



Abundance and distribution of ECSI Hector's dolphin

New Zealand Aquatic Environment and Biodiversity Report No. 123

D.L. MacKenzie,
D.M. Clement

ISSN 1179-6480 (online)
ISBN 978-0-478-42372-3 (online)

March 2014



Requests for further copies should be directed to:

Publications Logistics Officer
Ministry for Primary Industries
PO Box 2526
WELLINGTON 6140

Email: brand@mpi.govt.nz
Telephone: 0800 00 83 33
Facsimile: 04-894 0300

This publication is also available on the Ministry for Primary Industries websites at:
<http://www.mpi.govt.nz/news-resources/publications.aspx>
<http://fs.fish.govt.nz> go to Document library/Research reports

© Crown Copyright - Ministry for Primary Industries

TABLE OF CONTENTS

EXECUTIVE SUMMARY	1
1 INTRODUCTION	3
1.1 Background	3
1.2 Scope	4
2 METHODS	5
2.1 Survey design and effort	5
2.2 Survey platform and protocol	8
2.3 Abundance analyses	12
2.4 Availability bias	16
2.5 Distribution analyses	22
3 RESULTS	25
3.1 Abundance estimates	25
3.2 Distribution results	61
4 DISCUSSION	69
4.1 Abundance estimates	69
4.2 Distribution	73
4.3 Spatial management areas	74
5 ACKNOWLEDGMENTS	77
6 REFERENCES	77

EXECUTIVE SUMMARY

MacKenzie, D.I.; Clement, D.M. (2014). Abundance and distribution of ECSI Hector's dolphin.

New Zealand Aquatic Environment and Biodiversity Report No. 123. 79 p.

The Ministry for Primary Industries and the Department of Conservation are currently reviewing the Hector's dolphin threat management plan. For this review, up-to-date abundance and distribution estimates of Hector's dolphin are required. A survey programme specifically designed for sampling the ECSI population completed two aerial surveys over summer 2012/2013 and winter 2013. The ECSI survey area (about 42 677 km² between Farewell Spit and Nugget Point) was stratified into eight coastal sections with offshore substrata of 0–4 nmi (inner), 4–12 nmi (middle) and 12–20 nmi (outer). This design was expected to encompass the offshore limits of Hector's dolphin distribution. Double observer, line-transect methodology was used with transect lines orientated in the offshore direction and spaced parallel at equal intervals (according to strata-specific effort allocation) using systematic-random line placement. These aerial surveys constitute the only abundance study to date with substantial effort in offshore regions (more than 4 nmi from the coast) for Hector's dolphin along the entire east and north coastal waters of the South Island. Sightings results were similar across the two seasons with 354 dolphin groups (157 of which were seen by two observers) sighted along 7156 km of summer transect lines compared to 328 dolphin groups (103 observed by two observers) sighted along 7276 km of winter transect lines.

ECSI abundance was estimated using an extension of mark-recapture distance sampling (MRDS) techniques; a modern approach to analysing double observer line distance sampling data, enabling a more efficient use of the data compared to previous approaches. Availability bias is a fundamentally important component for obtaining a reliable estimate of total abundance, therefore, we tested the relative efficacy of two availability methods; helicopter observations of dive cycles and circle-back redetection.

Regional variation in dive cycle data was noticeable, with a slight north-south gradient (0.63–0.42 estimated surface availability) over summer indicating that groups are more available in the north. A similar range of regional dive cycle availability was observed over winter (0.62–0.33 estimated surface availability), but were geographically more random. Availability estimated from the circle back data exhibited less regional variation in the summer and a greater degree in the winter.

ECSI Hector's dolphin abundance was estimated to be 9130 (CV: 19%; 95% CI: 6342–13 144) in summer and 7456 (CV: 18%; 95% CI: 5224–10 641) in winter. These estimates were obtained by averaging the four sets of results for each season; from two different data sets using different truncation distances and two methods of estimating availability (dive cycle and circle-backs). These estimates do not include harbours and bays that were outside the survey region.

This agreement between seasonal abundance estimates confirms that the population of Hector's dolphin along the ECSI is larger than expected from previous estimates. This difference mainly corresponds to approximately half of the current summer estimate being distributed across previously unsurveyed regions in offshore waters between 4 nmi and 20

nmi. Density surface models (DSMs) confirm general offshore movements from summer to winter with lower winter relative densities closer to shore in Cloudy/Clifford Bay, Pegasus Bay and Banks Peninsula, and an increase in relative densities offshore of Timaru. Regional alongshore movements and a further than anticipated offshore shift may account for the slight difference between seasonal estimates.

In general, survey results suggest that, at least in summer, a large portion of the ECSI Hector's dolphin population occurs in waters around Banks Peninsula and within Clifford and Cloudy Bays. However, these results also suggest reasonable numbers of dolphins can be found outside designated spatial management areas, in more offshore regions or along the Timaru and Kaikoura/Clarence coastline, during both summer and, in particular, winter.

1 INTRODUCTION

Hector's dolphin, *Cephalorhynchus hectori hectori*, is only found within New Zealand waters and is currently listed as *Nationally Endangered* by the NZ threat classification scheme (Baker et al. 2010) and considered *Endangered* by the IUCN since 2000 (Reeves et al. 2008). From a series of surveys conducted from 1997–2001, the abundance of this species around the South Island has been estimated at approximately 7300 animals (95% 5303–9966; Slooten et al. 2004).

MPI and DOC have agreed to undertake a review of the Hector's dolphin threat management plan as this species' coastal distribution significantly overlaps with inshore setnet and trawl fisheries (DOC & MFish 2007). As part of this process, decision-makers must take into account sections 8, 9, and 15 of the Fisheries Act 1996, which include guidance to avoid, remedy or mitigate any adverse effects of fishing on the aquatic environment, including the effects of fishing related mortality on protected species. For this review, an up-to-date abundance estimate of Hector's dolphin is required as the previous estimate is now too old for management purposes and more recent research demonstrates that this species ranges further offshore than past abundance surveys have sampled (e.g. DuFresne & Mattlin 2009, Rayment et al. 2010a).

1.1 Background

The South Island population of Hector's dolphin is clumped, geographically and genetically, into three fairly distinct populations (Dawson & Slooten 1988, Pichler et al. 1998, Hamner et al. 2012). The majority of dolphins are found along the West Coast (between Farewell Spit and Milford Sound) with the remainder (about 1200 to 2900) found along the East Coast (ESCI; from Farewell Spit to Nugget Point) and South Coast (SCSI; from Nugget Point to Long Point; Dawson et al. 2004).

This abundance estimate is based on a series of four surveys, three undertaken by boat and one by airplane, over four consecutive summer seasons between 1997/1998 and 2000/2001. All four surveys were based on line-transect sampling methods and targeted the inshore waters between the coastline and four nautical miles (nmi) offshore. Sparse sampling effort was allocated to more offshore regions as previous research (Dawson & Slooten 1988) suggested that few dolphins occurred beyond four nmi. As a result, abundance was not estimated for more offshore waters (Dawson et al. 2004).

In 2008, the Ministry of Fisheries (now MPI) and Department of Conservation (DOC) released a draft Hector's and Maui's dolphin Threat Management Plan (TMP). This management document highlighted fishing-related mortalities as one of the main human-induced, yet highly uncertain, threats to this species. To mitigate these effects, the TMP established a range of fisheries prohibited zones and several non-fisheries protective measures throughout the three populations based on the above abundance estimates and all available data (DOC & MFish 2007). These measures focused on the waters out to four nmi where the majority of dolphins occur and overlap with both commercial and recreational setnet fisheries and inshore trawl fisheries.

Since the abundance surveys were completed and the TMP measures implemented, additional aerial-based studies have been undertaken within several localised regions around the South Island (DuFresne & Mattlin 2009, DuFresne et al. 2010, Rayment et al. 2010a, 2010b). There

are several advantages to using aerial platforms for research on Hector's dolphins. The biggest advantages include being able to synoptically sample a large study area in much shorter time periods than boat platforms, which minimises the effect of any directional or seasonal movement, while eliciting little to no responsive behaviours from the dolphins (Slooten et al. 2004).

All of these studies found Hector's dolphin regularly occurring past four nmi, and some much further offshore than it was previously thought that this species might normally occur (e.g. 16 nmi DuFresne & Mattlin 2009; 18 nmi Rayment et al. 2010a). In addition, DuFresne & Mattlin's (2009) study in Cloudy and Clifford Bay, along the top of the South Island, indicated a much larger population of Hector's dolphins (about 573–1577 dolphins), present over summer than the previous abundance survey estimated (about 56–474 dolphins; Clement et al. 2001). These findings suggest that the 1997–2001 abundance survey may have missed a proportion of dolphins from these offshore regions and that the overall population of Hector's dolphin along the ECSI is likely to be larger than previously estimated.

1.2 Scope

The Cawthron Institute (Cawthron), in conjunction with Proteus Wildlife Research Consultants and Marine Wildlife Research Limited, were contracted by MPI to conduct two aerial surveys along the ECSI in summer 2012/2013 and winter 2013. The resulting survey programme was designed specifically for the ECSI population and based on previous aerial methods on this species (Slooten et al. 2004, DuFresne & Mattlin 2009, Clement et al. 2011). To ensure appropriate allocation of survey effort, pre-survey simulation testing assessed several possible options based on previous and recent information on dolphin density and distribution, and utilised different levels of sampling intensity and stratification (MacKenzie et al. 2012). The specific scope of this programme is outlined as follows.

Overall objective:

To estimate critical aspects of the biology, abundance and distribution of Hector's and Maui's dolphin populations to assess the effects of fishing-related mortality on these populations.

Specific objectives:

1. To estimate the abundance of Hector's dolphins along the ECSI in summer 2012/13 applying an agreed aerial survey methodology;
2. To estimate the distribution of Hector's dolphins along the ECSI in summer 2012/13 applying an agreed aerial survey methodology;
3. To estimate the abundance of Hector's dolphins along the ECSI in winter 2013 applying an agreed aerial survey methodology; and
4. To estimate the distribution of Hector's dolphins along the ECSI in winter 2013 applying an agreed aerial survey methodology.

In addition to this report, a second report containing relevant supplementary material is also available. References to items in the supplementary material report are prefixed by SM.

2 METHODS

The survey programme was based on the general aerial survey design outlined in MacKenzie et al. (2012) that relies on distance sampling techniques and appropriate allocation of survey effort. Abundance is estimated by mark-recapture distance sampling (MRDS; Buckland et al. 2004) and density surface models (DSM) are used to estimate dolphin distribution.

2.1 Survey design and effort

The ECSI survey area was stratified into eight coastal sections with offshore substrata of 0–4 nmi (inner), 4–12 nmi (middle) and 12–20 nmi (outer - see Table 1), as determined in previous Aquatic Environment Working Group (AEWG) meetings during 2012 and as outlined in MacKenzie et al. (2012). The final survey design was based on simulations that demonstrated equal coverage probability using DISTANCE 6 (Thomas et al. 2010) and a lack of difference in offshore versus 45 degree orientation of lines (MacKenzie et al. 2012). This design was expected to encompass the offshore limits of Hector's dolphin distribution. Transect lines were orientated generally in the offshore direction and spaced parallel at equal intervals (according to effort allocation in Table 1) using systematic-random line placement (i.e., the first line is randomly placed within a stratum and subsequent lines are placed parallel to that at a set distance) as recommended by Buckland et al. (2004) and Dawson et al. (2008). Golden Bay and Banks Peninsula were further subdivided to allow suitable orientation of transect lines in regards to local shoreline and bathymetry as seen in Figure 1 as recommended and approved in previous AEWG meetings during 2012.

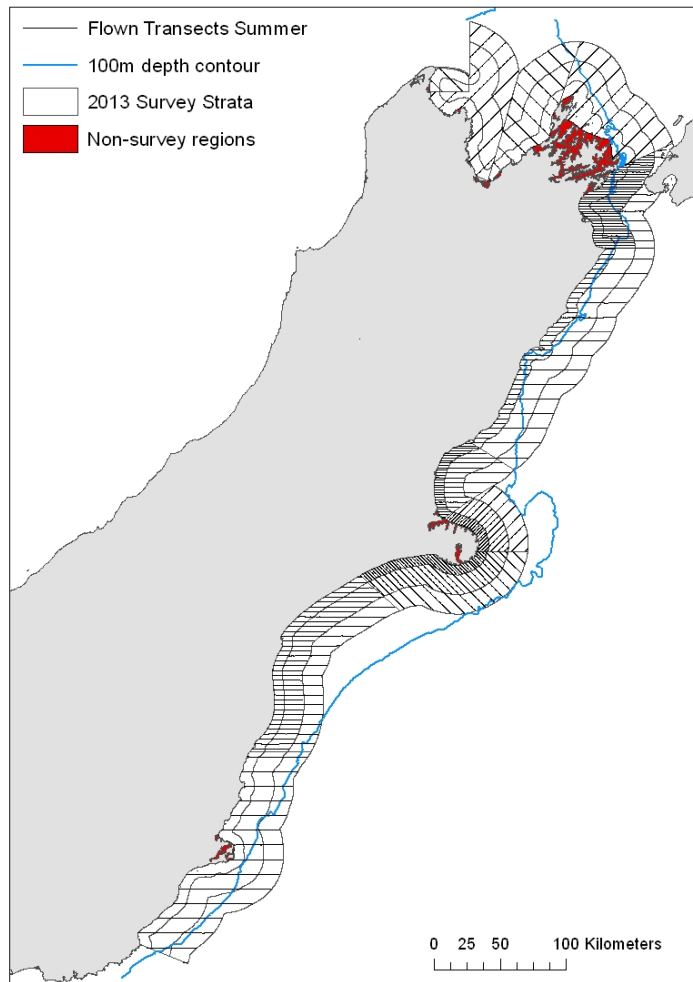
To ensure a sufficient number of sightings (60–80 is typically a recommended minimum; Buckland et al. 2001), priority was given to more intensive sampling within known high-density regions (e.g. Banks Peninsula and Clifford/Cloudy Bay; Table 1). Less intensive sampling was carried out in suspected low-density strata, although effort was still greater than what would be considered optimal for estimating abundance (MacKenzie et al. 2012), in recognition that little survey work has been conducted in those areas and because of the dual survey objectives of estimating both abundance and distribution. The extra effort in the suspected low-density strata was also intended to ensure that low density estimates were not obtained simply due to a low level of survey effort, which may have arisen if the 'optimal' allocation had been used.

The summer survey of all continuous transect lines (276 lines, 7156 km) was carried out between 28 January and 13 March 2013. Note that the offshore stratification subdivides many of the continuous transects, hence there was a total of 540 transect lines for the purpose of the analysis (Figure 1; i.e. one continuous transect line may be considered as three lines for analysis purposes if it spans across all three offshore substrata). Based on summer sighting results, the survey design was further optimised for winter sampling by reallocating sampling effort to and from particular coastal sections and offshore substrata. Effort changes included reducing effort off Cloudy Bay (previously over-sampled as the summer survey suggested that local abundance was a smaller proportion of ECSI population than anticipated) and increasing effort around Banks Peninsula (previously under-sampled based on summer sightings; Table 1; Figure 1). The winter survey sampled 245 continuous transect lines (7276 km between 1 July and 18 August 2013 for a total of 539 lines for analysis).

Table 1: Summer and winter survey line spacing with estimated and achieved levels of effort in each stratum.

Coastal Section	Offshore Stratum	Summer			Winter		
		Line Spacing (km)	Approximate Length of Transects (km)	Achieved Length of Transects (km)	Line Spacing (km)	Approximate Length of Transects (km)	Achieved Length of Transects (km)
Golden Bay	Inner	11.10	169	156	11.10	169	160
	Middle	11.10	267	267	11.10	267	267
	Outer	11.10	197	197	11.10	197	197
Marlborough Sounds	Inner	11.10	95	88	11.10	95	88
	Middle	11.10	130	136	11.10	130	136
	Outer	11.10	139	137	11.10	139	137
Cloudy Bay	Inner	1.85	377	366	3.70	185	182
	Middle	1.85	708	712	3.70	353	352
	Outer	7.40	125	138	7.40	121	119
Clarence	Inner	3.70	163	156	3.70	163	156
	Middle	11.10	102	89	11.10	102	89
	Outer	11.10	98	86	11.10	98	86
Kaikoura	Inner	3.70	235	233	3.70	235	234
	Middle	11.10	162	159	11.10	162	159
	Outer	11.10	168	168	11.10	168	168
Banks Peninsula	Inner	1.85	865	846	1.85	723	713
	Middle	3.70	863	864	1.85	1490	1489
	Outer	7.40	426	430	7.40	614	612
Timaru	Inner	3.70	340	338	3.70	340	341
	Middle	3.70	634	631	3.70	634	631
	Outer	7.40	292	284	7.40	292	283
Otago	Inner	11.10	144	131	11.10	144	131
	Middle	11.10	269	277	11.10	269	277
	Outer	11.10	268	267	11.10	268	268
Total			7236	7156		7358	7276

A)



B)

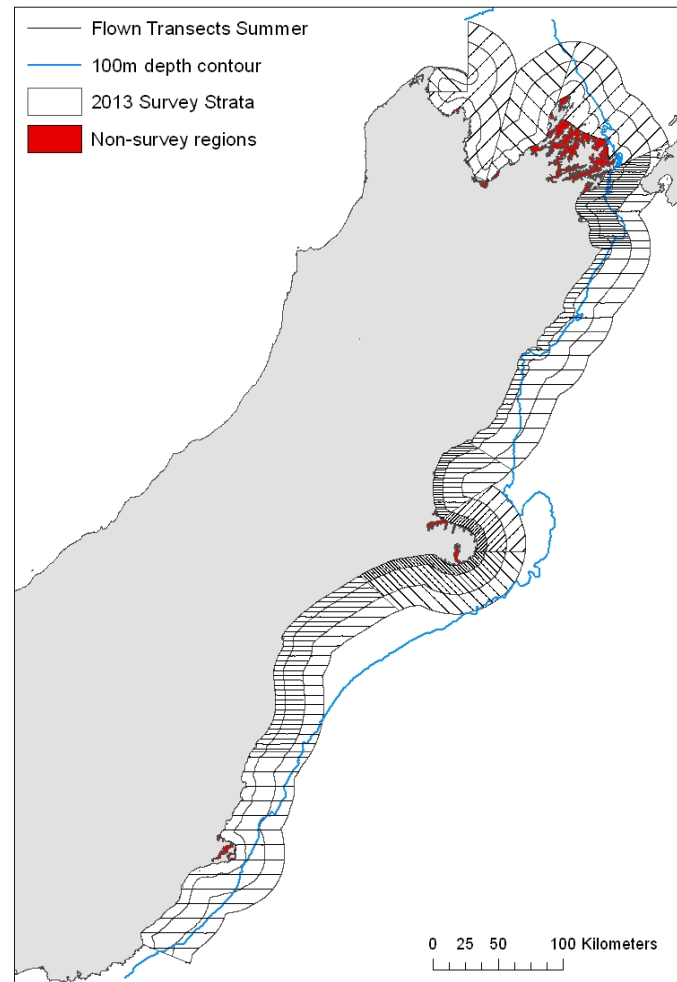


Figure 1: A) Summer survey transects flown between 28 January and 13 March 2013. B) Winter survey transects flown between 1 July and 18 August 2013.

2.2 Survey platform and protocol

The survey protocol was developed based upon the protocols that are typically used for double-observer line-transect aerial surveys in general (e.g., Manly et al. 1996), and for Hector's and Maui's dolphins in particular (Slooten et al. 2004, 2006; DuFresne & Mattlin 2009; Clement et al. 2011).

A high-wing, seven-seater Cessna 207 aircraft allowed two observers on each side of the aircraft to independently search for Hector's dolphins. Rear bubble windows permitted observers in the back seats to see directly underneath the plane while surveying. Transects were surveyed at an altitude of 152.4 metres (500 feet) at a speed of about 100 knots (185.2 km/h). Pilot(s) navigated transects using the aircraft's in-built GPS navigation system that was pre-loaded with all transect information. Surveys were only undertaken in suitable conditions; sea state (Beaufort 3 or less), weather (low glare, no fog or obstructive clouds), and light (at least one hour after sunrise and before sunset). One observer on each flight was designated to take note of the sighting conditions at the start of each transect and whenever they changed. Sighting conditions recorded included Beaufort sea state, water colour (categorised as blue, blue-green, green or brown), swell height and glare intensity (1 to 3), percentage (recorded as the proportion of the field of view obscured) and glare direction. Sighting conditions were discussed between transect lines to ensure consistency.

The search zone for the front observers was between the downward angles of 20° and 70° and for the rear observers using the bubble window it was between 25° and 90°. We used the maximum possible overlap zone of approximately 40° between the downward angles of 25° and 65° degrees. This overlap zone is larger than the 20° used previously in Hector's dolphin surveys (Slooten et al. 2004, 2006; DuFresne & Mattlin 2009; Clement et al. 2011) in an effort to collect more data that is relevant for the effective estimation of dolphin detection on the trackline (MacKenzie et al. 2012). Observers were instructed to use a consistent level of effort both inside and outside of the overlapping view zones. When dolphins were sighted, each observer recorded downward angle and time (to the second) of each observation into individual dictaphones, as well as other relevant sighting information (e.g. group size, presence of calves, sighting conditions). The downward angle of observation (used in calculation of sighting distance) is taken perpendicular to the aircraft's track using a hand-held inclinometer (Suunto PM5/360PC). Time is recorded from a digital timepiece that is synchronised with the GPS at the beginning of each survey and placed within each survey window. To minimise the chance of one observer visually cueing off the other, black sheets of fabric were hung between the two seats on each side of the plane. Observers were rotated amongst all positions in the aircraft so that each person spent approximately the same amount of time in each position.

Given the lengthy time-frame estimated to complete each survey (6–10 weeks in each season, dependent on weather), a team of five observers was trained to ensure consistency across survey results while keeping observers fresh and attentive, and avoiding costly delays due to observer sickness or other unforeseen circumstances that may have made observer(s) unavailable for surveying. Four of these observers were used across both survey seasons. One observer (Ob5) had to leave the project soon after summer training for personal reasons. A replacement observer (Ob6) was trained while the summer survey was in progress, undertaking training flights between survey flights and when in transit to and from survey areas (Table 2). The observer was able to directly train against the rear observer on the same side during surveys as the co-pilot window was also fitted with a bubble window. A new

observer (Ob7) joined the original core team of observers for the winter survey as neither Ob5 nor Ob6 were available for the winter survey period.

As observers had various levels of marine mammal observing and marine survey experience, extensive pre-survey training was conducted within Clifford and Cloudy Bays (high-density regions for Hector's dolphins) in both seasons; 14–27 January 2013 and 12–19 June 2013. Training flights helped confirm the size of the fields of view for observers, ensured that observers were skilled in the field protocols and recording requirements, and helped to familiarise the pilot with the survey design, protocols and communication with observers.

Approximately 41 hours of summer (about 20 flights) and 24 hours of winter (about 14 flights) training flights were completed, with individual observer training hours varying from 20.5 to 27.5 hrs (Table 2). Observers initially recorded as many objects that they could see (e.g. dolphins, birds, seals, sharks, seaweed) to practice the sighting protocol while fine-tuning their search image for Hector's dolphins. After several initial flights, observers kept track of all on- and off-effort sightings of Hector's dolphins and any other observed marine mammal species. Summer observers flew 112 transects and made 223 training sightings and winter observers recorded 160 sightings across 64 transects while on-effort. All newly trained observers recorded 34 or more sightings each (Table 2, Figure 2) before surveying commenced, well over the recommended 20 sightings minimum (Dawson et al. 2008).

Table 2: Observer statistics from training flights in Clifford and Cloudy Bay, Blenheim.

		Ob1	Ob2	Ob3	Ob4	Ob5	Ob6	Ob7
	Flying Hours	25.50	27.50	27.25	26.25	26.50	20.50	-
Summer	On-effort Sight	60	43	52	79	35	41	-
	Training Detection Rate	67%	100%	94%	100%	73%	83%*	
	Average Survey Detection Rate	73%	85%	88%	82%		80%	-
	Flying Hours	19.00	18.50	17.50	12.75	-	-	20.50
Winter	On-effort Sight	50	53	29	32	-	-	34
	Training Detection Rate	75%	100%	71%	100%	-	-	67%
	Average Survey Detection Rate	73%	76%	73%	79%	-	-	68%

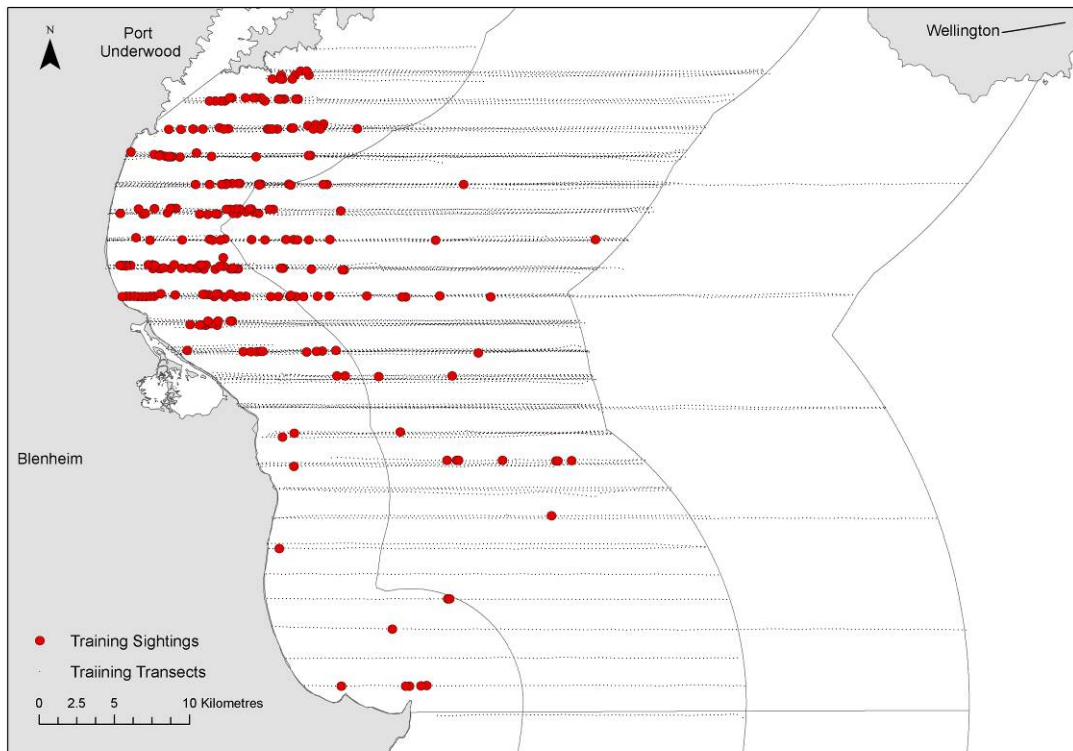
* compared to the rear seat observer during survey flights.

To gauge observer performance, each observer's training sightings were compared against the most experienced observer when on the same side of the plane (i.e. number of duplicate sightings versus number of experienced observer sightings within shared viewing zone only). By the end of both training periods, the detection rates of observers ranged between 67 and 100% (Table 2). We also compared observer performance over the last two-thirds of each

survey season. An observer's survey detection rate was calculated as the average of their duplicate sightings versus the number of the other observers' sightings from the same side of the plane and within the shared viewing zone only. Average survey detection rates remained high and were fairly comparable across observers within a season, however; winter rates were generally lower than summer.

Training data were used for training purposes only and not included in any further analyses.

A)



B)

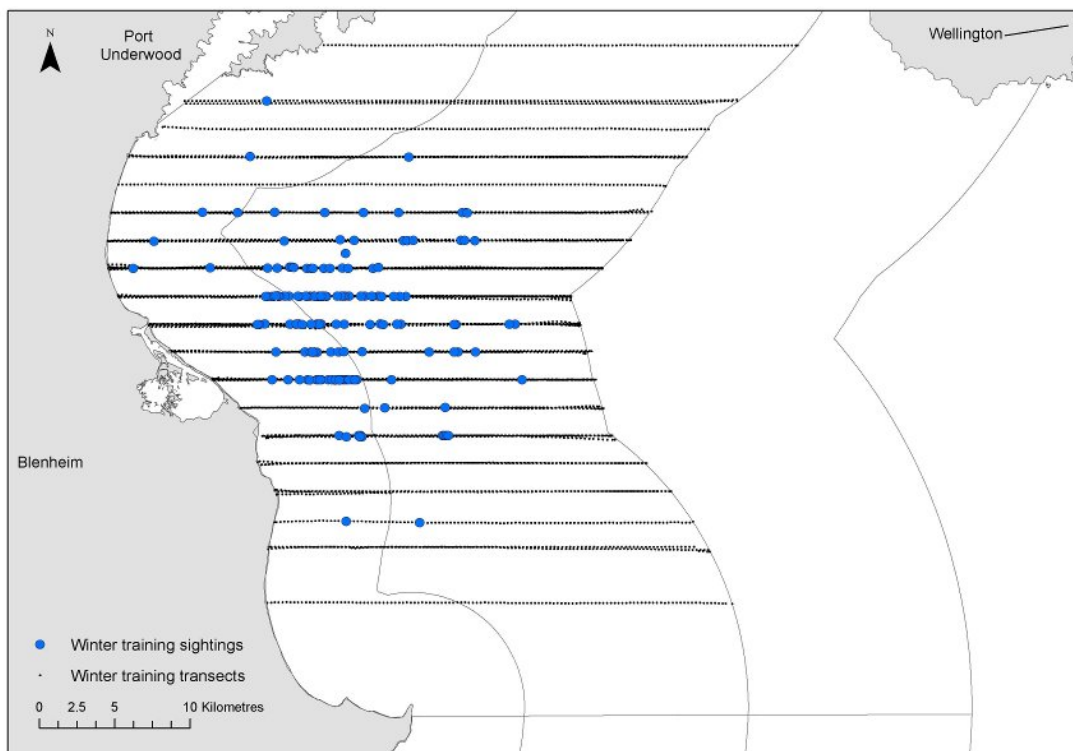


Figure 2: The locations of Hector's dolphin sightings and on-effort transects flown during observer training off Clifford and Cloudy Bays for A) summer: 13-27 January 2013 and B) winter: 12-19 June 2013.

2.3 Abundance analyses

Data selection

Any sightings that were data deficient (e.g. angle not measured, seconds not recorded, uncertain about species' identification) were removed prior to analysis (Table 3). Buckland et al. (2001) recommends right truncation of sightings at the further perpendicular distances by 5–10% of the dataset, or alternatively, such that the probability of detection at the truncation distance is (approximately) greater than 0.15. After some initial analyses, a right truncation distance of 0.3 km (27 degrees) was used for both front and rear observer positions (see Table 3). This is smaller than the truncation distance used in other aerial surveys for Hector's dolphin (0.33 km - Slooten et al. 2004; 0.337 km – Clement et al. 2011), but was decided upon in an effort to be conservative, and minimise the effect of angle measurement error on perpendicular distance, which has a greater effect at shallower angles. A left-truncation distance of 0.071 km (65 degrees) was used for the front observer position as not all observers could consistently survey to 70 degrees due to their height. Any angles recorded at greater than 90 degrees from the rear observer position were presumed to be 90 degrees. A subset of the data was also analysed where a left truncation distance of 0.071 km was applied to both front and rear observer data as a comparison with the results obtained from the full analysis. This reduced data set is more typical of double-observer line transect surveys where sightings can be made from either observer position across the entire range of distances.

Table 3: The numbers of sightings removed through data verification prior to inclusion in abundance or distribution analyses. Sightings were initially removed due to either uncertainty around species identification or missed information about the exact time or angle of the sighting. Additional sightings were removed as part of the left and right truncation process. Final sightings numbers represent those sightings used in the final full analyses. The numbers in brackets list the percentage of the total raw sightings that each verification step represents.

	Number of Raw sightings	Uncertain about identification	Missed angle/time	Truncated [^]	Number of Final Sighting
Summer	391	13 * (3%)	9 [#] (2%)	15 (4%)	354
Winter	346	10 (3%)	2 (0.6%)	6 (2%)	328

[^] Sightings were left truncated at 0.071 km for the front observer position, and right truncated at 0.300 km for both observer positions.

* 4 of which were beyond 0.30 km

[#] 7 of which were beyond 0.30 km

Duplicate sightings were those in which the same group of animals was recorded by both the front and rear observer (on the same side of the plane). Duplicates were manually identified by comparing three different sighting variables; sighting time (within ± 5 seconds), sighting angle (within ± 5 degrees) and group size (± 1 individual), in line with criteria from previous Hector's dolphin aerial surveys (e.g. DuFresne & Mattlin 2009, Clement et al. 2011). Matching criteria helped identify those sightings with agreement in at least two of the three variables while observer experience and any distinguishing comments recorded by observers at the time (e.g. mother/calf pair) were also important factors considered in final duplicate decisions, particularly in cases where a sighting fell just outside one or more of the matching criteria. Duplicate sightings were retained in the final database as a single sighting in which

the average angle was used to calculate distance from the trackline, and where the recorded groups sizes differed, the larger value was retained (17% of duplicates in both summer and winter). As observers were instructed to record the minimum group size they were certain of rather than approximating group size, the larger value was used as it was believed that undercounting of a group would be more likely than over-counting. The final datasets contained a record for each unique sighting, the number of individuals in the group, distance from the trackline and whether the group was detected by the front and/or rear observer.

Detection function analysis

Hector's dolphin abundance was estimated using mark-recapture distance sampling (MRDS) techniques (e.g., Buckland et al. 2004, Borchers et al. 2006). MRDS methods are a more modern approach to analysing distance sampling data from double observers enabling a more efficient use of the data compared to the multi-step approaches that have been used previously for estimating Hector's dolphin abundance (Slooten et al. 2004, 2006; DuFresne & Mattlin 2009; Clement et al. 2011). However, given that the range of angles being searched from each observer position was different, current MRDS methods had to be extended (MacKenzie et al. 2012). An alternative approach to dealing with a lack of independence between the observer detections was also developed. A brief summary of the method is given below with full details in SM §A.

For the purpose of abundance estimation, the key probability to be determined from the data is the probability of detecting a dolphin group by at least one of the observers in the aircraft. Denote this as $p_{\bullet}(d_i, s_i)$ where d_i and s_i are the distance and group size measured for the i th group respectively. With the double observer setup, there are four possible outcomes in terms of sighting a dolphin group within a survey transect; 1) sighted by both observers; 2) sighted from the front position, but not the rear; 3) sighted from the rear position, but not the front; or 4) sighted by neither observer. These four outcomes are mutually exclusive and each outcome has an associated probability, the sum of which must equal 1, therefore three of these probabilities can be estimated with the fourth being obtained by subtraction. Note that $p_{\bullet}(d_i, s_i)$ is the sum of the probabilities for the first three outcomes, hence $1 - p_{\bullet}(d_i, s_i)$ is the probability associated with the outcome of a dolphin group not being sighted by either observer.

There are multiple parameterizations that could be used for determining $p_{\bullet}(d_i, s_i)$ (e.g., Laake & Borchers 2004, Buckland et al. 2010) and the one used here is:

$$p_{\bullet}(d_i, s_i) = p_F(d_i, s_i) + [1 - p_F(d_i, s_i)]p_{R|NF}(d_i, s_i) \quad (\text{Eqn. 1})$$

where $p_F(d_i, s_i)$ is the probability of the dolphin group being observed from the front observer position and $p_{R|NF}(d_i, s_i)$ is the probability of the dolphin group being observed from the rear position given it *was not* detected by the front observer (NF =not front). A third probability that could be estimated with this parameterisation is the probability of the dolphin group being observed from the rear position given that it *was* detected by the front observer ($p_{R|F}(d_i, s_i)$). While not included in Eqn. 1, $p_{R|F}(d_i, s_i)$ is important in terms of accounting for the potential dependence of detecting the same group from each observer position with $p_{R|F}(d_i, s_i) = p_{R|NF}(d_i, s_i)$ if detections are independent and $p_{R|F}(d_i, s_i) \neq p_{R|NF}(d_i, s_i)$

otherwise. However, the approach developed here does not estimate $p_{R|F}(d_i, s_i)$ directly, and instead estimates an odds ratio ($v_{R|F}(d_i, s_i)$) for how the *odds* of detection from the rear position change if the dolphin group was also detected from the front position, with an odds ratio of 1 implying independence.

In summary, the three components being estimated in the approach developed here are $p_F(d_i, s_i)$, $p_{R|NF}(d_i, s_i)$ and $v_{R|F}(d_i)$. How these components are used with the double observer distance sampling data to estimate abundance follows the standard MRDS theory (e.g., Laake & Borchers 2004, Buckland et al. 2010; see SM §A), although a key element is that $p_F(d_i, s_i)$ was set equal to zero for distances less than 0.071 km (i.e., angles deeper than 65 degrees) as an observer cannot see dolphin groups in this portion of the transect from the front position.

A simulation study was conducted that verified the performance of this approach for modelling the detection function to estimate the number of available groups within the transect width (see SM §B).

Covariates

In the primary analysis, the effects of distance, observer, and group size on detection probabilities were considered by fitting a range of models to the collected data. All covariates were included by using the logit-link function, which is equivalent to performing logistic regression. How detection varied with distance was investigated using three different functional forms (on the logit scale); 1) linear; 2) quadratic; and 3) a natural spline with two internal knots. A natural spline is a method for fitting a flexible, non-parametric curve to data. For each functional relationship for distance ($f(d)$), general equations can be expressed for each of $p_F(d_i, s_i)$ and $p_{R|NF}(d_i, s_i)$ (Eqns 2 and 3, respectively) from which six models were considered, resulting from applying various constraints across the regression coefficients.

$$\text{logit}(p_F(d_i, s_i)) = \ln\left(\frac{p_F(d_i, s_i)}{1 - p_F(d_i, s_i)}\right) = a_1 + \beta_1 f(d_i) + c_1 s_i \quad (2)$$

$$\text{logit}(p_{R|NF}(d_i, s_i)) = \ln\left(\frac{p_{R|NF}(d_i, s_i)}{1 - p_{R|NF}(d_i, s_i)}\right) = a_2 + \beta_2 f(d_i) + c_2 s_i \quad (3)$$

The six models were:

1. different intercept terms and different coefficients for $f(d)$ for each observer position, i.e., $a_1 \neq a_2$, $\beta_1 \neq \beta_2$ and $c_1 = c_2 = 0$;
2. different intercept terms, but the same coefficients for $f(d)$ for each observer position, i.e., $a_1 \neq a_2$, $\beta_1 = \beta_2$ and $c_1 = c_2 = 0$;
3. same intercept and same coefficients for $f(d)$ for each observer position, i.e., $a_1 = a_2$, $\beta_1 = \beta_2$ and $c_1 = c_2 = 0$;

4. as model 1, with constant effect of group size for both observer positions, i.e., $a_1 \neq a_2$, $\beta_1 \neq \beta_2$ and $c_1 = c_2$;
5. as model 2, with constant effect of group size for both observer positions, i.e., $a_1 \neq a_2$, $\beta_1 = \beta_2$ and $c_1 = c_2$;
6. as model 3, with constant effect of group size for both observer positions, i.e., $a_1 = a_2$, $\beta_1 = \beta_2$ and $c_1 = c_2$.

Apparent lack of independence between observers (which may be due to response to cues from the other observer, or unmodelled heterogeneity in detection; Laake & Borchers 2004) was incorporated through the odds ratio $v_{R|F}(d_i)$ which was modelled on the natural log scale. That is,

$$\ln(v_{R|F}(d_i)) = a_3 + \beta_3 d_i \quad (4)$$

noting that only a linear effect with distance was considered. This approach for incorporating potential dependence differs from that used by Laake & Borchers (2004) and Buckland et al. (2010), and was considered as a potentially more numerically stable method than that developed by Buckland et al. (2010). Four models for dependence were considered:

1. full independence, i.e., $a_3 = \beta_3 = 0$ (hence $v_{R|F}(d_i) = 1$);
2. constant dependence at all distances i.e., $a_3 \neq 0$ and $\beta_3 = 0$;
3. dependence between observer position changes linearly with distance, with full independence at the track line, i.e., $a_3 = 0$ and $\beta_3 \neq 0$ (point independence);
4. as for model 3, but dependence between observers at track line is estimated rather than assuming point independence i.e., $a_3 \neq 0$ and $\beta_3 \neq 0$ (limiting independence, Buckland et al., 2010).

Note that under full independence, and a linear effect of distance, models 3, 2, 1 and 4 are equivalent to models 1–4 considered by Manly et al. (1996), though the model likelihoods are formulated slightly differently.

In total, 72 models were considered for the analysis ($3 \times 6 \times 4$) and compared using Akaike's Information Criterion (AIC; Burnham & Anderson 2002) to determine the level of evidence for each effect. Model averaging was used to obtain an overall estimate of abundance based upon AIC model weights where there was model selection uncertainty (i.e., models incorporating different factors that have similar levels of support from the data; Anderson 2008). Stratum-specific detection functions were not considered as few strata would have had sufficient sightings to do so.

Goodness-of-fit of the detection functions was assessed using quantile-quantile (q-q) plots along with a Kolmogorov-Smirnov (KS) test and Cramer-von Mises (CvM) test (Buckland et al. 2004).

At the request of the AEWG members after a presentation of preliminary results, some secondary analyses were also conducted on the full summer data set to assess the effects on detection of water depth, water colour, wind, glare and distance from shore.

2.4 Availability bias

MacKenzie et al. (2012) emphasised the importance of the availability bias for Hector's dolphins given that it is a fundamentally important component for obtaining a reliable estimate of total abundance. Hence, we undertook a series of field tests to determine the relative efficacy of two methods: helicopter observations of dive cycles and circle-back redetection. Both methods require certain assumptions to be made that may be questionable in some circumstances (discussed further below). However, these were the only practical approaches that could be implemented within the budgetary constraints of the project. We suggest that the accurate estimation of availability for Hector's dolphins during aerial surveys is an area that needs further work. It is noted that helicopter observations of dive cycles has been used previously for Hector's dolphins (Slooten et al. 2004, 2006; DuFresne & Mattlin, 2009; Clement et al. 2011).

Field tests

The two methods for assessing availability were evaluated during the summer training period in Clifford and Cloudy Bays. The first method was based on previous methods used to estimate the availability of Hector's dolphins using helicopters (Slooten et al. 2004, 2006; DuFresne & Mattlin, 2009; Clement et al. 2011). Single-engine helicopters (i.e. Robinson R44), while successfully used in past studies, are only allowed beyond 10 nmi from the coast if equipped with the proper safety gear (e.g. skid floats, life raft, personal survival suits), and even then, many pilots are not prepared to operate such aircraft beyond a few nautical miles from shore at low altitude. Therefore, most companies recommend the use of twin-engine helicopters instead when operating further offshore. However, DuFresne & Mattlin (2009) noted that twin-engine helicopters (i.e. Jet rangers) substantially altered Hector's dolphin behaviour while hovering overhead. Given the need to assess possible differences in dolphin availability in more offshore waters (over 10 nmi), this first method further examined whether the type of helicopter (single-engine versus twin-engine) affected dolphin diving behaviours given the twin-engine's tendency for greater noise and vibrations.

The second field method was a variation of the 'circle-back' method originally proposed by Hiby (1999) using a single fixed-wing aircraft. This option has the advantage of being used in areas where other techniques might be impractical (e.g. helicopters in offshore areas) and can be employed when dolphins are sighted rather than trying to re-locate the same group at a later time.

Helicopter protocols

Surface availability was estimated using dive/surface intervals of Hector's dolphins collected using a modified sampling protocol and analysis in Slooten et al. (2004) and Clement et al. (2011). Helicopters searched for dolphins using a similar transect pattern to the fixed-wing

airplane; a perpendicular transect was flown out from the shore to approximately 5–10 nmi (depending on location and water depth), the helicopter then travelled parallel to the shore for approximate 1–2 nmi before surveying back towards the shore. Helicopters travelled at 100 kn or slower and maintained a height of 500 ft. Foretrex GPS was used to record the track of the helicopter and the location of any sighted dolphin groups.

Once a group of dolphins was sighted, the helicopter hovered off to one side rather than directly above to minimise any possible noise disturbance, and either maintained position or slowly circled the group. While hovering/circling, the observer recorded the duration of the groups' dive and surface intervals into a continuously running dictaphone for a maximum of ten minutes or until the group disappeared. Groups were recorded as either near the surface (i.e. visible to the observer in the helicopter, even if below the surface) or not. A range of group sizes, dive behaviours (synchronous, independent, etc.) and age classes were observed. We also noted any distinct behaviour changes that occurred between the initial sighting and helicopter approach, and with any later changes in behaviour with changes in the helicopter's position or activities. In an attempt to directly compare the effect of helicopter type on the dolphins' behaviour, the same observer surveyed from both the single and twin-engine platform and attempted to survey within similar regions (e.g. location, depth, distance from shore) of Cloudy Bay.

Our analysis included only complete dive cycles (i.e. dropping the first surface and last dive interval) to calculate the average time a group was visible near the surface and average time below the surface. As a group's dive cycles are not independent from each other, our overall sample size represents the number of groups observed rather than the total number of dive cycles.

From Laake & Borchers (2004), the probability of a group being available (P_α) can be estimated from dive cycle data by:

$$P_\alpha = 1 - \frac{\bar{b} \exp(-t/\bar{b})}{\bar{u} + \bar{b}} \quad (5)$$

where \bar{b} is the average time below the surface, \bar{u} the average time up or near the surface and t is the time frame for which the group is within the view of the observers from the aircraft. The standard error for \hat{P}_α can be calculated as:

$$SE(\hat{P}_\alpha) = \sqrt{\left[\frac{\bar{b} \exp(t/\bar{b})}{(\bar{u} + \bar{b})^2} \right]^2 V_{\bar{u}} - 2\bar{u}\bar{b} \left[1 + \frac{t(\bar{u} + \bar{b})}{\bar{u}\bar{b}} \right] V_{\bar{u}\bar{b}} + \bar{u}^2 \left[1 + \frac{t(\bar{u} + \bar{b})}{\bar{u}\bar{b}} \right]^2 V_{\bar{b}}} \quad (6)$$

where $V_{\bar{u}}$ and $V_{\bar{b}}$ are the variances for \bar{u} and \bar{b} respectively, and $V_{\bar{u}\bar{b}}$ is the covariance for the two means.

Note that the above analysis of the dive-cycle information differs from that used previously (Slooten et al. 2004, 2006; DuFresne & Mattlin, 2009; Clement et al. 2011) as the time a dolphin group is within the observer's field of view is explicitly accounted for. Previous applications have estimated instantaneous availability probabilities (i.e. $t = 0$), which will be lower, leading to higher estimates of abundance.

We collected regional information on availability using only single-engine helicopters (no twin-engines), based on field test results and given budget constraints. The goal was to allocate sufficient helicopter flight time among six regional locations such that availability could be estimated with a CV of at most 10% for each area. The six locations included Clifford/Cloudy Bays, Kaikoura, Pegasus Bay, northern Banks Peninsula, southern Banks Peninsula and Otago. These six regional locations were sampled over summer, however; due to longer winter search times and the lack of sufficient sample size from summer sampling, the Otago region was not sampled over winter. Regional estimates of availability were calculated and incorporated into estimates of total abundance. The value from Clifford/Cloudy Bays was also applied to Golden Bay and the Marlborough Sounds; the Kaikoura estimate applied to Clarence; and the southern Banks Peninsular value also applied to Timaru (and Otago in the winter).

Circle-back protocols

Circle-backs were carried out from the survey plane while on-effort and flying along training transects. Once a dolphin group was sighted by an observer, and the other observer on the same side had an opportunity to detect the same group (e.g. 5–10 s), the observer would call ‘availability’. The pilot would mark the location on his GPS while confirming ‘off-effort’ and carry on along the transect for another 20 s (1 nmi) before beginning a gentle turn that would bring the plane onto the next parallel transect. The pilot would back-track along the parallel transect for approximately 2–3 nmi (1–2 mins), using the GPS mark to ensure sufficient space of the plane to turn back onto the original transect, flatten its wings and re-survey the transect well before the location of the original sighting and the off-effort mark. The same procedure was repeated for a second circle-back with observers going back on-effort when the plane crossed over the original off-effort GPS mark, as called by the pilot, and carried on surveying the rest of the transect. Information about availability comes from the proportion of passes where the original dolphin group was observed on (or near) the surface. Other groups recorded after or before the original sighting by the other observers could also be used as part of the availability calculation.

To aid in the re-identification of the original sightings, observers kept detailed records of all circle-back activities. The observer who called availability would record the original sighting details using the normal survey protocol. All observers would note the time in their dictaphones when off-effort was called by the pilot while continuing to survey until the plane started to turn. Observers would rest as the plane back-tracked. As the plane turned back onto the original transect, observers would note the time and circle number and then begin surveying according to normal on-effort protocols. Analysis of this method could be difficult in high density areas where multiple groups were sighted in the same general location. As a result, observers had the ability to cancel an availability call if they observed multiple groups before or after the original call or if the pilot was too far off the original track (see example Figure 3A).

Circle-back sightings and duplicates were verified in a similar manner to on-effort sightings. The resulting sightings (position corrected for perpendicular distance off the transect line) and all circle-back information were visually plotted in ArcGIS (ESRI 2011) to aid in identifying re-sightings (Figure 3B). It was noted during summer training that the observer who called availability often reported the time of the original sighting later than the other observer reporting the same sighting. Hence, observers were asked to note when they thought this was the case (see example in Figure 3C).

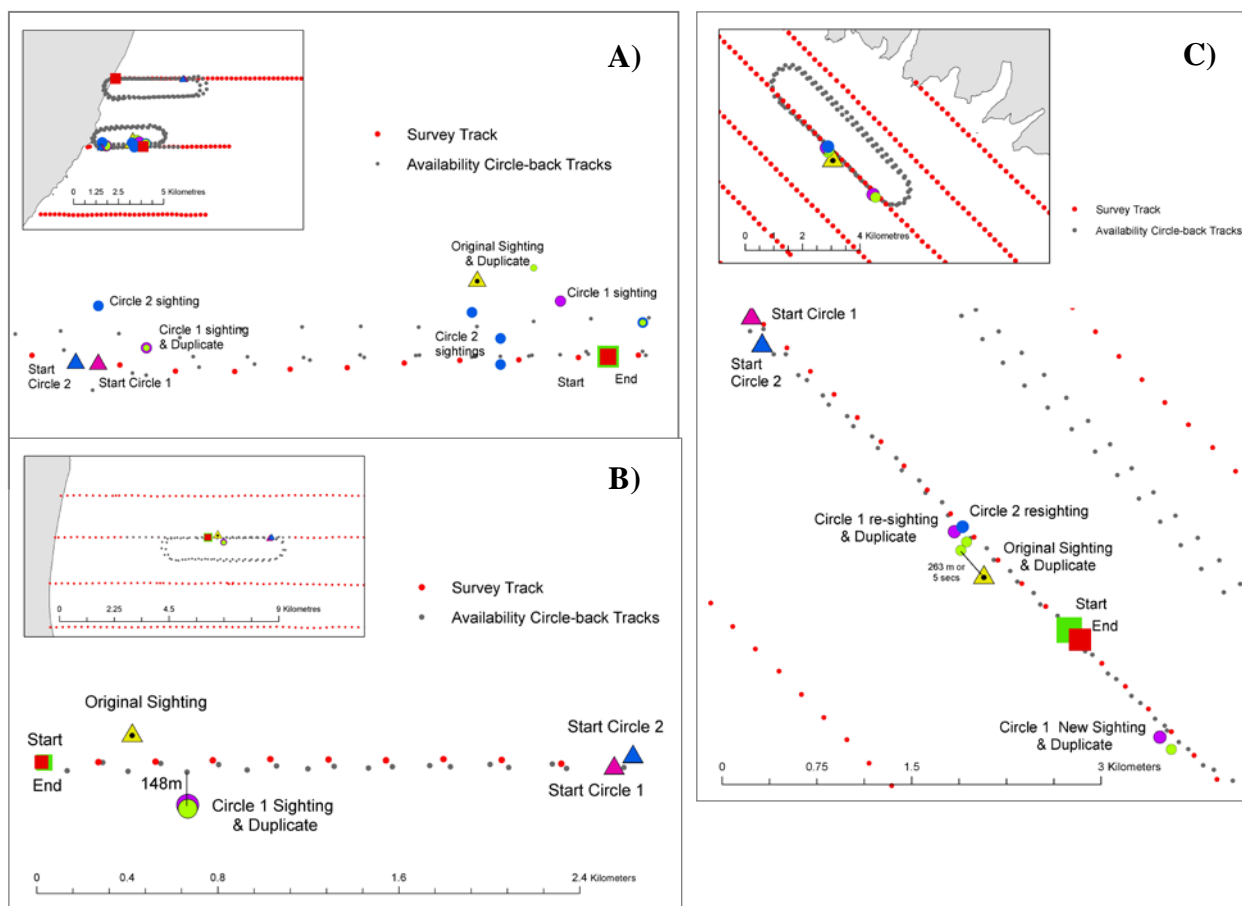


Figure 3: Examples of circle-back redetections in which A) the availability data were not used as the plane was too far off the original track and too many sightings hindered identification of any resightings; B) the original and additional sightings are distinguishable and C) as the original sighting was indicated as being late, duplicate and resightings were easier to identify. The location of the actual transect (red dots) and the circle-back track (grey dots) and all circle-back sightings and additional information (labelled) are displayed.

With this method, the idea is to re-survey the same portion of transect using exactly the same protocol (i.e. flying at 500 ft travelling 100 knts) in an attempt to re-detect the same group of dolphins with each new pass. It is assumed that the dolphin group remains within the transect strip being surveyed during each of the circle-backs. This assumption would be difficult to relax without information on fine-scale dolphin movement patterns. Dolphin groups may not be detected either because they have become unavailable (i.e. dived below the surface), or they have been available but missed by the observers. This aspect can be easily accounted for by using the information from the detection function collected from the on-effort sightings. For example, if P_a is the availability probability and $E(p_{\bullet}(s_i))$ is the expected probability of detecting a group of size s_i from at least one of the observer positions, then the probability of redetecting the group during a circle-back is $P_a E(p_{\bullet}(s_i))$ and the probability of not detecting the group would be $1 - P_a E(p_{\bullet}(s_i))$. Note that the inclusion of $E(p_{\bullet}(s_i))$ to account for perception bias in the estimation of availability does not amount to double-correcting for

perception bias when it is also included for abundance estimation. Estimates and standard errors for P_α can be obtained using maximum likelihood techniques. An important point is that the initial detection of the group that initiated the circle-backs is not used to estimate availability otherwise a biased estimate would result. This estimation procedure differs from that originally used by Hiby (1999).

The effect of region (corresponding to the same regions used in the helicopter-based surveys), offshore stratum (0–4 nmi versus further out) and water colour (blue, green, blue/green or turbid) on availability were investigated. Availability was modelled as:

$$\text{logit}(P_\alpha) = \delta_0 + \delta_1 \text{Region} + \delta_2 \text{Offshore} + \delta_3 \text{Colour} . \quad (7)$$

The factors *Region* and *Colour* have more than two levels and require multiple indicator variables to represent these effects; hence the regression coefficient is indicated as a vector quantity. Eight models were fit to the data by setting various combinations of δ_1 , δ_2 and δ_3 to zero, and ranked according to AIC. For the purpose of abundance estimation, the stratum-specific availability estimates (both regionally and offshore) were modelled averaged from the four models that excluded the water colour factor as there was insufficient evidence of it being an important factor. These model averaged estimates of availability were used in the estimation of abundance.

Note that the availability estimates may vary depending on which detection function is used to estimate $E(p_\bullet(s_i))$; hence the procedure outlined above was repeated for each detection function that was used to estimate abundance. That is, for each detection function that was ranked highly according to AIC, it was used to estimate both the number of dolphins in the area covered by the survey and the probability of them being available. These were then combined to estimate total abundance.

Note that similar truncation rules used for the detection function sighting data were applied to the circle-back data, whereby if the initial sighting was outside the truncation distances for the front or rear observer, the circle-back data for that group was not used. Therefore, for the analyses where only the sighting data between 0.071 and 0.300 km is used for both observers, availability is estimated from a subset of the full circle-back data set.

Abundance estimation

Estimation of abundance from line transect data requires that detection and availability biases be appropriately accounted for. Based upon Laake & Borchers (2004) and Buckland et al. (2010), dolphin abundance was estimated in the following manner.

The number of dolphins within the area of stratum k covered by the surveys is estimated using a Horvitz-Thomson type estimator, i.e.,

$$\hat{N}_{c\ k} = \sum_{i=1}^{n_k} \frac{s_i}{E(p_\bullet(s_i))} \quad (8)$$

where n_k is the number of groups detected in the stratum, s_i is the size of the i th group and $E(p_\bullet(s_i))$ is the expected probability of the i th group being detected given its size, which is obtained from the detection function analysis.

The number of *available* dolphins (i.e., near the surface with a non-zero chance of detection by the observers in the plane) within the stratum is therefore

$$\hat{N}_{ak} = \frac{A_k \hat{N}_{ck}}{a_k} \quad (9)$$

where, A_k is the total area of the stratum; $a_k = 2wL_k$ is the area covered by the survey transects with w being the truncated width (0.3 km) and L_k the total transect length flown. Accounting for availability, that total number of dolphins within a stratum is therefore:

$$\hat{N}_k = \frac{\hat{N}_{ak}}{\hat{P}_{ak}} \quad (10)$$

with total abundance being

$$\hat{N} = \sum_{k=1}^K \hat{N}_k \quad (11)$$

Details on the calculation of the standard errors are given in SM §A, but note that they are extensions of the methods used by Buckland et al. (2010). It should also be noted that given that some strata share parameters (either through the detection function or availability estimates), the standard errors from the stratum-specific abundance estimates should not be simply combined to obtain the standard error for total dolphin abundance.

As there may be model selection uncertainty associated with the detection function analysis, which would lead to different estimates of abundance (and availability using the circle-back data), AIC-based model averaging was used to combine the abundance estimates resulting from each detection function model (Burnham & Anderson, 2002; Anderson 2008; SM §C).

For both summer and winter surveys, four sets of abundance estimates are obtained: those resulting from the full and truncated distance data sets with either circle-back or dive-profile-based estimates of availability. The model averaging equations from SM §C were used to combine the four estimates into a single result, where each set of estimates were given equal weight.

Based upon an averaged estimate of abundance (\hat{N}) and its associated standard error (SE), the lower and upper limits of a Wald-lognormal 95% confidence interval were calculated as:

$$C = \exp \left(1.96 \sqrt{\ln \left(1 + \left(\frac{\hat{N}}{SE} \right)^2 \right)} \right)$$

$$Lower : \frac{\hat{N}}{C} \quad (12)$$

$$Upper : \hat{N}C$$

Note that an effective strip width (ESW) has not been used to estimate abundance as in previous studies for Hector's dolphin (e.g. Dawson et al. 2004, Slooten et al. 2004, 2006), but it can be determined from the results. ESW is really a conceptually convenient term to aid interpretation of the consequence of imperfect detection; its value is derived from the estimated detection function and transect width. Rather than describing the coverage of a survey of an area in terms of K lines with a half-width (i.e., one side of the aircraft) of w and

an average detection rate of \bar{p} , the effective coverage is of K lines with a half-width of ESW and perfect detection; that is, $ESW = w\bar{p}$. Comparison of ESW values between studies should therefore be made with caution as variation may be due to either w or \bar{p} . For interpretation, ESW values presented later have been calculated as:

$$ESW = w \frac{n_g}{\hat{N}_{cg}} \quad (13)$$

where n_g is the number of groups detected and \hat{N}_{cg} is the estimated number of groups in the covered region.

2.5 Distribution analyses

Simple plots of where Hector's dolphins were sighted, along with other marine mammal species (see SM §D), during the summer and winter surveys can be initially informative about their seasonal distributions. Assuming that detection and availability are approximately constant across regions and seasons, changes in sighting intensities would be indicative of distributional shifts. Where those assumptions are questionable, then a more quantitative approach is required.

Density surface modelling (DSM; Buckland et al. 2004) was used to examine Hector's dolphin distribution and potentially identify seasonal shifts, where distribution is defined as those areas with a non-negligible predicted density. DSM techniques combine the survey data with a spatial analysis to model how density at the time of surveying varies across a region according to spatial and habitat variables (e.g. bathymetry, distance from shore) while taking into account the probability of detecting the animals (Gomez de Segura et al. 2007). Further corrections can be made to account for dolphin availability.

It is important to note that a DSM produces a predicted density surface based upon line-transect data from a single survey. Spatial and habitat information is used to explain variability in where dolphins were sighted at the time of the survey, which results in the prediction surface. The estimated prediction surface may be sensitive to the exact location of the sightings with an alternative data set leading to a different prediction surface. Even though a DSM may use habitat variables, it is not a study of habitat preferences of the animals. The results cannot be used to make broad conclusions about the habitat preference of Hector's dolphins.

DSM protocols

Separate DSMs were developed to estimate the summer- and winter-time distribution of Hector's dolphins. For each season, the DSM was developed by using the top-ranked detection function model from the full distance sampling data set (Tables 4 and 10 for summer and winter, respectively). Easting, northing, depth and distance from shore were included as covariates for the DSM. The analyses were undertaken within the statistical software R using a combination of custom code and the package *dsm* (v.1.2).

Transect lines were divided into segments approximately 1 km long and 0.6 km wide, with the easting and northing coordinates for the centre point of the segment determined. Values

for easting, northing, depth and distance from shore were obtained from a prediction grid with 5×5 km cells. Dolphin abundance was estimated for each transect segment based upon the number of dolphins sighted in each segment, the estimated detection function and helicopter-based estimates of regional availability (Buckland et al. 2004). That is:

$$\hat{N}_i = \sum_{j=1}^{n_i} \frac{s_{ij}}{E(p_{\bullet}(s_{ij}))} \hat{P}_{ck}$$

where \hat{N}_i is the estimated abundance for segment i , n_i is the number of groups in the segment, s_{ij} is the size of the j th group in the segment, $E(p_{\bullet}(s_{ij}))$ is the expected probability of detecting a group of size s_{ij} , and \hat{P}_{ck} is the estimated availability probability for stratum k (which segment i is contained within).

A generalised additive model (GAM) was used to model the segment-specific abundance estimates based on the above covariates (with easting and northing entered as a bivariate spline term). The results of the GAM were used to predict dolphin density across the study region using the prediction grid that was defined at a scale of 5×5 km cells. No attempts were made to simplify the GAM by removing covariates that appeared to have little effect on the prediction surface.

Standard errors were obtained using a parametric bootstrap to accommodate uncertainty in both the detection function and DSM. It was implemented in the following steps:

1. Fit the detection function and DSM to the observed data to estimate the number of individual dolphins.
2. Refit DSM to estimate the density of available dolphin groups (as sightings are made of groups not individually).
3. Generate locations of available (e.g., near surface) groups using a random Poisson point process where the process intensity is obtained from the adjusted group-level DSM fitted in step 2.
4. Determine perpendicular distance of the group from nearest transect line. Retain groups that are within the area covered by the survey (i.e., within 0.3 km). Other groups are not retained as they have no chance of being sighted.
5. Randomly generate group size using a group-size frequency table. This table is based on the observed group frequency, with correction for detection probability being different for different group sizes. That is, $\hat{f}_s = \frac{n_s / E[p_{\bullet}(s)]}{\hat{N}_{gc}}$, where \hat{f}_s is the estimated frequency of group size s , n_s is the number of observed groups of size s , $E(p_{\bullet}(s))$ is the expected probability of detecting a group of size s within the covered area and \hat{N}_{gc} is the estimated number of groups within the covered area.
6. Using the detection function estimated in step 1, determine the probability of detection for each group given its distance from the line and size, from each observer position.
7. Generate a Bernoulli random variable (i.e., 0 or 1) to indicate whether each group was sighted from each observer position.
8. Using the groups sighted at least once, refit the detection function model used in step 1 to obtain detection estimates pertinent to the generated (i.e., bootstrapped) data set.

9. For each region, generate a new availability estimate by drawing a random value from a logit-normal distribution with mean and standard deviation equal to the logit-transformed regional availability estimate and associated standard error.
10. Using the detection function model fit in step 8, and availability estimates obtained in step 9, refit the DSM used in step 1 to obtain a predicted density surface (of individuals) for the bootstrap data set.
11. Repeat steps 3–10 a sufficiently large number of times. The standard deviation of summaries calculated from the bootstrapped DSMs can be used to approximate the standard errors of the corresponding quantities from the DSM for the real data.

MacKenzie et al. (2012) noted from simulation studies that resulting maps from a DSM analysis were sensitive to the exact location of detections when using a 5×5 km prediction grid and recommended that for the purpose of robust inferences about distribution, coarser spatial scales (e.g., cells of hundreds of square kilometres) should be used. While the results of the DSM are presented at the prediction grid scale, extreme caution is advised in terms of using the DSM to make such fine scale inferences because the maps will be sensitive to where dolphins were observed at the time of the survey. Changes in where dolphins were sighted, either due to dolphin movement or random chance, may lead to quite different maps. Hence, the DSM results may not accurately represent distribution information over a longer timeframe. It is recommended that the results from the prediction grid that have been aggregated to the courser scale of the strata be used for distribution and abundance inferences. A grid cell was defined to be associated with a defined stratum if its centroid was within the stratum boundaries, therefore given the resolution of the prediction grid, stratum areas are slightly different compared to those used previously.

Maps of the DSM results are expressed as relative densities. That is, the estimated density for a grid cell or stratum relative to the overall density;

$$\frac{\hat{N}_k/A_k}{\hat{N}/A},$$

as a means to identify areas of relative higher or lower density that are robust to the magnitude of absolute abundance estimates. Values over 1 indicate areas with densities that are greater than the overall average. Note that the relative density can also be interpreted as the fraction of the total population in cell or stratum k , relative to the proportion of the total area contained within that cell or stratum, i.e.,

$$\frac{\hat{N}_k/\hat{N}}{A_k/A}.$$

3 RESULTS

3.1 Abundance estimates

Line transect data

A summary of the summer and winter sighting data is given in Table 4. These sample sizes far exceed the recommended minimum of 60–80 sightings for estimating abundance (Buckland et al. 2001). From the summer survey, for the front observer position, 14 sightings were left truncated (had distances less than 0.071 km) and 12 sightings were right truncated (distance more than 0.300 km). For the rear observer position, two sightings had a recorded angle greater than 90 degrees that were set equal to 90 degrees (0 km) and four sightings were right truncated. An additional 83 sightings made from the rear observer position were left truncated for the data analysis where both observers had the same viewing area.

From the winter survey, for the front observer position, 18 sightings were left truncated (had distances less than 0.071 km) and five sightings were right truncated (distance more than 0.300 km). Two sightings were right truncated for the rear observer position. 109 sightings made from the rear observer position were left truncated for the data analysis where both observers had the same viewing area.

Table 4: Summary of the sighting data from the summer and winter aerial surveys. ‘Verified’ indicates the numbers post-verification; ‘Full’ indicates the numbers used in the full analysis where sightings were left truncated at 0.071 km for the front observer position, and right truncated at 0.300 km for both observer positions; and ‘Truncated’ indicates the numbers used in the subset analysis where sightings were left truncated at 0.071 km and right truncated at 0.300 km for both observer positions. Note that the number of groups sighted from both positions are also included in the front and rear totals.

	Summer			Winter		
	Verified	Full	Truncated	Verified	Full	Truncated
Total Sightings	369	354	271	333	328	219
Total Front	246	220	220	192	169	169
Total Rear	295	291	208	262	262	153
Both (duplicates)	172	157	157	121	103	103
Individuals	849	815	635	543	537	365
Average Group Size	2.3	2.3	2.3	1.6	1.6	1.7
SD Group Size	1.6	1.6	1.6	1.0	1.0	1.0
Range Group Size	1–10	1–10	1–10	1–8	1–8	1–6
Transect Length (km)	7155.8	7155.8	7155.8	7276.2	7276.2	7276.2

Figure 4 is the histogram of the verified distance data from the summer, prior to any truncation, and Figures 5–6 are the histograms of the distance data after truncation. Figure 7 is the histogram of the verified distance data from winter prior to any truncation, and Figures 8–9 are the histograms of the distance data after truncation. Note that for the data set where all data was left truncated, distances have been rescaled such that the original distance of 0.071 km now equals 0 km.

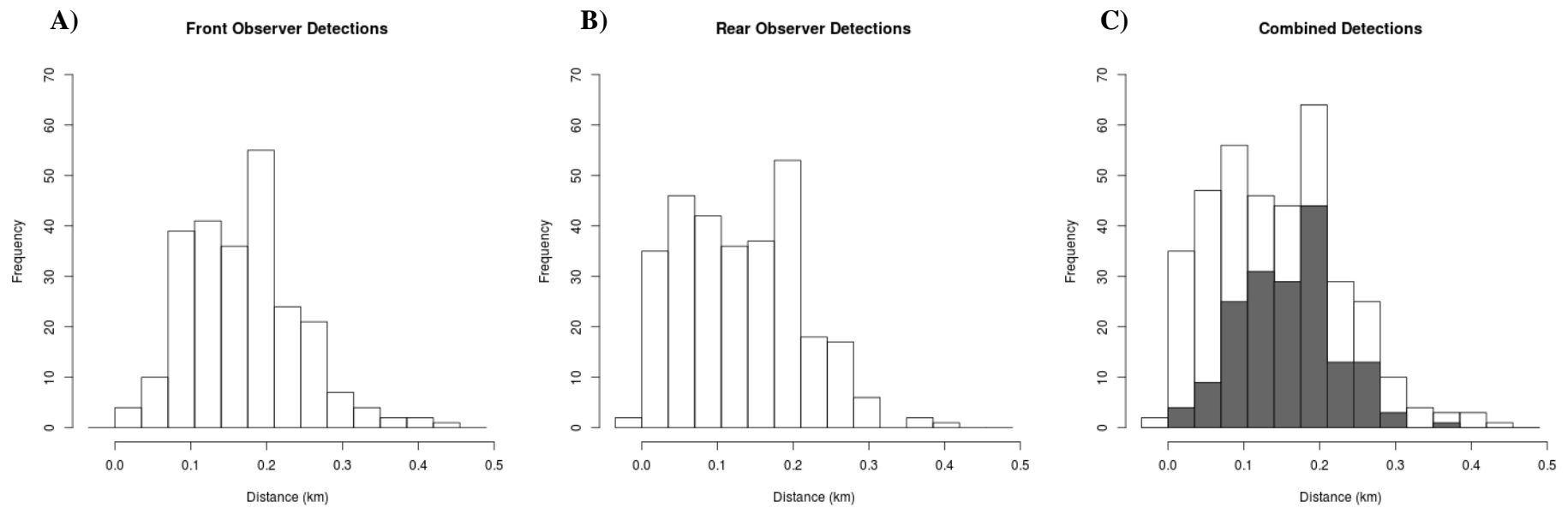


Figure 4: Histogram of the verified distance data prior to any truncation of sightings from A) the front observer position, B) the rear observer position, and C) from either observer position in the summer survey. Grey bars indicate sightings made by both observers (duplicates).

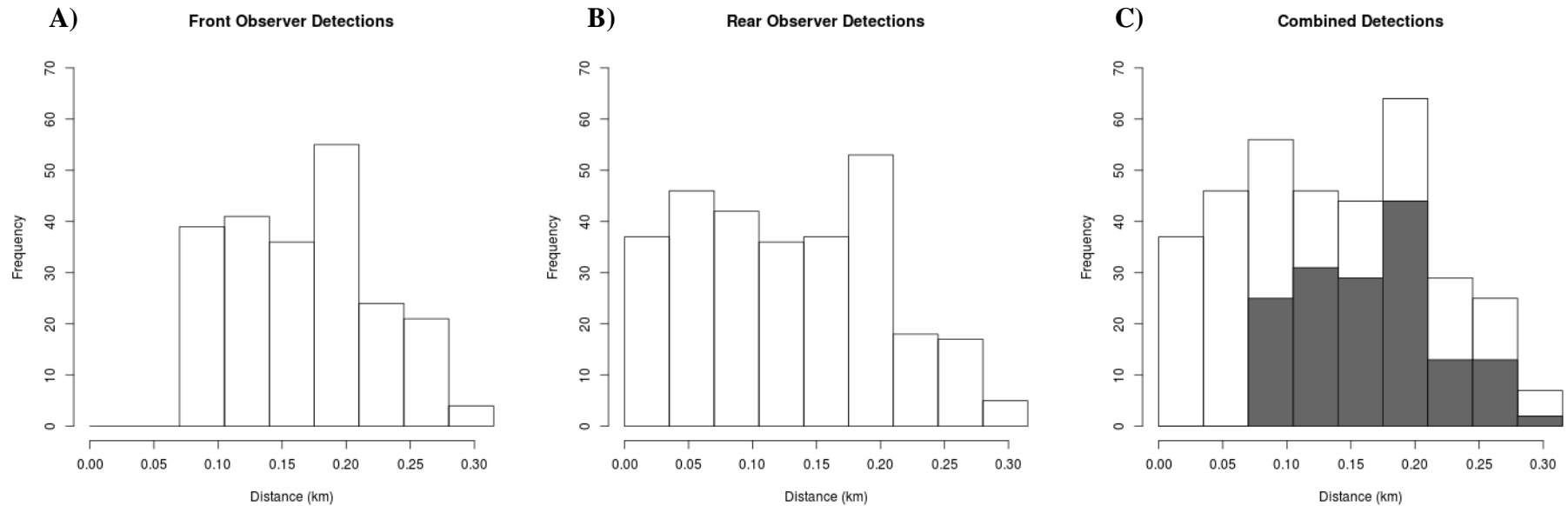


Figure 5: Histogram of the full distance data for sightings in the summer survey from A) the front observer position following left truncation at 0.071 km and right truncation at 0.300 km, B) from the rear observer position following setting two sightings with angles over 90 degrees to 90 degrees and right truncation at 0.300 km, and C) either observer position following left truncation at 0.071 km for the front position, setting two sightings with angles over 90 degrees to 90 degrees for the rear position, and right truncation at 0.300 km for both positions. Grey bars indicate the number of sightings made by both observers (duplicates).

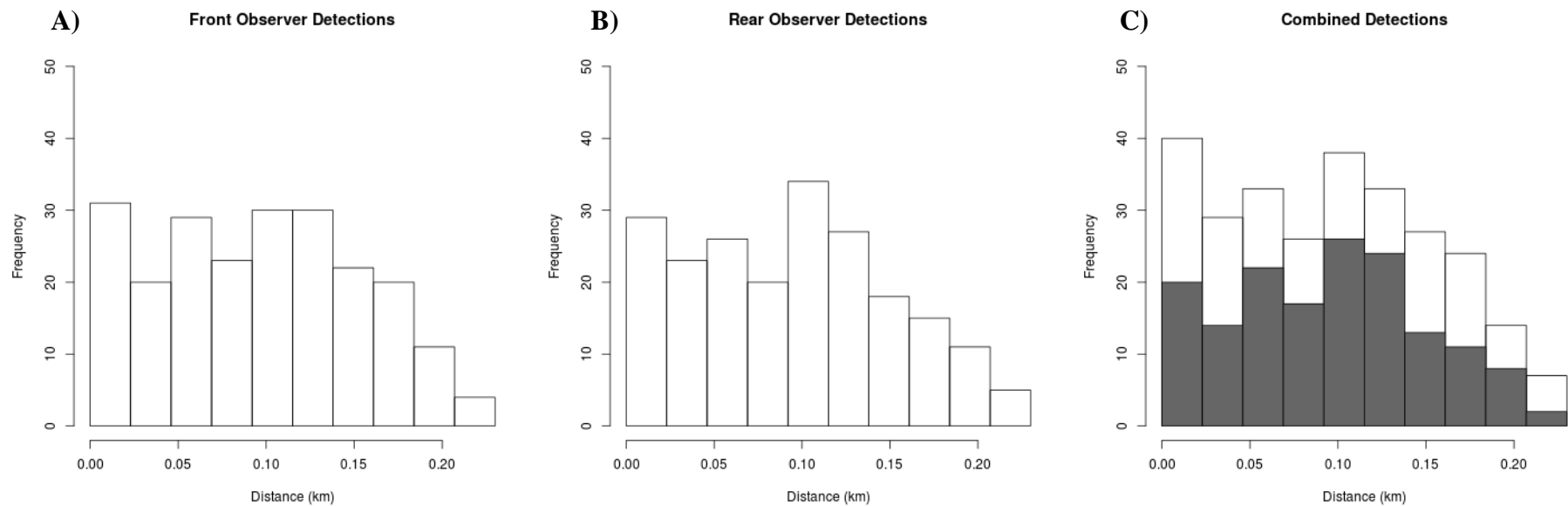


Figure 6: Histogram of the truncated distance data for sightings in the summer survey from A) the front observer position following left truncation at 0.071 km, right truncation at 0.300 km, B) the rear observer position following left truncation at 0.071 km and right truncation at 0.300 km, and C) either observer position following left truncation at 0.071 km and right truncation at 0.300 km for both positions. Distances have been rescaled such that the original distance of 0.071 km becomes 0 km. Grey bars indicate the number of sightings made by both observers (duplicates).

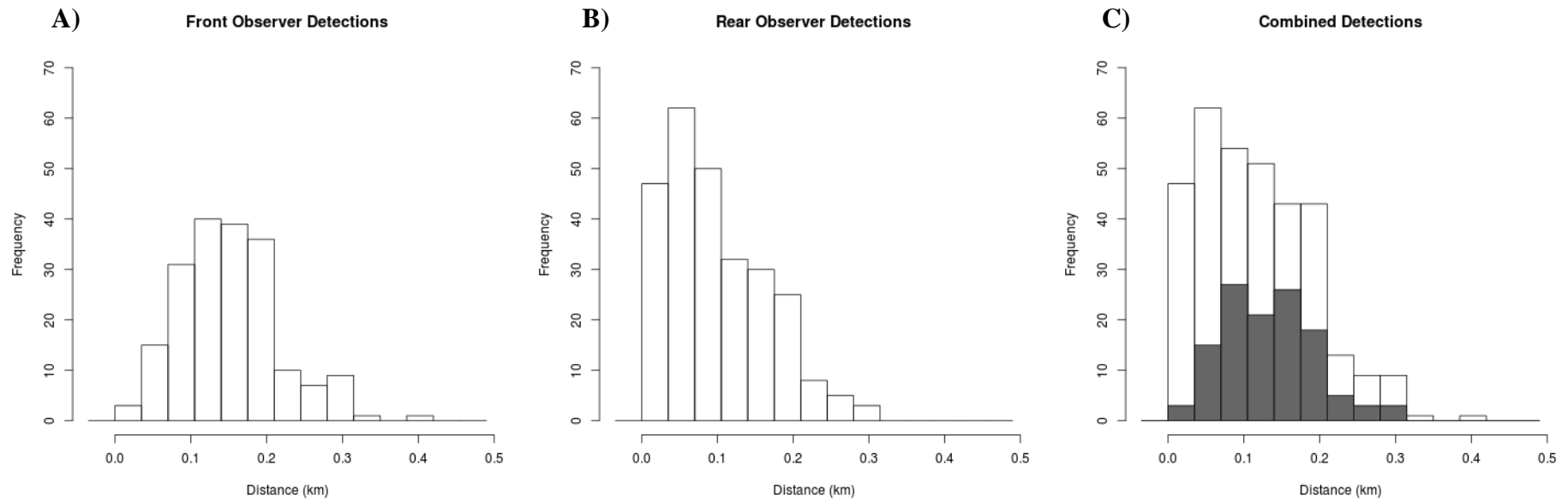


Figure 7: Histogram of the verified distance data prior to any truncation of sightings from A) the front observer position, B) the rear observer position, and C) from either observer position in the winter survey. Grey bars indicate sightings made by both observers (duplicates).

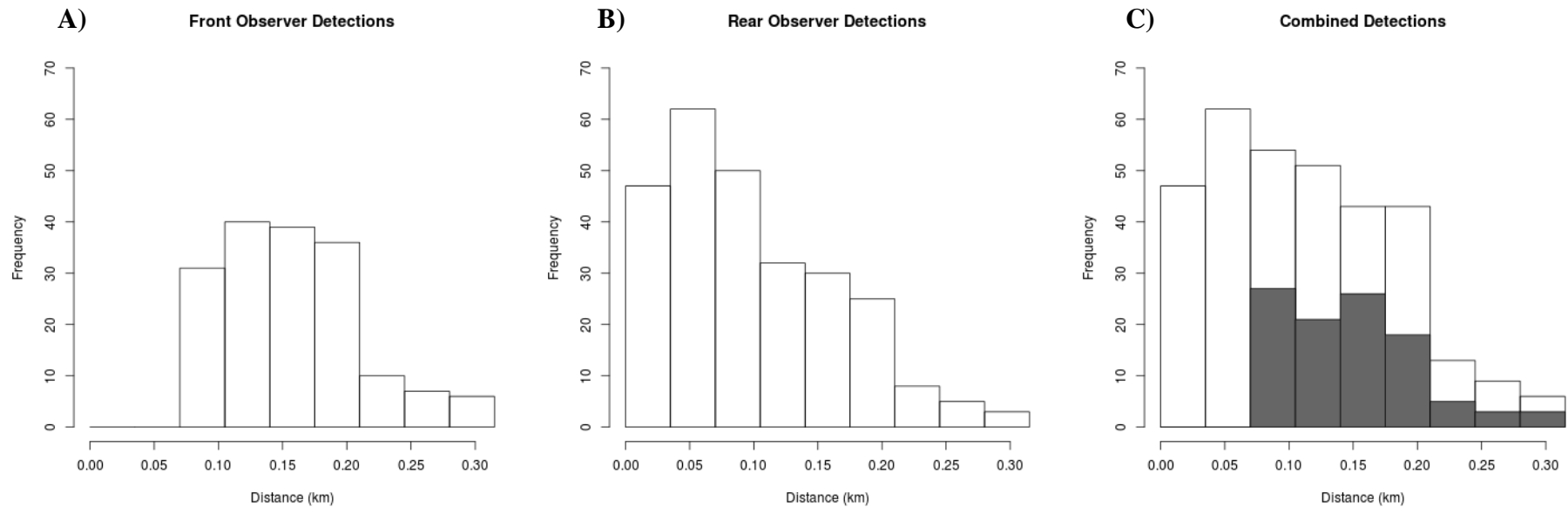


Figure 8: Histogram of the full distance data for sightings in the winter survey from A) the front observer position following left truncation at 0.071 km and right truncation at 0.300 km, B) from the rear observer position following setting two sightings with angles over 90 degrees to 90 degrees and right truncation at 0.300 km, and C) either observer position following left truncation at 0.071 km for the front position, setting two sightings with angles over 90 degrees to 90 degrees for the rear position, and right truncation at 0.300 km for both positions. Grey bars indicate the number of sightings made by both observers (duplicates).

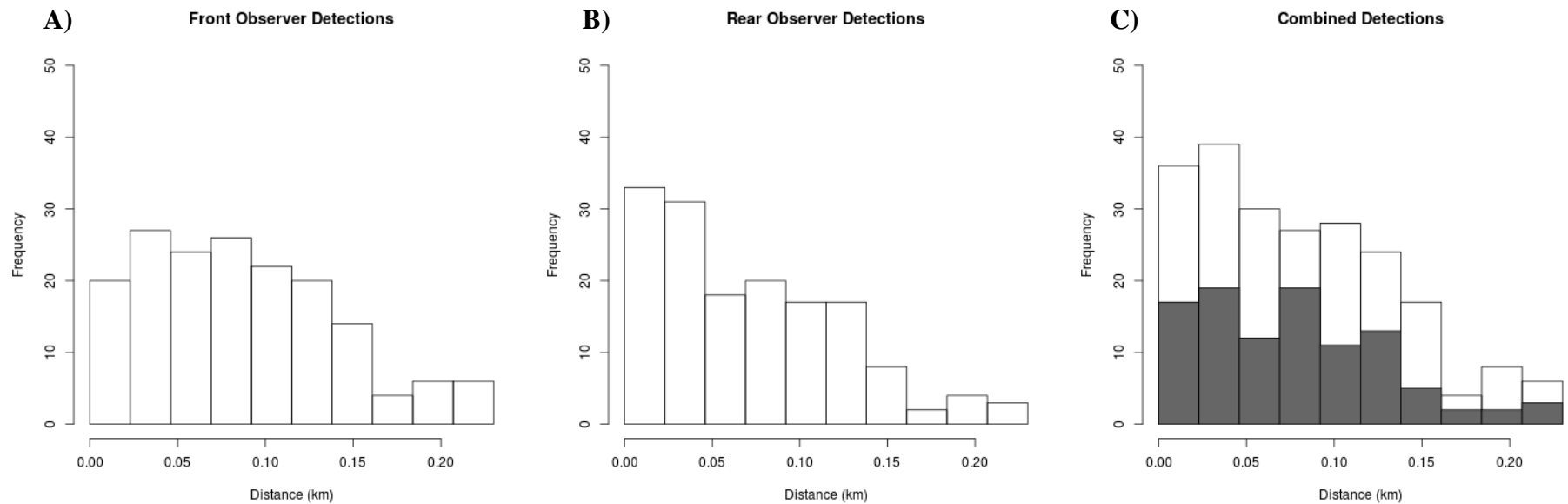


Figure 9: Histogram of the truncated distance data for sightings in the winter survey from A) the front observer position following left truncation at 0.071 km, right truncation at 0.300 km, B) the rear observer position following left truncation at 0.071 km and right truncation at 0.300 km, and C) either observer position following left truncation at 0.071 km and right truncation at 0.300 km for both positions. Distances have been rescaled such that the original distance of 0.071 km becomes 0 km. Grey bars indicate the number of sightings made by both observers (duplicates).

A breakdown of the number of sightings and number of dolphins sighted within each stratum during the summer and winter surveys is given in SM §E. Note that these tables include the calculation of a naïve estimate (that does not account for detection or availability) of the number of dolphins in each strata and in total. These calculations are simply the number of dolphins detected in the strata, divided by the area surveyed, multiplied by the total stratum area, i.e.,

$$\tilde{N}_k = A_k \frac{\sum_{i=1}^{n_k} s_i}{a_k} \quad \text{and} \quad \tilde{N} = \sum_{k=1}^K \tilde{N}_k .$$

These naïve estimates of overall summer abundance are 3641 and 3747 from the full and reduced data set, respectively, and 3029 and 2725 from the corresponding winter surveys. This clearly indicates that from this study, the number of Hector's dolphin along the ECSI is likely to be much larger than anticipated based upon previous studies (Dawson & Slooten, 1988; Dawson et al. 2004), especially after accounting for detection and availability.

Detection function analysis

Summer

The top 10 models (as ranked by AIC) for the full data set are given in Table 5. Most of the AIC weight is associated with the top two models, but lower ranked models also have non-negligible weight; therefore the top six models were used to produce model averaged estimates of abundance after adjusting their AIC model weights such that they sum to 1. The correlation between the intercepts of the detection and dependence functions are well away from -1, giving no indication of potential overestimation (see SM §B). All of the top six models have different intercept terms for each observer position, and group size as a covariate for detection. The top four models suggest that the shape of relationship between distance and detection is different for each observer position, while the top two models use a quadratic relationship between distance and detection and the next four models use a spline relationship. Three of the top six models use limiting independence and the remaining three use point independence.

Plots of the fitted detection functions and empirical histograms of detection rates do not indicate any systematic concerns about lack of fit for any of the top six models, particularly for $p_{\bullet}(d_i, s_i)$, which is the most relevant in terms of estimating abundance. The fitted detection functions for the top ranked model are presented in Figure 10 for illustration, and the plots for all six models are given in SM §F. Note that there is no theoretical argument that requires the highest detection rate to be at the point closest to the transect line, although typically one would expect it to be close to the transect line. Provided a flexible family of relationships between distance and detection are being considered, valid abundance estimates would still be obtained even if the highest detection rate was at the furthest limit of the survey strip.

Table 5: Top 10 AIC-ranked models for the detection function analysis for sightings between 0–0.3 km from the transect line in the summer. Model components identify the structure of the detection function model; $f(d)$ is the functional relationship with distance on the logit scale (L=linear, Q=quadratic, S=Spline), Obs indicates whether the intercept term is different for each observer position (Y=Yes, N=No), $\beta_1 \neq \beta_2$ indicates whether the regression coefficients for the effect of distance on detection is different for each observer position (Y= Yes, N= No), Size indicates whether group size has an effect on detection (Y=Yes, N=No) and Dep. indicates the form of dependence in detection between observer positions (FI=Full Independence, C = Constant Dependence, P = Point Independence and L= Limiting Independence). ΔAIC is the relative difference in AIC values, wgt is the AIC model weight, wgt* is the adjusted AIC weight for the models used for inference, $-2l$ is twice the negative log-likelihood, pars. is the number parameters in the model, \hat{N}_{cg} is the estimated number of dolphin groups in the covered area, ESW is the effective strip width and corr is the correlation between the intercepts of the detection and dependence functions (only relevant for constant dependence and limiting independence models).

Model Components					Model Fitting Summaries							
$f(d)$	Obs	$\beta_1 \neq \beta_2$	Size	Dep.	ΔAIC	wgt	wgt*	$-2l$	pars	\hat{N}_{cg}	ESW	corr
Q	Y	Y	Y	L	0.00	0.47	0.50	469.17	9	464	0.229	0.18
Q	Y	Y	Y	P	1.23	0.25	0.27	472.41	8	568	0.187	-
S	Y	Y	Y	L	3.67	0.07	0.08	468.85	11	456	0.233	0.07
S	Y	Y	Y	P	4.14	0.06	0.06	471.32	10	553	0.192	-
S	Y	N	Y	P	4.21	0.06	0.06	477.38	7	528	0.201	-
S	Y	N	Y	L	6.19	0.02	0.02	477.36	8	520	0.204	0.13
Q	Y	Y	N	L	7.68	0.01		478.85	8	466		0.20
Q	Y	N	Y	P	7.99	0.01		483.17	6	570		-
Q	Y	Y	N	P	8.62	0.01		481.79	7	550		-
S	N	N	Y	L	8.85	0.01		482.03	7	438		0.13

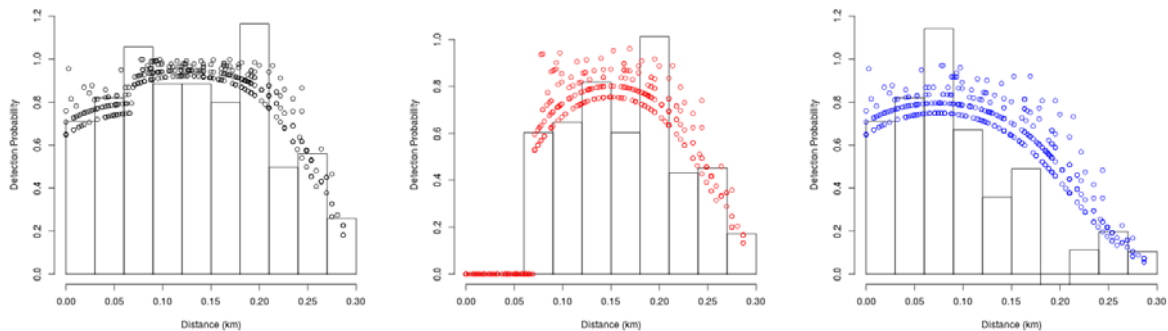


Figure 10: Fitted detection functions and histograms of empirical detection probabilities from the top ranked model in Table 5. Left is $p_*(d_i, s_i)$, centre is $p_F(d_i, s_i)$, and right is $p_{R/NF}(d_i, s_i)$.

The q-q plots (Figure 11A and SM §F) and goodness of fit tests (Table 6) do not indicate any evidence of lack of fit for the top six models. For a comparison, and to demonstrate that these methods have some power to detect lack of fit, the results are also presented for the simple model which assumes a linear relationship between detection distance that is different for each observer position, and detections are fully independent. This model was ranked last with a ΔAIC 43.84 and clearly shows a systematic lack of fit (Figure 11B).

Table 6: Goodness of fit tests for top six ranked models and the lowest ranked model for the detection function analysis of the full summer data set. Given are the Cramer-von Mises (CvM) and Kolmogorov-Smirnov (KS) tests with associated p-values.

Model Rank	CvM	p-value	KS	p-value
1	0.051	0.87	0.033	0.83
2	0.083	0.67	0.045	0.48
3	0.048	0.89	0.033	0.83
4	0.084	0.67	0.042	0.56
5	0.106	0.56	0.043	0.52
6	0.107	0.55	0.044	0.51
72	1.375	0.00	0.123	0.00

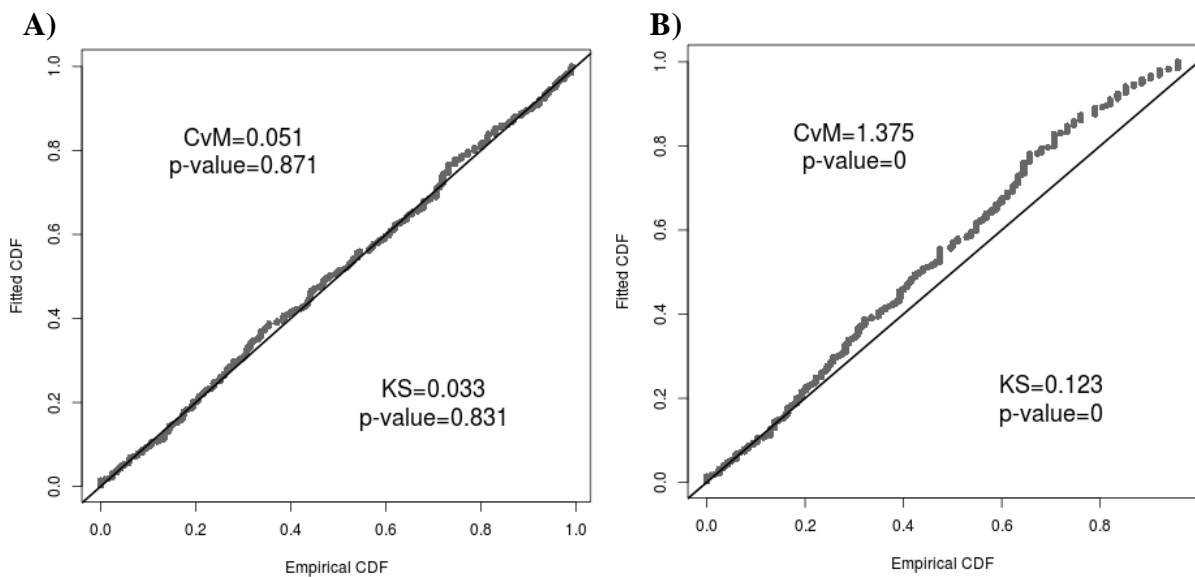


Figure 11: Q-Q plot of the fitted and empirical cumulative density functions (CDF) for the A) top ranked model and B) lowest ranked model of the detection function analysis of the full summer data.

Using the detection data from the portion of the transect that can be viewed from both observer positions (0.071–0.300 km) results in greater model selection uncertainty (Table 7). However, there are a number of common features in the top-ranked models. Firstly, the relationship with distance appears to be non-linear on the logit scale with the top models having either a quadratic (primarily) or spline. Observer position and group size are also important factors. The top-ranked models all contain terms indicating some form of dependence in detection of dolphin groups from each observer position, with models that assume point independence being slightly preferred over models with limiting independence. Note that the fourth-ranked model assumes constant dependence and provides an unrealistic estimate of abundance in the covered area. The simulation results (SM §B) indicate that the constant dependence model is prone to such results when the sighting data for both observers has been truncated to the same distances, and the correlation between the intercepts of the detection and dependence functions was -1.0. Therefore, the fourth-ranked model has not been used for final inferences, and model averaging has been performed based upon the models ranked 1–3 and 5–8. The correlation value between the intercepts of the detection and

dependence functions for the fifth ranked model is getting near the zone when one might be concerned about potential overestimation (SM §B), while the correlation value for the ninth ranked model is close to -1.0 indicating likely overestimation hence it was excluded from the model averaging.

Table 7: Top 10 AIC-ranked models for the detection function analysis for sightings between 0.071–0.300 km from the transect line in the summer. Model components identify the structure of the detection function model; $f(d)$ is the functional relationship with distance on the logit scale (L=linear, Q=quadratic, S=Spline), Obs indicates whether the intercept term is different for each observer position (Y=Yes, N=No), $\beta_1 \neq \beta_2$ indicates whether the regression coefficients for the effect of distance on detection is different for each observer position (Y= Yes, N= No), Size indicates whether group size has an effect on detection (Y=Yes, N=No) and Dep. indicates the form of dependence in detection between observer positions (FI=Full Independence, C = Constant Dependence, P = Point Independence and L= Limiting Independence). ΔAIC is the relative difference in AIC values, wgt is the AIC model weight, wgt* is the adjusted AIC weight for the models used for inference, $-2l$ is twice the negative log-likelihood, pars. is the number parameters in the model, \hat{N}_{cg} is the estimated number of dolphin groups in the covered area, ESW is the effective strip width and corr is the correlation between the intercepts of the detection and dependence functions (only relevant for constant dependence and limiting independence models).

Model Components					Model Fitting Summaries							
$f(d)$	Obs	$\beta_1 \neq \beta_2$	Size	Dep.	ΔAIC	wgt	wgt*	$-2l$	pars	\hat{N}_{cg}	ESW	corr
Q	Y	Y	Y	P	0.00	0.30	0.39	469.50	8	382	0.162	-
Q	Y	Y	Y	L	1.76	0.12	0.16	469.26	9	357	0.174	-0.66
Q	Y	N	Y	P	2.07	0.11	0.14	475.57	6	366	0.169	-
S	Y	N	Y	C	2.46	0.09		473.97	7	1515113		-1.00
Q	Y	N	Y	L	2.74	0.08	0.10	474.25	7	428	0.145	-0.83
S	Y	Y	Y	P	2.98	0.07	0.09	468.49	10	383	0.162	-
S	Y	N	Y	P	3.72	0.05	0.06	475.22	7	368	0.168	-
S	Y	Y	Y	L	4.08	0.04	0.05	467.58	11	344	0.180	-0.46
Q	Y	N	Y	C	4.20	0.04		477.71	6	593	0.162	-0.98
S	Y	N	Y	L	4.46	0.03		473.96	8	437	0.174	-0.87

Plots of the fitted detection functions and empirical histograms of detection rates for the seven models used for model averaging do not indicate any systematic concerns about lack of fit for either model, particularly for $p_{\bullet}(d_i, s_i)$, which is most relevant for abundance estimation. Figure 12 presents the fitted detection functions for the top-ranked model with SM §G including the plots for all eight models. The q-q plots (Figure 13 and SM §G) and goodness of fit tests (Table 8) do not indicate any evidence of lack of fit for the seven models either.

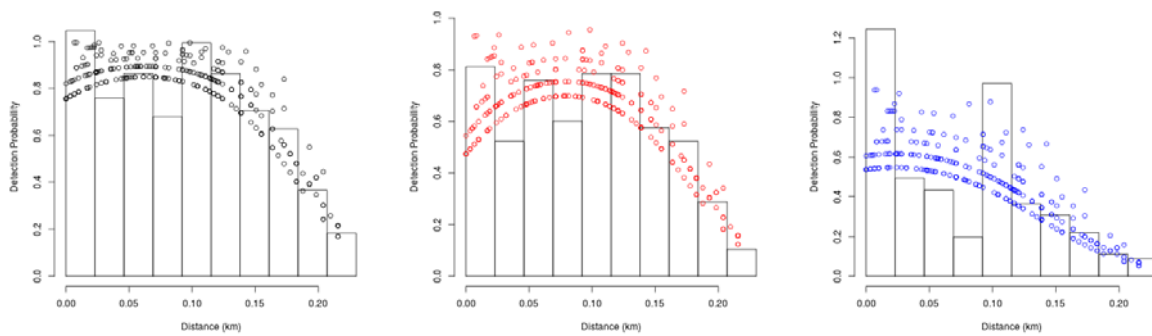


Figure 12: Fitted detection functions and histograms of empirical detection probabilities from the top ranked model in Table 7. Left is $p_{\bullet}(d_i, s_i)$, centre is $p_F(d_i, s_i)$, and right is $p_{R/NF}(d_i, s_i)$. Note that distance from the transect line has been rescaled such that an original distance of 0.071 km is now 0 km.

Table 8: Goodness of fit tests for top six ranked models and the lowest ranked model for the detection function analysis of the full summer data set. Given are the Cramer-von Mises (CvM) and Kolmogorov-Smirnov (KS) tests with associated p-values.

Model Rank	CvM	p-value	KS	p-value
1	0.102	0.58	0.049	0.52
2	0.098	0.59	0.046	0.62
3	0.150	0.39	0.053	0.43
5	0.118	0.50	0.054	0.41
6	0.104	0.57	0.051	0.48
7	0.135	0.44	0.053	0.43

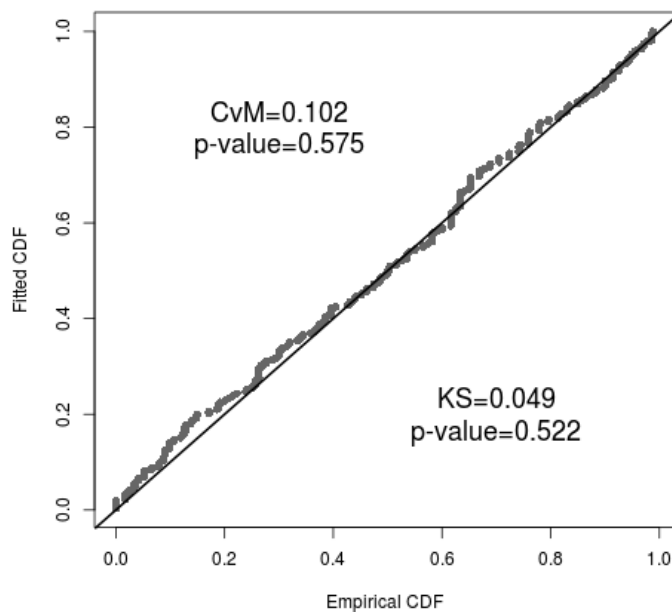


Figure 13: Q-Q plot of the fitted and empirical cumulative density functions (CDF) for the top ranked model of the detection function analysis of the reduced summer data. Q-Q plots for all seven models used for model averaging are given in SM §G.

Exploratory analyses.

An additional exploratory analysis was conducted for other covariates that may affect detection including: Beaufort sea state (as a continuous measure), glare, water depth (m), water colour (blue, green, blue/green and turbid) and distance from the shore (km). These covariates were added individually to the top- and second-ranked detection function models using the full summer data set (Table 5; Base model). A model was also considered where sea state, glare and water colour were all added to the base model together (Tables 9 and 10). While the additional covariates appear to have some explanatory power for explaining variation in detection; importantly, their inclusion does not substantially alter the estimated abundance in the covered region. This is consistent with the findings of the simulation study in which abundance estimates were robust to the effects of unmodelled random variation in detection (SM §B). Given that the primary aim of these analyses is to estimate abundance, these additional covariates are not considered further in the interests of avoiding further complications to the analyses.

Table 9: Exploratory analysis on the full summer data investigating the effect of other covariates on detection. Covariates were added to the top-ranked model from Table 5 (Base). Additional covariates considered are Beaufort sea state (as a continuous measure), glare, water depth (m), water colour (blue, green, blue/green and turbid) and distance from the shore (km). Parameters given are the relative difference in AIC (ΔAIC), twice the negative log-likelihood ($-2l$), number of parameters (K), estimated abundance in the area covered by the survey (\hat{N}_c) and its associated standard error (SE).

Model	ΔAIC	$-2l$	K	\hat{N}_c	SE
+ Sea State + Glare + Water Colour	0.00	454.34	14	1027	84
+ Glare	1.77	464.11	10	1013	81
+ Depth	2.66	465.00	10	1051	105
+ Water Colour	4.21	462.54	12	1047	89
+ Sea State	4.64	466.98	10	1004	76
Base	4.84	469.17	9	1021	83
+ Distance to Shore	5.78	468.12	10	1006	75

Table 10: Exploratory analysis on the full summer data investigating the effect of other covariates on detection. Covariates were added to the second-ranked model from Table 5 (Base). Additional covariates considered are Beaufort sea state (as a continuous measure), glare, water depth (m), water colour (blue, green, blue/green and turbid) and distance from the shore (km). Parameters given are the relative difference in AIC (ΔAIC), twice the negative log-likelihood ($-2l$), number of parameters (K), estimated abundance in the area covered by the survey (\hat{N}_c) and its associated standard error (SE).

Model	ΔAIC	$-2l$	K	\hat{N}_c	SE
+ Sea State + Glare + Water Colour	0.00	458.88	13	1238	112
+ Depth	0.28	467.16	9	1253	147
+ Glare	0.93	467.81	9	1213	123
+ Water Colour	2.91	465.79	11	1221	120
Base	3.53	472.41	8	1202	116
+ Sea State	4.05	470.93	9	1201	131
+ Distance to Shore	5.23	472.11	9	1193	113

Winter

The top 10 models (as ranked by AIC) for the full data set are given in Table 11. Most of the AIC weight is associated with the top model, but lower ranked models also have non-negligible weight; therefore the top four models were used to produce model averaged estimates of abundance after adjusting their AIC model weights such that they sum to 1. The correlation between the intercepts of the detection and dependence functions are well away from -1, giving no indication of potential overestimation (SM §B) All of the top four models have different intercept terms for each observer position, the shape of relationship between distance and detection is different for each observer position, and group size as a covariate for detection. The top two models use a spline relationship between distance and detection and the next two models (with much less overall model weight) involve a quadratic relationship. The modelling of limiting independence or point independence alternates for the top four models, although the top model includes limiting independence.

Plots of the fitted detection functions and empirical histograms of detection rates do not indicate any systematic concerns about lack of fit for any of the top four models, particularly for $p_{\bullet}(d_i, s_i)$, which is the most relevant in terms of estimating abundance. The fitted detection functions for the top ranked model is presented in Figure 14 for illustration, and the plots for all four models are given in SM §H. The q-q plots (Figure 15 and SM §H) and goodness of fit tests (Table 12) do not indicate any evidence of lack of fit for the top four models.

Table 11: Top 10 AIC-ranked models for the detection function analysis for sightings between 0–0.3 km from the transect line in the winter. Model components identify the structure of the detection function model; $f(d)$ is the functional relationship with distance on the logit scale (L=linear, Q=quadratic, S=Spline), Obs indicates whether the intercept term is different for each observer position (Y=Yes, N=No), $\beta_1 \neq \beta_2$ indicates whether the regression coefficients for the effect of distance on detection is different for each observer position (Y= Yes, N= No), Size indicates whether group size has an effect on detection (Y=Yes, N=No) and Dep. indicates the form of dependence in detection between observer positions (FI=Full Independence, C = Constant Dependence, P = Point Independence and L= Limiting Independence). ΔAIC is the relative difference in AIC values, wgt is the AIC model weight, wgt* is the adjusted AIC weight for the models used for inference, $-2l$ is twice the negative log-likelihood, pars. is the number parameters in the model, \hat{N}_{cg} is the estimated number of dolphin groups in the covered area, ESW is the effective strip width and corr is the correlation between the intercepts of the detection and dependence functions (only relevant for constant dependence and limiting independence models).

Model Components					Model Fitting Summaries							
$f(d)$	Obs	$\beta_1 \neq \beta_2$	Size	Dep.	ΔAIC	wgt	wgt*	$-2l$	pars	\hat{N}_{cg}	ESW	corr
S	Y	Y	Y	L	0.00	0.76	0.77	337.94	11	473	0.208	0.36
S	Y	Y	Y	P	4.12	0.10	0.10	344.06	10	517	0.190	-
Q	Y	Y	Y	L	4.19	0.09	0.09	346.14	9	486	0.202	0.04
Q	Y	Y	Y	P	5.87	0.04	0.04	349.82	8	563	0.175	-
L	Y	Y	Y	P	12.44	0.00		360.38	6	650		-
S	Y	Y	N	L	12.63	0.00		352.58	10	483		0.34
L	Y	Y	Y	L	12.75	0.00		358.70	7	542		-0.50
S	Y	Y	Y	C	13.83	0.00		353.77	10	513		-0.32
Q	Y	Y	Y	C	15.56	0.00		359.50	8	634		*
S	Y	Y	N	P	16.36	0.00		358.30	9	634		-

* estimation procedure failed to obtain valid correlation

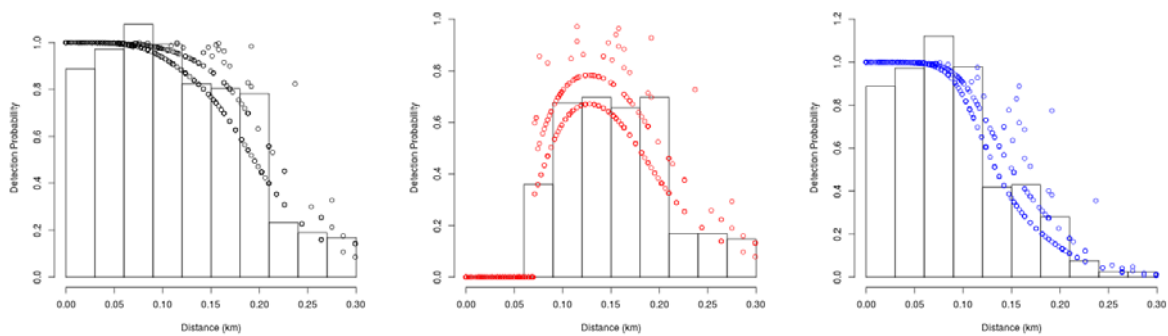


Figure 14: Fitted detection functions and histograms of empirical detection probabilities from the top ranked model in Table 11. Left is $p_{\bullet}(d_i, s_i)$, centre is $p_F(d_i, s_i)$, and right is $p_{R|NF}(d_i, s_i)$.

Table 12: Goodness of fit tests for top four ranked models for the detection function analysis of the full winter data set. Given are the Cramer-von Mises (CvM) and Kolmogorov-Smirnov (KS) tests with associated p-values.

Model Rank	CvM	p-value	KS	p-value
1	0.057	0.83	0.036	0.78
2	0.196	0.28	0.053	0.31
3	0.083	0.68	0.037	0.76
4	0.175	0.32	0.053	0.32

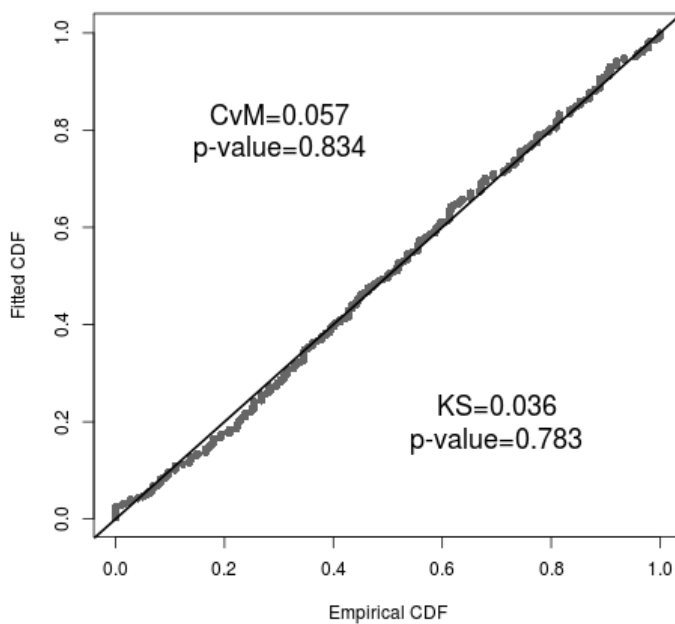


Figure 15: Q-Q plot of the fitted and empirical cumulative density functions (CDF) for the top ranked model of the detection function analysis of the full winter data.

For the detection function analysis on the data from the portion of the transect that can be viewed from both observer positions (0.071–0.300 km), the top two models have most of the AIC model weight (Table 13). Lower-ranked models also have some weight, although the fourth–sixth ranked models result in unrealistic abundance estimates and have correlation values between the intercepts of the detection and dependence functions that are essentially -1 indicating overestimation (SM §B). Therefore, model averaging was performed using the top three models. The top two models (with the majority of the AIC weight) involve a spline relationship between detection and distance that is different from each observer position, and group size as a covariate. The models differ only in terms of whether point or limiting independence is assumed.

Table 13: Top 10 AIC-ranked models for the detection function analysis for sightings between 0.071–0.300 km from the transect line in the winter. Model components identifies the structure of the detection function model; $f(d)$ is the functional relationship with distance on the logit scale (L= linear, Q=quadratic, S=Spline), Obs indicates whether the intercept term is different for each observer position (Y=Yes, N=No), $\beta_1 \neq \beta_2$ indicates whether the regression coefficients for the effect of distance on detection is different for each observer position (Y= Yes, N= No), Size indicates whether group size has an effect on detection (Y=Yes, N=No) and Dep. indicates the form of dependence in detection between observer positions (FI=Full Independence, C = Constant Dependence, P = Point Independence and L= Limiting Independence). ΔAIC is the relative difference in AIC values, wgt is the AIC model weight, wgt* is the adjusted AIC weight for the models used for inference, $-2l$ is twice the negative log-likelihood, pars. is the number parameters in the model, \hat{N}_{cg} is the estimated number of dolphin groups in the covered area, ESW is the effective strip width and corr is the correlation between the intercepts of the detection and dependence functions (only relevant for constant dependence and limiting independence models).

Model Components					Model Fitting Summaries							
$f(d)$	Obs	$\beta_1 \neq \beta_2$	Size	Dep.	ΔAIC	wgt	wgt*	$-2l$	pars	\hat{N}_{cg}	ESW	corr
S	Y	Y	Y	P	0.00	0.49	0.55	351.94	10	428	0.117	-
S	Y	Y	Y	L	0.67	0.35	0.39	350.61	11	355	0.141	0.18
Q	Y	Y	Y	P	4.42	0.05	0.06	360.36	8	444	0.113	-
S	Y	Y	Y	C	5.17	0.04		357.11	10	13819		-1.00
Q	Y	Y	Y	L	5.40	0.03		359.33	9	2289		-0.99
Q	Y	Y	Y	C	5.71	0.03		361.65	8	260702		-1.00
S	Y	Y	N	P	10.21	0.00		364.15	9	422		-
L	Y	Y	Y	P	11.19	0.00		371.13	6	480		-
S	Y	Y	N	L	11.55	0.00		363.48	10	374		0.05
L	Y	Y	Y	L	12.13	0.00		370.06	7	689		-0.92

Plots of the fitted detection functions and empirical histograms of detection rates for the top three models do not indicate any systematic concerns about lack of fit for either model, particularly for $p_{\bullet}(d_i, s_i)$, which is most relevant for abundance estimation. Figure 16 presents the fitted detection functions for the top-ranked model with SM §I including the plots for all three models. The q-q plots (Figure 17 and SM §I) and goodness of fit tests (Table 14) do not indicate any evidence of lack of fit for the three models either.

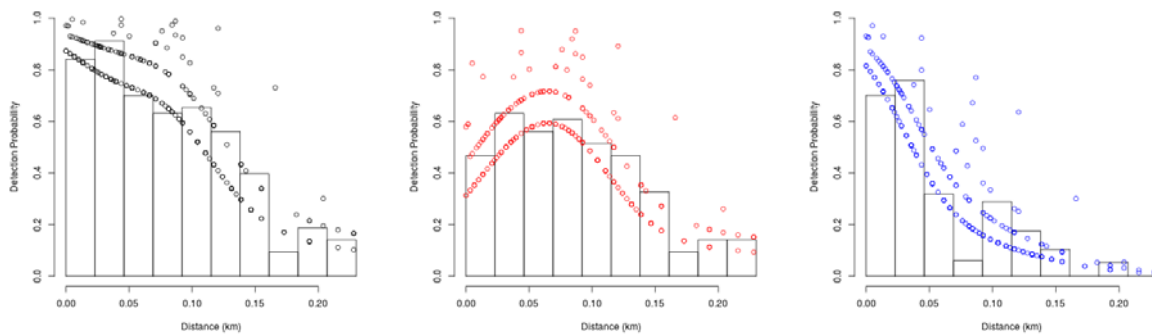


Figure 16: Fitted detection functions and histograms of empirical detection probabilities from the top ranked model in Table 13. Left is $p_{\bullet}(d_i, s_i)$, centre is $p_F(d_i, s_i)$, and right is $p_{R/NF}(d_i, s_i)$. Note that distance from the transect line has been rescaled such that an original distance of 0.071 km is now 0 km.

Table 14: Goodness of fit tests for top three ranked models and the lowest ranked model for the detection function analysis of the reduced winter data set. Given are the Cramer-von Mises (CvM) and Kolmogorov-Smirnov (KS) tests with associated p-values.

Model Rank	CvM	p-value	KS	p-value
1	0.023	0.99	0.035	0.95
2	0.044	0.91	0.040	0.87
3	0.045	0.91	0.046	0.75

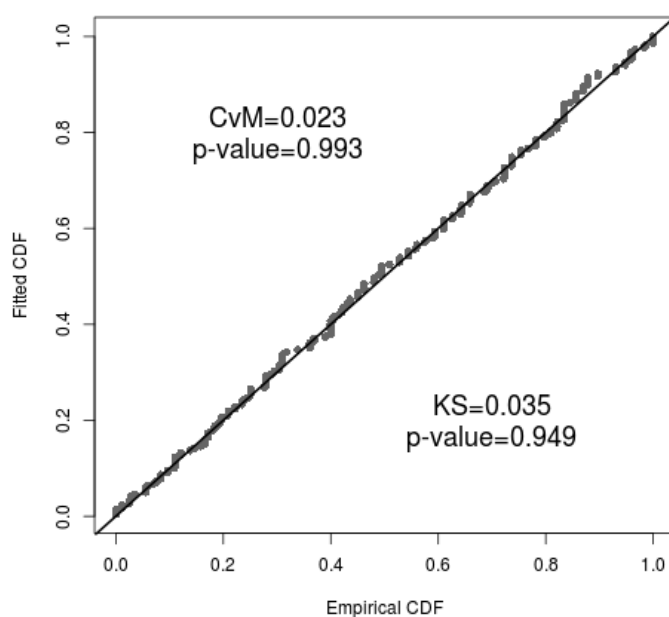


Figure 17: Q-Q plot of the fitted and empirical cumulative density functions (CDF) for the top ranked model of the detection function analysis of the reduced winter data. Q-Q plots for all three models used for model averaging are given in SM §I.

Availability bias

Helicopter dive profiles

The helicopter observer recorded very few distinct behavioural responses (i.e. startled dive) or changes (i.e. socialising to travel) to either helicopter type (single- or double-engine) or between the different hovering and circling techniques. The only obvious dolphin response occurred when the helicopter turned slightly on its side to execute a quick circle, causing the dolphins to immediately dive. During such turns, the noise from the blades was noticeably different to the observer and appeared to be directed more towards the surface of the water. Given that useable data could be collected from the twin-engine platform, the dive data collected from both helicopter types during the trials were used for further comparisons with circle-back methods.

As the data collected during the training period did not indicate a clear preference or discrepancies between either dive-cycle or circle-back based estimates of availability, further collection of availability data from both techniques was considered necessary and attainable given the cost effectiveness of circle-back methods.

During the summer survey, dive information was collected on 86 different dolphin groups equating to 520 complete dive cycles (Table 15, Figure 18). On a regional level, dive sightings ranged from 12 to 22 groups and 24 to 192 dive cycles. Note that for each group, only the average time spent near or the below the surface has been used, not the times for individual dives. Therefore, the mean and variances given in Table 15 are means and variances of average surface/dive times per group. Availability estimates would suggest that there is some regional variation, with a possible north-south gradient indicating that groups are more available in the north (largely due to shorter dive periods; Figure 19). During the training period, it was determined that fixed objects are within an observers view for about six seconds on average, hence $t=6$ has been used to correct for availability bias when estimating abundance (Table 15). The effect of varying t was considered and for every three second change in t the estimated availability changed by approximately 0.02–0.03.

Table 15: Summary of summer dive-cycle data and availability estimates. Given is the number of groups data were collected on (n), average time on or near the surface (\bar{u}), average dive time (\bar{b}), variance for the average surface time ($V_{\bar{u}}$), variance for the average dive time ($V_{\bar{b}}$) and covariance between average surface and dive time ($V_{\bar{u}\bar{b}}$). All times are given in seconds. Estimated probability of a group being available (\hat{P}_α) for $t = 6$ seconds and associated standard error (SE).

Area	n	\bar{u}	\bar{b}	$V_{\bar{u}}$	$V_{\bar{b}}$	$V_{\bar{u}\bar{b}}$	\hat{P}_α	SE
Cloudy	17	47.0	36.6	143.1	36.8	18.7	0.63	0.08
Kaikoura	22	33.8	35.8	14.3	14.5	3.4	0.57	0.05
Nth Banks	21	46.0	50.7	41.5	37.3	14.4	0.53	0.05
Sth Banks	14	48.3	80.0	70.2	76.1	54.6	0.42	0.03
Otago	12	48.2	88.4	33.3	100.2	-8.2	0.40	0.05

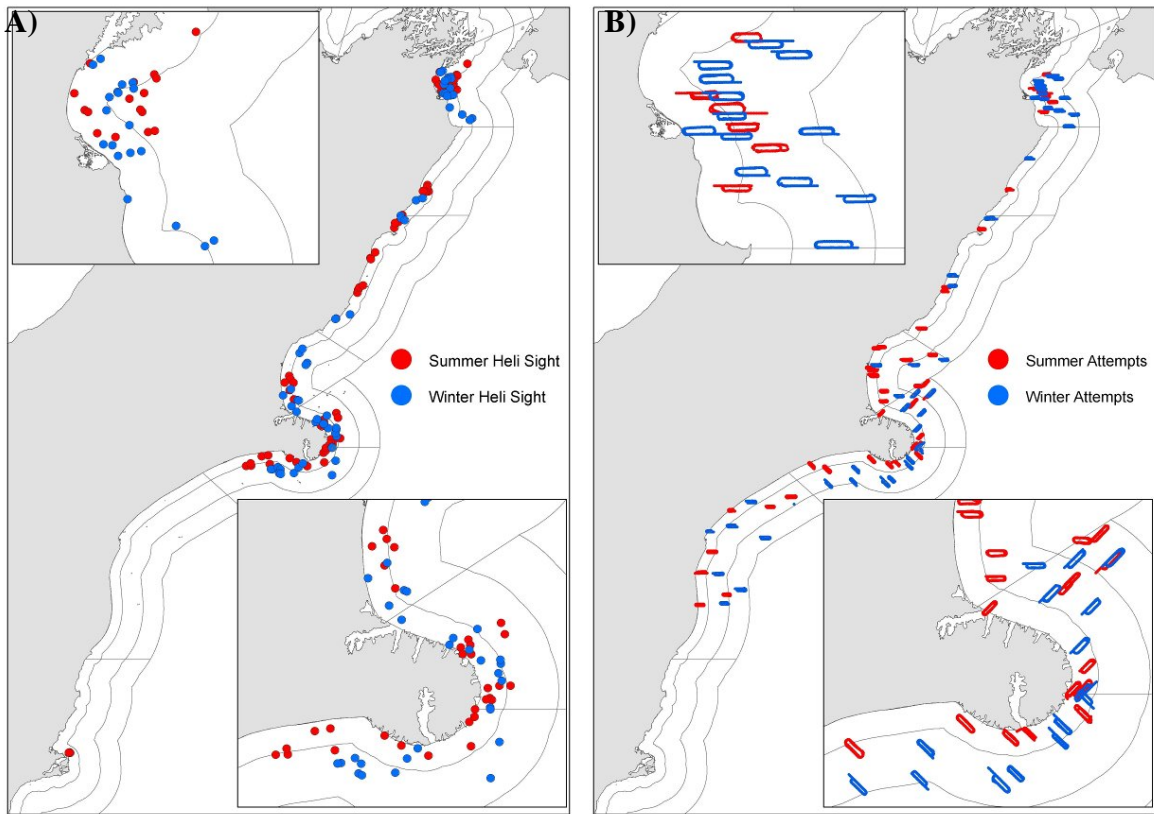


Figure 18: A comparison between the locations of summer (red dots) and winter (blue dots) availability sightings from A) helicopter observations and B) circle-back track attempts within each of the survey stratum.

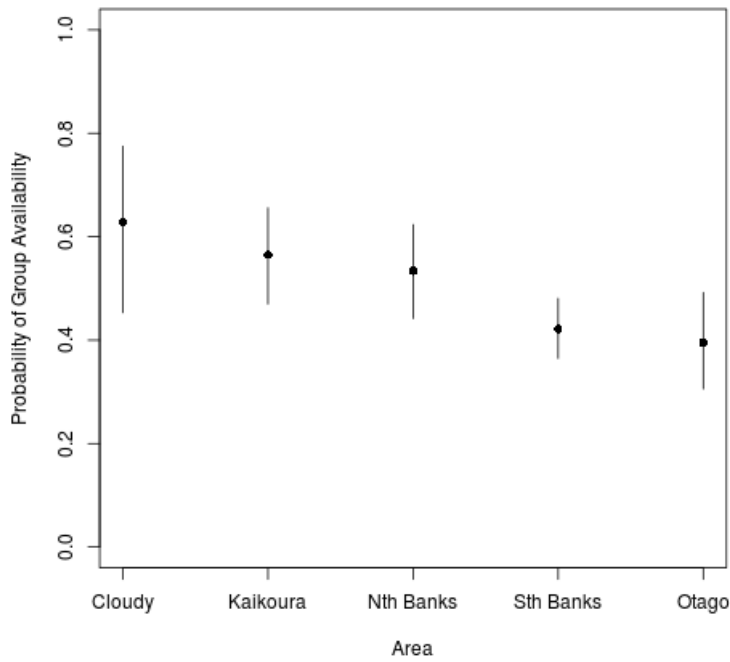


Figure 19: Estimated availability and 95% confidence intervals obtained from the dive-cycle data during summer.

During the winter survey, dive information was collected on 52 different dolphin groups equating to 592 complete dive cycles. On a regional level, dive sightings ranged from 6 to 16 groups and 73 to 257 dive cycles (Table 16, Figure 18). Availability estimates would suggest that there is some regional variation, although unlike the summer surveys there is no suggestion of a north-south gradient (Figure 20). As for the summer surveys, $t=6$ has been used to correct for availability bias when estimating abundance.

While availability has been calculated differently here to account for the time that dolphins are in the view of observers, the estimates are broadly similar to the instantaneous rates that have been determined previously using dive-cycle data for Hector's dolphin (0.36, Clement et al. 2011; 0.46 Slooten et al. 2004; 0.60 DuFresne & Mattlin 2009) and Maui's dolphin (0.56, Slooten et al. 2006).

Table 16: Summary of winter dive-cycle data and availability estimates. Given is the number of groups data were collected on (n), average time on or near the surface (\bar{u}), average dive time (\bar{b}), variance for the average surface time ($V_{\bar{u}}$), variance for the average dive time ($V_{\bar{b}}$) and covariance between average surface and dive time ($V_{\bar{u}\bar{b}}$). All times are given in seconds. Estimated probability of a group being available (\hat{P}_α) for $t = 6$ seconds and associated standard error (SE).

Area	n	\bar{u}	\bar{b}	$V_{\bar{u}}$	$V_{\bar{b}}$	$V_{\bar{u}\bar{b}}$	\hat{P}_α	SE
Cloudy	16	37.59	56.86	37.20	79.20	44.21	0.46	0.03
Kaikoura	6	17.12	51.63	22.38	498.43	99.46	0.33	0.08
Nth Banks	17	28.56	26.53	39.43	14.02	14.06	0.62	0.06
Sth Banks	13	56.69	54.87	55.82	62.24	21.63	0.56	0.05

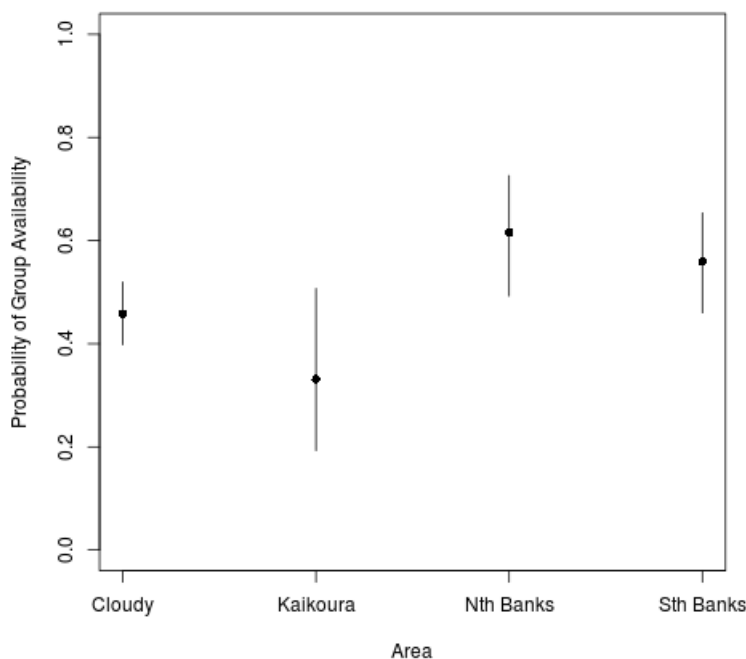


Figure 20: Estimated availability and 95% confidence intervals obtained from the dive-cycle data during winter.

At the AEWG meeting on 11 October 2013, estimates of availability for 20 m seabed depth intervals were requested to investigate for any apparent relationship. There is no indication of a consistent relationship from either the summer or winter data (Figures 21–22). The number of groups observed in each distance interval were 34, 39, 9 and 4 respectively in summer, and 12, 25, 7 and 8 respectively in winter.

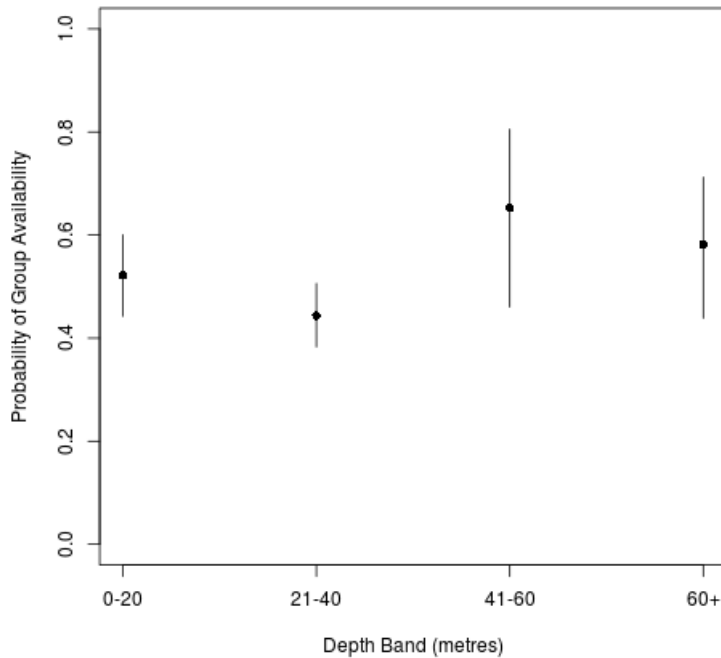


Figure 21: Estimated availability and 95% confidence intervals obtained from the dive-cycle data during summer for different 20 m depth intervals.

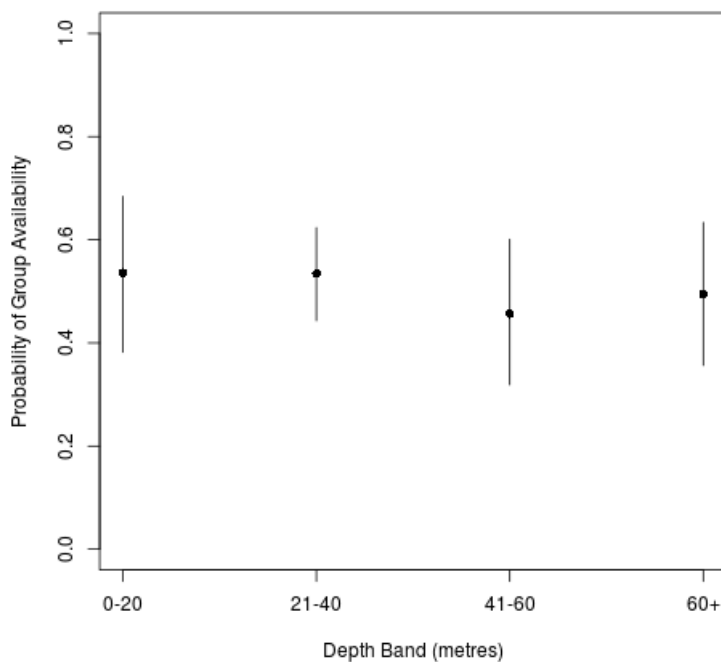


Figure 22: Estimated availability and 95% confidence intervals obtained from the dive-cycle data during winter for different 20 m depth intervals.

Summer

Following data verification, 41 circle-backs were completed during the summer survey (see Figure 18), with data used from 87 dolphin groups (often multiple groups were spotted during a circle-back) and a total of 215 attempts to resight dolphin groups with 93 successful detections by either observer. The six detection function models identified in Table 5 were used in the modelling of the circle-back data. Investigation of the three factors of interest (region, offshore and water colour) resulted in similar AICs regardless of the detection function used (Table 17). Only the results from the top detection function model in Table 5 are presented here, although model selection summaries for all detection functions are given in SM §J. There is little indication of water colour being an important factor for availability from these analyses (i.e., low AIC model weights; Table 17 and SM §J), hence it was not incorporated into the estimation of abundance.

For each detection function used, model averaged estimates of availability were calculated (Table 18), which were then used to estimate dolphin abundance. Standard errors have not been presented in Table 18, but are included with the stratum-specific abundance estimates from each detection function (SM §K).

Table 17: Model selection summary for factors affecting summer availability as assessed from circle-back protocol, using the detection function from the top-ranked model in Table 5. Parameters given are the relative difference in AIC values (ΔAIC), AIC model weights (w), adjusted weights for the four models used to obtain model averaged availability estimates (w^*), twice the negative log-likelihood ($-2l$) and the number of parameters in the model ($NPar$). The ‘.’ model assumes equal availability across all factors.

Model	ΔAIC	w	w^*	$-2l$	$NPar$
.	0.00	0.60	0.65	175.58	1
offshore	1.80	0.24	0.27	175.38	2
region	4.81	0.05	0.06	174.39	4
colour	4.85	0.05		174.42	4
offshore+colour	6.61	0.02		174.19	5
region+offshore	6.80	0.02	0.02	174.37	5
region+colour	9.93	0.00		173.51	7
region+offshore+colour	11.85	0.00		173.43	8

Table 18: Model averaged availability estimates from the full summer data for each detection function. Column labels indicate the order of the detection function models in Table 5 with the values in parentheses indicating the corresponding adjusted AIC model weight for each detection function model.

	Offshore Stratum (nmi)	1 (0.50)	2 (0.27)	3 (0.08)	4 (0.06)	5 (0.06)	6 (0.02)
Coastal Section							
Golden Bay North	0–4	0.56	0.68	0.54	0.65	0.62	0.61
	4–12	0.55	0.66	0.53	0.64	0.61	0.60
Golden Bay A	0–4	0.56	0.68	0.54	0.65	0.62	0.61
	4–12	0.55	0.66	0.53	0.64	0.61	0.60
	12–20	0.55	0.66	0.53	0.64	0.61	0.60
Golden Bay B	0–4	0.56	0.68	0.54	0.65	0.62	0.61
	4–12	0.55	0.66	0.53	0.64	0.61	0.60
	12–20	0.55	0.66	0.53	0.64	0.61	0.60
Marlborough Sounds	0–4	0.56	0.68	0.54	0.65	0.62	0.61
	4–12	0.55	0.66	0.53	0.64	0.61	0.60
	12–20	0.55	0.66	0.53	0.64	0.61	0.60
Cloudy/Clifford Bay	0–4	0.56	0.68	0.54	0.65	0.62	0.61
	4–12	0.55	0.66	0.53	0.64	0.61	0.60
	12–20	0.55	0.66	0.53	0.64	0.61	0.60
Kaikoura	0–4	0.57	0.68	0.55	0.65	0.63	0.62
	4–12	0.56	0.67	0.54	0.64	0.62	0.61
	12–20	0.56	0.67	0.54	0.64	0.62	0.61
Clarence	0–4	0.57	0.68	0.55	0.65	0.63	0.62
	4–12	0.56	0.67	0.54	0.64	0.62	0.61
	12–20	0.56	0.67	0.54	0.64	0.62	0.61
Pegasus Bay	0–4	0.57	0.69	0.55	0.66	0.63	0.62
	4–12	0.56	0.67	0.54	0.64	0.62	0.61
	12–20	0.56	0.67	0.54	0.64	0.62	0.61
Banks Pen. North	0–4	0.57	0.69	0.55	0.66	0.63	0.62
	4–12	0.56	0.67	0.54	0.64	0.62	0.61
	12–20	0.56	0.67	0.54	0.64	0.62	0.61
Banks Pen. South	0–4	0.57	0.69	0.55	0.66	0.63	0.62
	4–12	0.56	0.68	0.54	0.65	0.62	0.61
	12–20	0.56	0.68	0.54	0.65	0.62	0.61
Timaru	0–4	0.57	0.69	0.55	0.66	0.63	0.62
	4–12	0.56	0.68	0.54	0.65	0.62	0.61
	12–20	0.56	0.68	0.54	0.65	0.62	0.61
Otago	0–4	0.57	0.69	0.55	0.66	0.63	0.62
	4–12	0.56	0.68	0.54	0.65	0.62	0.61
	12–20	0.56	0.68	0.54	0.65	0.62	0.61

For the reduced summer analysis, data was used from 72 dolphin groups with 176 attempted sightings and 73 successful detections. The seven detection function models identified in Table 7 were used in the modelling of the circle-back data. As for the full data set model selection, results were very similar for all detection functions; hence only the results from the top detection function model in Table 7 are presented here (Table 19), with summaries for all detection functions given in SM §J. There is little indication of water colour being an important factor for availability from these analyses (i.e., low AIC model weights; Table 19 and SM §J), hence it was not incorporated into the estimation of abundance.

For each detection function used, model averaged estimates of availability were calculated (Table 20), which were used to estimate dolphin abundance. Standard errors have not been presented in Table 20, but are included with the stratum-specific abundance estimates from each detection function (SM §L).

Table 19: Model selection summary for factors affecting summer availability as assessed from circle-back protocol, using the detection function from the top-ranked model in Table 7. Given is the relative difference in AIC values (ΔAIC), AIC model weights (w), adjusted weights for the four models used to obtain model averaged availability estimates (w^*), twice the negative log-likelihood ($-2l$) and the number of parameters in the model ($NPar$). The ‘.’ model assumes equal availability across all factors.

Model	ΔAIC	w	w^*	$-2l$	$NPar$
.	0.00	0.50	0.55	143.89	1
offshore	1.58	0.23	0.25	143.47	2
region	2.61	0.14	0.15	140.50	4
region+offshore	4.51	0.05	0.06	140.40	5
colour	5.11	0.04		143.00	4
offshore+colour	6.60	0.02		142.49	5
region+colour	6.85	0.02		138.74	7
region+offshore+colour	8.81	0.01		138.70	8

Table 20: Model averaged availability estimates from the reduced summer data for each detection function. Column labels indicate the order of the detection function models in Table 7 with the values in parentheses indicating the corresponding adjusted AIC model weight for each detection function model.

	Offshore Stratum (nmi)	1 (0.39)	2 (0.16)	3 (0.14)	5 (0.10)	6 (0.09)	7 (0.06)	8 (0.05)
Coastal Section								
Golden Bay North	0-4	0.56	0.53	0.54	0.63	0.55	0.53	0.49
	4-12	0.54	0.51	0.52	0.61	0.53	0.51	0.47
Golden Bay A	0-4	0.56	0.53	0.54	0.63	0.55	0.53	0.49
	4-12	0.54	0.51	0.52	0.61	0.53	0.51	0.47
	12-20	0.54	0.51	0.52	0.61	0.53	0.51	0.47
Golden Bay B	0-4	0.56	0.53	0.54	0.63	0.55	0.53	0.49
	4-12	0.54	0.51	0.52	0.61	0.53	0.51	0.47
	12-20	0.54	0.51	0.52	0.61	0.53	0.51	0.47
Marlborough Sounds	0-4	0.56	0.53	0.54	0.63	0.55	0.53	0.49
	4-12	0.54	0.51	0.52	0.61	0.53	0.51	0.47
	12-20	0.54	0.51	0.52	0.61	0.53	0.51	0.47
Cloudy/Clifford Bay	0-4	0.56	0.53	0.54	0.63	0.55	0.53	0.49
	4-12	0.54	0.51	0.52	0.61	0.53	0.51	0.47
	12-20	0.54	0.51	0.52	0.61	0.53	0.51	0.47
Kaikoura	0-4	0.57	0.54	0.55	0.64	0.56	0.54	0.50
	4-12	0.55	0.52	0.53	0.62	0.54	0.52	0.48
	12-20	0.55	0.52	0.53	0.62	0.54	0.52	0.48
Clarence	0-4	0.57	0.54	0.55	0.64	0.56	0.54	0.50
	4-12	0.55	0.52	0.53	0.62	0.54	0.52	0.48
	12-20	0.55	0.52	0.53	0.62	0.54	0.52	0.48
Pegasus Bay	0-4	0.58	0.55	0.56	0.65	0.57	0.55	0.51
	4-12	0.57	0.53	0.54	0.63	0.55	0.53	0.50
	12-20	0.57	0.53	0.54	0.63	0.55	0.53	0.50
Banks Pen. North	0-4	0.58	0.55	0.56	0.65	0.57	0.55	0.51
	4-12	0.57	0.53	0.54	0.63	0.55	0.53	0.50
	12-20	0.57	0.53	0.54	0.63	0.55	0.53	0.50
Banks Pen. South	0-4	0.62	0.58	0.59	0.68	0.60	0.58	0.54
	4-12	0.60	0.56	0.57	0.66	0.58	0.56	0.53
	12-20	0.60	0.56	0.57	0.66	0.58	0.56	0.53
Timaru	0-4	0.62	0.58	0.59	0.68	0.60	0.58	0.54
	4-12	0.60	0.56	0.57	0.66	0.58	0.56	0.53
	12-20	0.60	0.56	0.57	0.66	0.58	0.56	0.53
Otago	0-4	0.62	0.58	0.59	0.68	0.60	0.58	0.54
	4-12	0.60	0.56	0.57	0.66	0.58	0.56	0.53
	12-20	0.60	0.56	0.57	0.66	0.58	0.56	0.53

Winter

Following data verification, 43 circle-backs were completed during the winter survey (see Figure 18), with data used from 75 dolphin groups (often multiple groups were spotted during a circle-back) and a total of 181 attempts to resight dolphin groups with 68 successful detections by either observer. The four detection function models identified in Table 11 were used in the modelling of the circle-back data. Investigation of the three factors of interest (region, offshore and water colour) were similar in terms of AICs regardless of the detection function used. Only the results from the top detection function model in Table 11 are presented here (Table 21), although model selection summaries for all detection functions are given in SM §J. There is little indication of water colour being an important factor for availability from these analyses (i.e., low AIC model weights; Table 21 and SM §J), hence it was not incorporated into the estimation of abundance.

For each detection function used, model averaged estimates of availability were calculated (Table 22), which were used to estimate dolphin abundance. Standard errors have not been presented in Table 22, but are included with the stratum-specific abundance estimates from each detection function (SM §M).

Table 21: Model selection summary for factors affecting winter availability as assessed from circle-back protocol, using the detection function from the top-ranked model in Table 11. Given is the relative difference in AIC values (ΔAIC), AIC model weights (w), adjusted weights for the four models used to obtain model averaged availability estimates (w^*), twice the negative log-likelihood ($-2l$) and the number of parameters in the model ($NPar$). The ‘.’ model assumes equal availability across all factors.

Model	ΔAIC	w	w^*	$-2l$	$NPar$
region	0.00	0.45	0.57	144.53	4
region+offshore	1.92	0.17	0.22	144.45	5
region+colour	2.50	0.13		141.03	7
.	2.69	0.12	0.15	153.22	1
region+offshore+colour	4.47	0.05		141.00	8
offshore	4.48	0.05	0.06	153.01	2
colour	5.95	0.02		150.48	4
offshore+colour	7.92	0.01		150.45	5

Table 22: Model averaged availability estimates from the full winter data for each detection function. Column labels indicate the order of the detection function models in Table 11 with the values in parentheses indicating the corresponding adjusted AIC model weight for each detection function model.

	Offshore Stratum (nmi)	1 (0.77)	2 (0.10)	3 (0.09)	4 (0.04)
Coastal Section					
Golden Bay North	0–4	0.43	0.46	0.51	0.44
	4–12	0.42	0.44	0.47	0.43
Golden Bay A	0–4	0.43	0.46	0.51	0.44
	4–12	0.42	0.44	0.47	0.43
	12–20	0.42	0.44	0.47	0.43
Golden Bay B	0–4	0.43	0.46	0.51	0.44
	4–12	0.42	0.44	0.47	0.43
	12–20	0.42	0.44	0.47	0.43
Marlborough Sounds	0–4	0.43	0.46	0.51	0.44
	4–12	0.42	0.44	0.47	0.43
	12–20	0.42	0.44	0.47	0.43
Cloudy/Clifford Bay	0–4	0.43	0.46	0.51	0.44
	4–12	0.42	0.44	0.47	0.43
	12–20	0.42	0.44	0.47	0.43
Kaikoura	0–4	0.26	0.27	0.28	0.26
	4–12	0.25	0.25	0.26	0.25
	12–20	0.25	0.25	0.26	0.25
Clarence	0–4	0.26	0.27	0.28	0.26
	4–12	0.25	0.25	0.26	0.25
	12–20	0.25	0.25	0.26	0.25
Pegasus Bay	0–4	0.67	0.73	0.81	0.69
	4–12	0.66	0.72	0.79	0.68
	12–20	0.66	0.72	0.79	0.68
Banks Pen. North	0–4	0.67	0.73	0.81	0.69
	4–12	0.66	0.72	0.79	0.68
	12–20	0.66	0.72	0.79	0.68
Banks Pen. South	0–4	0.60	0.65	0.71	0.62
	4–12	0.59	0.64	0.68	0.61
	12–20	0.59	0.64	0.68	0.61
Timaru	0–4	0.60	0.65	0.71	0.62
	4–12	0.59	0.64	0.68	0.61
	12–20	0.59	0.64	0.68	0.61
Otago	0–4	0.60	0.65	0.71	0.62
	4–12	0.59	0.64	0.68	0.61
	12–20	0.59	0.64	0.68	0.61

For the reduced winter analysis, data was used from 59 dolphin groups with 142 attempted sightings and 55 successful detections. The three detection function models identified in Table 13 were used in the modelling of the circle-back data. As for the full data set, model selection results were very similar for all detection functions; hence only the results from the top detection function model in Table 13 are presented here (Table 23), with summaries for all detection functions given in SM §J. There is little indication of water colour being an important factor for availability from these analyses (i.e., low AIC model weights; Table 23 and SM §J), hence it was not incorporated into the estimation of abundance.

For each detection function used, model averaged estimates of availability were calculated (Table 24) which were used to estimate dolphin abundance. Standard errors have not been presented in Table 24, but are included with the stratum-specific abundance estimates from each detection function (SM §N).

Table 23: Model selection summary for factors affecting winter availability as assessed from circle-back protocol, using the detection function from the top-ranked model in Table 13. Given is the relative difference in AIC values (ΔAIC), AIC model weights (w), adjusted weights for the four models used to obtain model averaged availability estimates (w^*), twice the negative log-likelihood ($-2l$) and the number of parameters in the model ($NPar$). The ‘.’ model assumes equal availability across all factors.

Model	ΔAIC	w	w^*	$-2l$	$NPar$
region	0.00	0.47	0.52	115.06	4
region+offshore	1.75	0.20	0.22	114.81	5
.	2.02	0.17	0.19	123.08	1
offshore	4.00	0.06	0.07	123.06	2
region+colour	4.24	0.06		113.30	7
region+offshore+colour	5.88	0.02		112.95	8
colour	7.33	0.01		122.39	4
offshore+colour	9.32	0.00		122.39	5

Table 24: Model averaged availability estimates from the reduced winter data for each detection function. Column labels indicate the order of the detection function models in Table 13 with the values in parentheses indicating the corresponding adjusted AIC model weight for each detection function model.

	Offshore Stratum (nmi)	1 (0.55)	2 (0.39)	3 (0.06)
Coastal Section				
Golden Bay North	0-4	0.59	0.49	0.60
	4-12	0.55	0.49	0.56
Golden Bay A	0-4	0.59	0.49	0.60
	4-12	0.55	0.49	0.56
	12-20	0.55	0.49	0.56
Golden Bay B	0-4	0.59	0.49	0.60
	4-12	0.55	0.49	0.56
	12-20	0.55	0.49	0.56
Marlborough Sounds	0-4	0.59	0.49	0.60
	4-12	0.55	0.49	0.56
	12-20	0.55	0.49	0.56
Cloudy/Clifford Bay	0-4	0.59	0.49	0.60
	4-12	0.55	0.49	0.56
	12-20	0.55	0.49	0.56
Kaikoura	0-4	0.43	0.38	0.44
	4-12	0.40	0.39	0.41
	12-20	0.40	0.39	0.41
Clarence	0-4	0.43	0.38	0.44
	4-12	0.40	0.39	0.41
	12-20	0.40	0.39	0.41
Pegasus Bay	0-4	0.91	0.75	0.93
	4-12	0.91	0.75	0.93
	12-20	0.91	0.75	0.93
Banks Pen. North	0-4	0.91	0.75	0.93
	4-12	0.91	0.75	0.93
	12-20	0.91	0.75	0.93
Banks Pen. South	0-4	0.79	0.66	0.81
	4-12	0.77	0.66	0.78
	12-20	0.77	0.66	0.78
Timaru	0-4	0.79	0.66	0.81
	4-12	0.77	0.66	0.78
	12-20	0.77	0.66	0.78
Otago	0-4	0.79	0.66	0.81
	4-12	0.77	0.66	0.78
	12-20	0.77	0.66	0.78

Summer abundance estimates

Summer estimates of dolphin abundance after correcting for each availability bias are given in Table 25. Table 26 contains the abundance estimates obtained by averaging the four sets of estimates, which provides an estimate of Hector's dolphin summer abundance along the ECSI (out to 20 nmi) of 9130 (CV: 19%; 95% CI: 6342–13 144). Note that this estimate excludes harbours and bays that were not included in the survey region (Figure 23).

Table 25: Model averaged summer abundance estimates and standard errors for each stratum from data of sightings between 0–0.3 km (Full Data) and 0.071–0.3 km (Reduced Data). Given are the estimated abundance of Hector's dolphins (corrected for availability bias; \hat{N}_k) using the availability estimates from the dive-cycle data and circle-back data).

	Offshore Stratum (nmi)	Full Data				Reduced Data			
		Dive Cycle		Circle-back		Dive Cycle		Circle-back	
		\hat{N}_k	SE	\hat{N}_k	SE	\hat{N}_k	SE	\hat{N}_k	SE
Coastal Section									
Golden Bay North	0–4								
	4–12								
Golden Bay A	0–4								
	4–12								
	12–20								
Golden Bay B	0–4								
	4–12								
	12–20								
Marlborough Sounds	0–4								
	4–12								
	12–20								
Cloudy/Clifford Bay	0–4	430	166	450	156	427	154	485	183
	4–12	499	184	531	175	455	145	536	181
	12–20								
Kaikoura	0–4	388	207	362	194	340	194	342	202
	4–12								
	12–20								
Clarence	0–4	143	121	134	113	186	156	187	159
	4–12								
	12–20								
Pegasus Bay	0–4	455	142	398	117	453	135	421	126
	4–12	294	171	262	151	333	192	320	187
	12–20	320	306	285	270	246	244	237	235
Banks Pen. North	0–4	938	220	822	181	918	231	854	220
	4–12	965	368	859	318	986	363	948	355
	12–20	475	340	423	300	568	396	546	383
Banks Pen. South	0–4	1969	407	1358	273	2009	428	1401	331
	4–12	1111	495	780	349	1261	560	907	420
	12–20								
Timaru	0–4	770	287	530	194	774	310	539	222
	4–12	1170	527	823	376	1101	535	793	400
	12–20								
Otago	0–4								
	4–12								
	12–20								
Total		9927	1617	8017	1246	10057	1565	8518	1415

Table 26: Estimated summer abundance of Hector’s dolphins in each stratum and overall obtained from averaging the four sets of results from the two different data sets and methods of estimating availability. Given is the average estimate and associated standard error, along with the lower and upper limits of a Wald-lognormal 95% confidence interval (see SM §K and §L).

Coastal Section	Offshore Stratum (nmi)	\widehat{N}_k	SE	Lower	Upper
Golden Bay North	0–4				
	4–12				
Golden Bay A	0–4				
	4–12				
	12–20				
Golden Bay B	0–4				
	4–12				
	12–20				
Marlborough Sounds	0–4				
	4–12				
	12–20				
Cloudy/Clifford Bay	0–4	448	167	221	908
	4–12	505	175	261	977
	12–20				
Kaikoura	0–4	358	200	129	995
	4–12				
	12–20				
Clarence	0–4	163	141	37	705
	4–12				
	12–20				
Pegasus Bay	0–4	432	132	240	777
	4–12	302	178	104	881
	12–20	272	267	54	1362
Banks Pen. North	0–4	883	219	547	1425
	4–12	940	355	459	1922
	12–20	503	361	142	1781
Banks Pen. South	0–4	1684	476	978	2900
	4–12	1015	498	408	2524
	12–20				
Timaru	0–4	653	284	289	1475
	4–12	972	494	380	2486
	12–20				
Otago	0–4				
	4–12				
	12–20				
Total		9130	1712	6342	13144

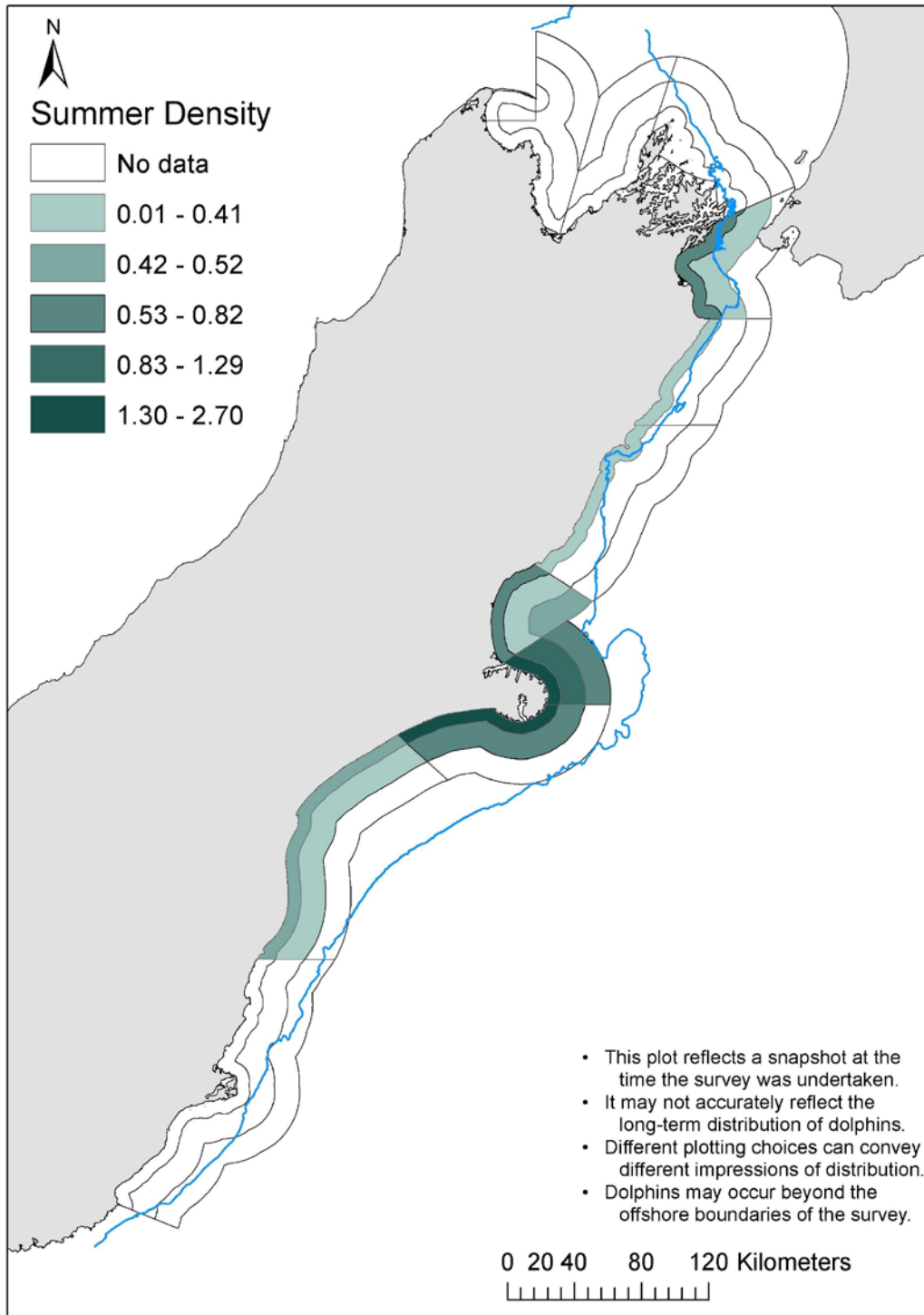


Figure 23: Estimated summer abundance of Hector's dolphins in each stratum obtained from averaging the four sets of results from the two different data sets and methods of estimating availability. 'No data' indicates regions with no sightings and does not necessarily indicate the absence of dolphins.

Winter abundance estimates

Winter estimates of dolphin abundance after correcting for each availability bias are given in Table 27. Table 28 contains the abundance estimates obtained by averaging the four sets of estimates, which provides an estimate of Hector's dolphin winter abundance along the ECSI (out to 20 nmi) of 7456 (CV: 18%; 95% CI: 5224–10 641). Note that this estimate excludes harbours and bays that were not included in the survey region (Figure 24).

Table 27: Model averaged winter abundance estimates and standard errors for each stratum from data of sightings between 0–0.3 km (Full Data) and 0.071–0.3 km (Reduced Data). Given is the estimated abundance of Hector's dolphins (corrected for availability bias; \hat{N}_k) using the availability estimates from the dive-cycle data and circle-back data.

	Offshore Stratum (nmi)	Full Data				Reduced Data			
		Dive Cycle		Circle-back		Dive Cycle		Circle-back	
		\hat{N}_k	SE	\hat{N}_k	SE	\hat{N}_k	SE	\hat{N}_k	SE
Coastal Section	0–4								
Golden Bay North	4–12								
Golden Bay A	0–4								
	4–12	154	165	166	182	230	247	200	220
	12–20								
Golden Bay B	0–4								
	4–12								
	12–20								
Marlborough Sounds	0–4								
	4–12								
	12–20								
Cloudy/Clifford Bay	0–4	116	69	122	79	61	68	51	59
	4–12	383	151	415	184	310	119	269	121
	12–20	212	148	229	167	199	120	173	111
Kaikoura	0–4	233	114	299	280	185	126	148	141
	4–12								
	12–20								
Clarence	0–4	410	213	527	501	321	203	256	236
	4–12								
	12–20								
Pegasus Bay	0–4	43	35	39	32	70	56	51	41
	4–12	509	250	466	240	630	401	458	297
	12–20	417	169	382	165	379	142	275	109
Banks Pen. North	0–4	280	83	252	86	329	115	239	90
	4–12	483	112	443	123	545	148	396	118
	12–20	486	225	445	218	524	270	382	204
Banks Pen. South	0–4	477	136	435	135	505	167	381	136
	4–12	260	70	242	72	301	103	232	84
	12–20	131	101	122	95	59	44	45	34
Timaru	0–4	268	92	244	89	214	83	161	65
	4–12	1841	398	1714	432	2088	523	1607	456
	12–20	1043	290	970	297	1295	421	997	350
Otago	0–4								
	4–12								
	12–20								
Total		7745	962	7513	1176	8246	1370	6320	1122

Table 28: Estimated winter abundance of Hector’s dolphins in each stratum and overall obtained from averaging the four sets of results from the two different data sets and methods of estimating availability. Given is the average estimate and associated standard error, along with the lower and upper limits of a Wald-lognormal 95% confidence interval (see SM §M and §N).

Coastal Section	Offshore Stratum (nmi)	\widehat{N}_k	SE	Lower	Upper
Golden Bay North	0–4				
	4–12				
	12–20				
Golden Bay A	0–4				
	4–12	187	208	32	1087
	12–20				
Golden Bay B	0–4				
	4–12				
	12–20				
Marlborough Sounds	0–4				
	4–12				
	12–20				
Cloudy/Clifford Bay	0–4	88	76	20	379
	4–12	344	157	147	808
	12–20	203	140	60	689
Kaikoura	0–4	216	187	50	935
	4–12				
	12–20				
Clarence	0–4	378	330	87	1650
	4–12				
	12–20				
Pegasus Bay	0–4	51	44	12	218
	4–12	516	311	173	1538
	12–20	363	157	161	820
Banks Pen. North	0–4	275	100	137	550
	4–12	467	137	265	822
	12–20	459	237	177	1188
Banks Pen. South	0–4	450	152	236	855
	4–12	259	87	136	493
	12–20	89	83	19	422
Timaru	0–4	221	92	101	484
	4–12	1813	489	1078	3047
	12–20	1076	367	562	2062
Otago	0–4				
	4–12				
	12–20				
Total		7456	1364	5224	10641

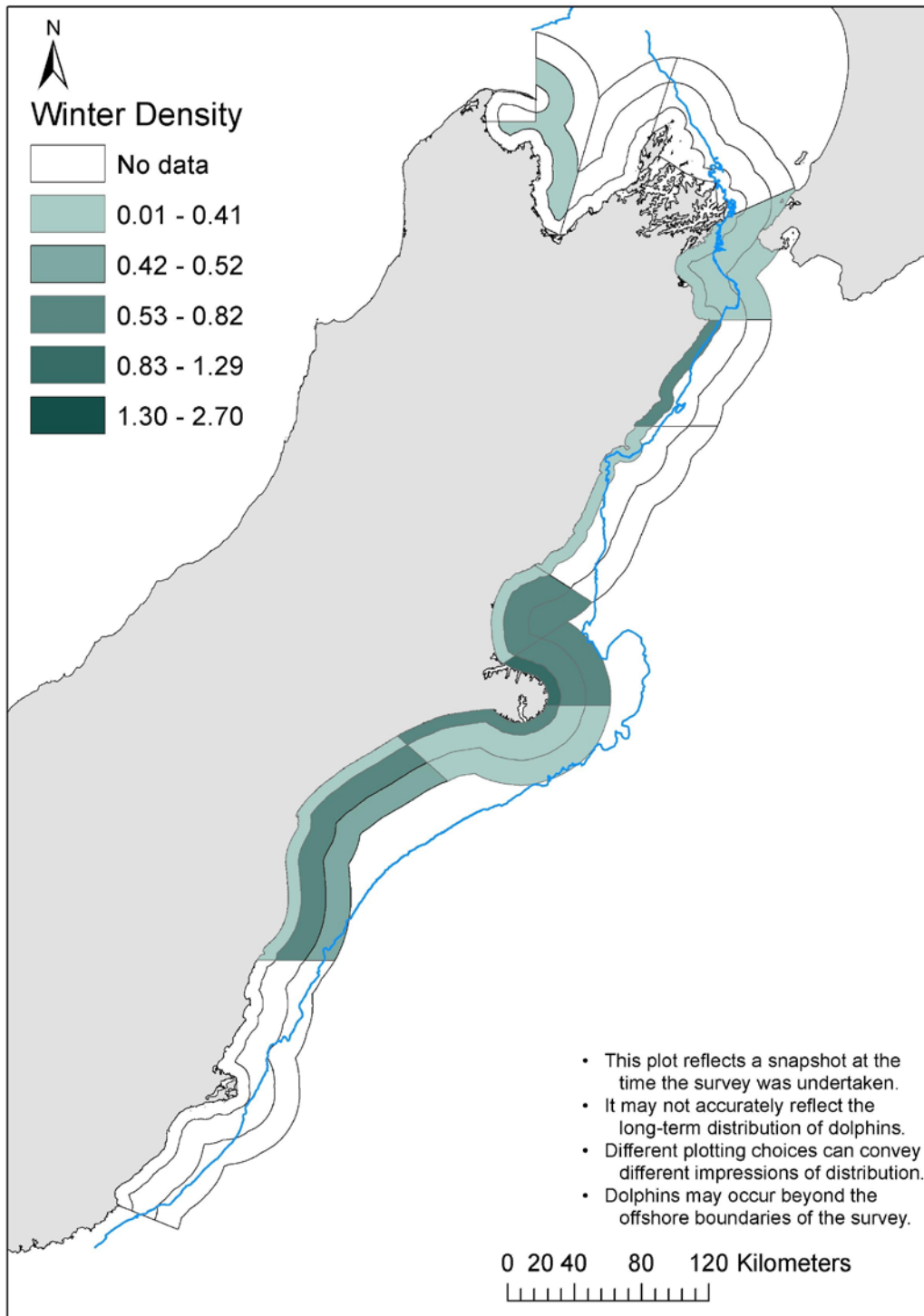


Figure 24: Estimated winter abundance of Hector’s dolphins in each stratum obtained from averaging the four sets of results from the two different data sets and methods of estimating availability. ‘No data’ indicates regions with no sightings and does not necessarily indicate the absence of dolphins.

3.2 Distribution results

The fact that there are more Hector’s dolphins along the east and north coast of the South Island than previously estimated does not preclude several other well-established facts about their general distribution and population structure along this coastline. This species clearly prefers water around Banks Peninsula and within Clifford and Cloudy Bays (Figures 25a–26b). Approximately 87% of all summer and 67% of all winter sightings were recorded within these general regions. Substantial breaks in population structure occur between these two regions and, in particular, waters to the south of Oamaru and west of Cloudy Bay where only smaller and semi-isolated communities were found and/or known to occur as indicated by previous research (Dawson & Slooten 1988, Turek et al. 2013, Clement pers. obs.).

The majority of dolphins were also found closer to shore in the summer than winter (Table 29). As has been observed previously (DuFresne & Mattlin 2009, Rayment et al. 2010a), Hector’s dolphins generally shift offshore over colder months, considerably further in some regions than others (i.e. Timaru with an extended continental shelf versus Kaikoura with a close in shelf). While most animals were sighted within the 100 m depth contour, animals within Clifford/Cloudy Bays and near Pegasus Canyon (NE Banks Peninsula) occurred near and across this contour on both surveys suggesting this species is not necessarily limited to waters of shallower depths (Table 29).

The results of the summer and winter DSM are given in Figures 25a–26b. Note how the visual impression of the estimated dolphin distribution can change depending on how the results of the DSM are presented (Figure 25a versus 25b and 26a versus 26b). The right-hand panels of Figures 25b and 26b indicate the precision of the relative abundance estimates from the DSM and tend to be greatest in those areas with higher relative density. As seen in the raw data, the DSMs support general offshore movement from summer to winter, with lower winter relative densities close to shore in Cloudy/Clifford Bay, Pegasus Bay and Banks Peninsula, and an increase in relative densities offshore of Timaru. Estimated summer and winter dolphin density (per 100 km²) for each strata are given in Table 30 and Table 31 lists the group-size frequencies used in the parametric bootstrap for each season.

Table 29: The mean and maximum distance from shore (km) and depths (m) at which summer and winter survey sightings of Hector’s dolphin occurred.

Stratum	Summer		Winter		Summer		Winter	
	Distance offshore (km)		Distance offshore (km)		Depth (m)		Depth (m)	
	Mean	Max	Mean	Max	Mean	Max	Mean	Max
ECSI	7.0	31.6	14.8	37.1	26.2	150.0	37.8	100.0
Golden Bay			8.9	8.9			30.0	30.0
Cloudy/Clifford Bay	7.7	22.1	12.5	23.2	42.0	150.0	51.6	100.0
Clarence	1.5	2.9	2.7	6.1	13.3	20.0	38.6	100.0
Kaikoura	1.8	6.0	4.7	6.7	16.3	20.0	32.9	50.0
Pegasus Bay	6.6	28.9	6.7	37.1	15.5	50.0	32.1	100.0
Banks Pen. North	9.7	31.6	15.9	35.2	22.3	50.0	39.0	100.0
Banks Pen. South	5.1	12.9	8.3	33.1	28.5	50.0	43.3	50.0
Timaru	6.9	20.3	17.3	33.7	20.6	30.0	33.8	50.0

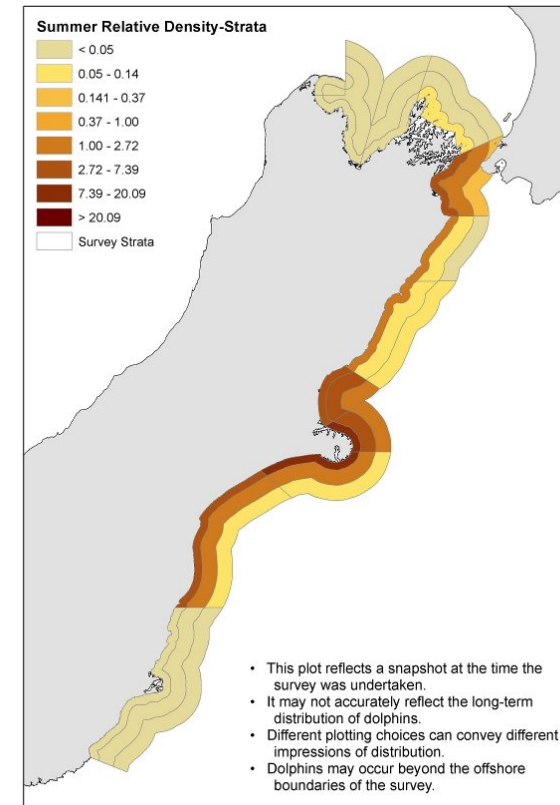
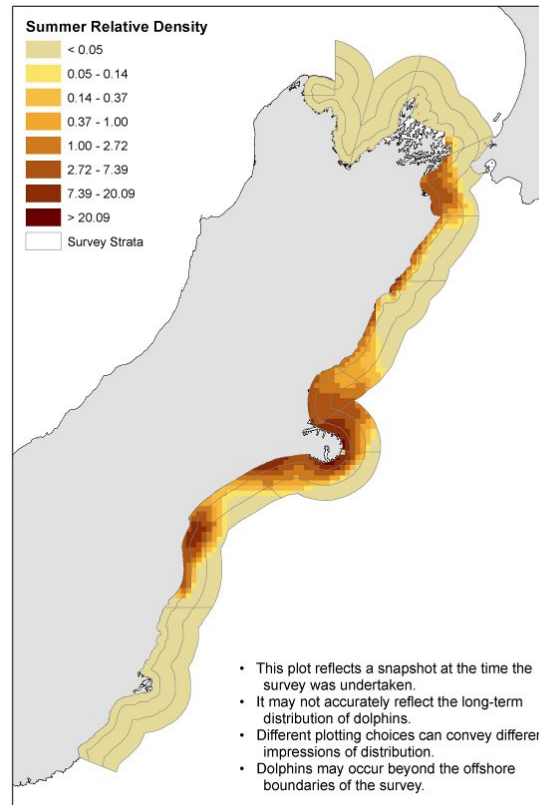
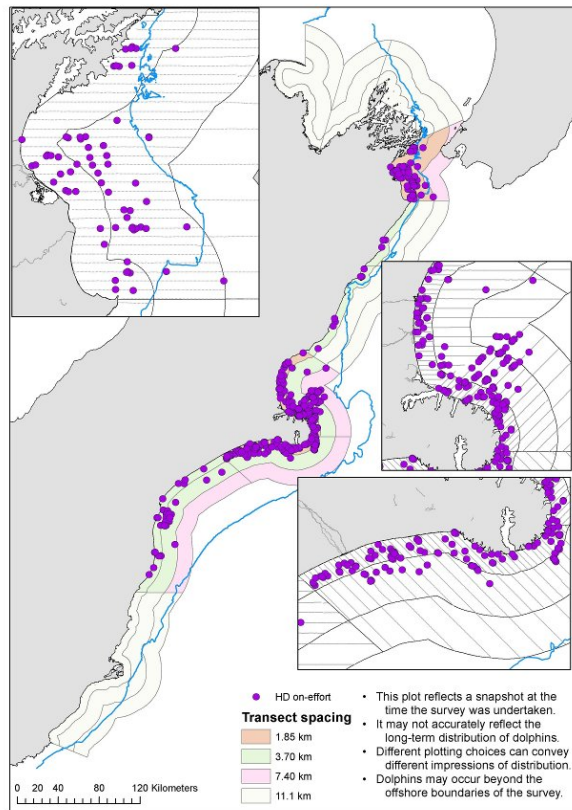


Figure 25a: Heceta's dolphin summer distribution assessed from aerial line-transect surveys. Panels represent patterns for an on-effort Heceta's dolphin sightings (left), the relative density of Heceta's dolphins within 5 km × 5 km grid cells generated from the Density Surface Models with eight categories (middle) and the relative density of Heceta's dolphins within survey strata generated from the Density Surface Models (right). Relative densities greater than 1 indicate areas with density greater than the overall average density.

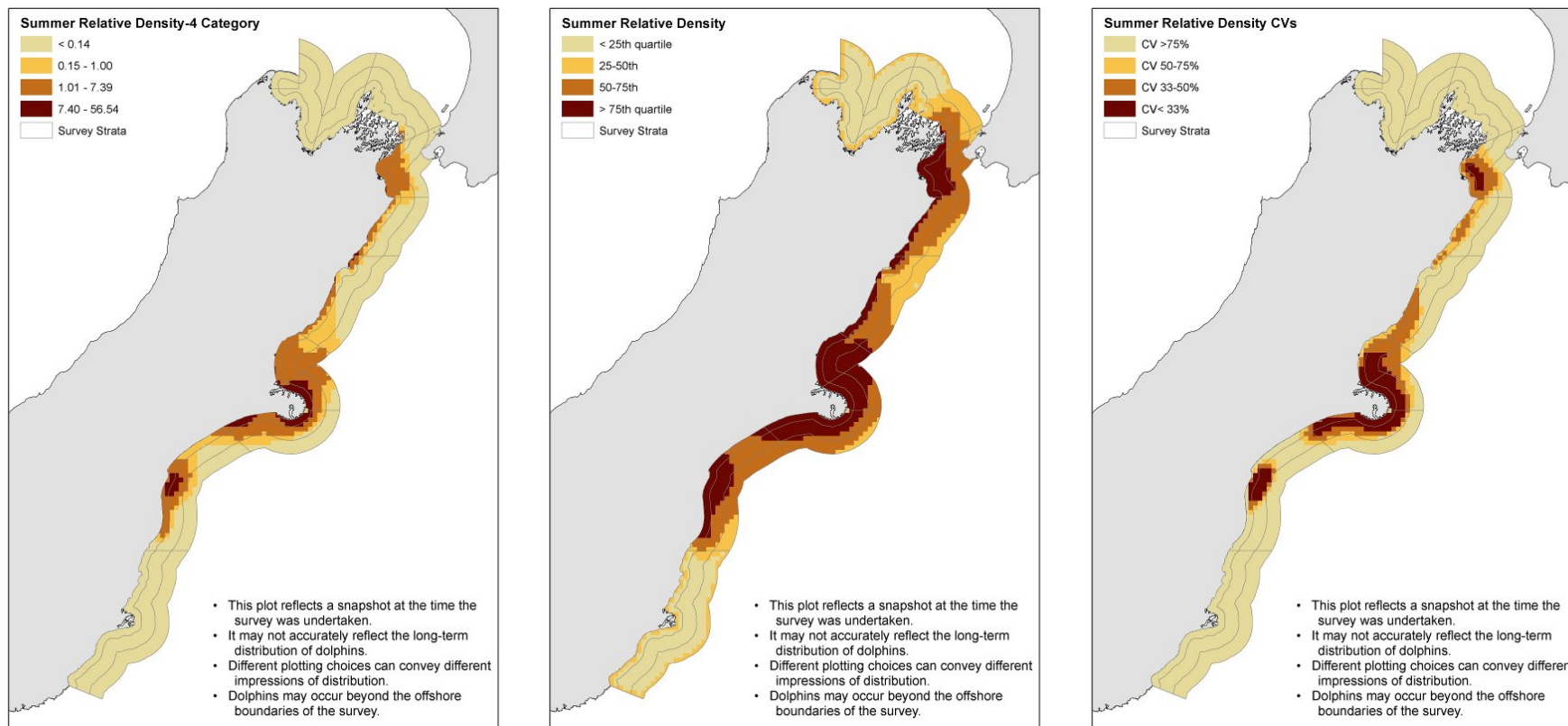


Figure 25b: Hector's dolphins summer distribution assessed from aerial line-transect surveys. Panels represent the relative density of Hector's dolphins within 5 km × 5 km grid cells generated from the Density Surface Model with four density categories (left), with density categories defined in terms of quartiles of estimated relative density values (middle), and precision of estimated relative density with darker colours indicating greater precision; i.e. smaller CVs (right). Relative densities greater than 1 indicate areas with density greater than the overall average density.

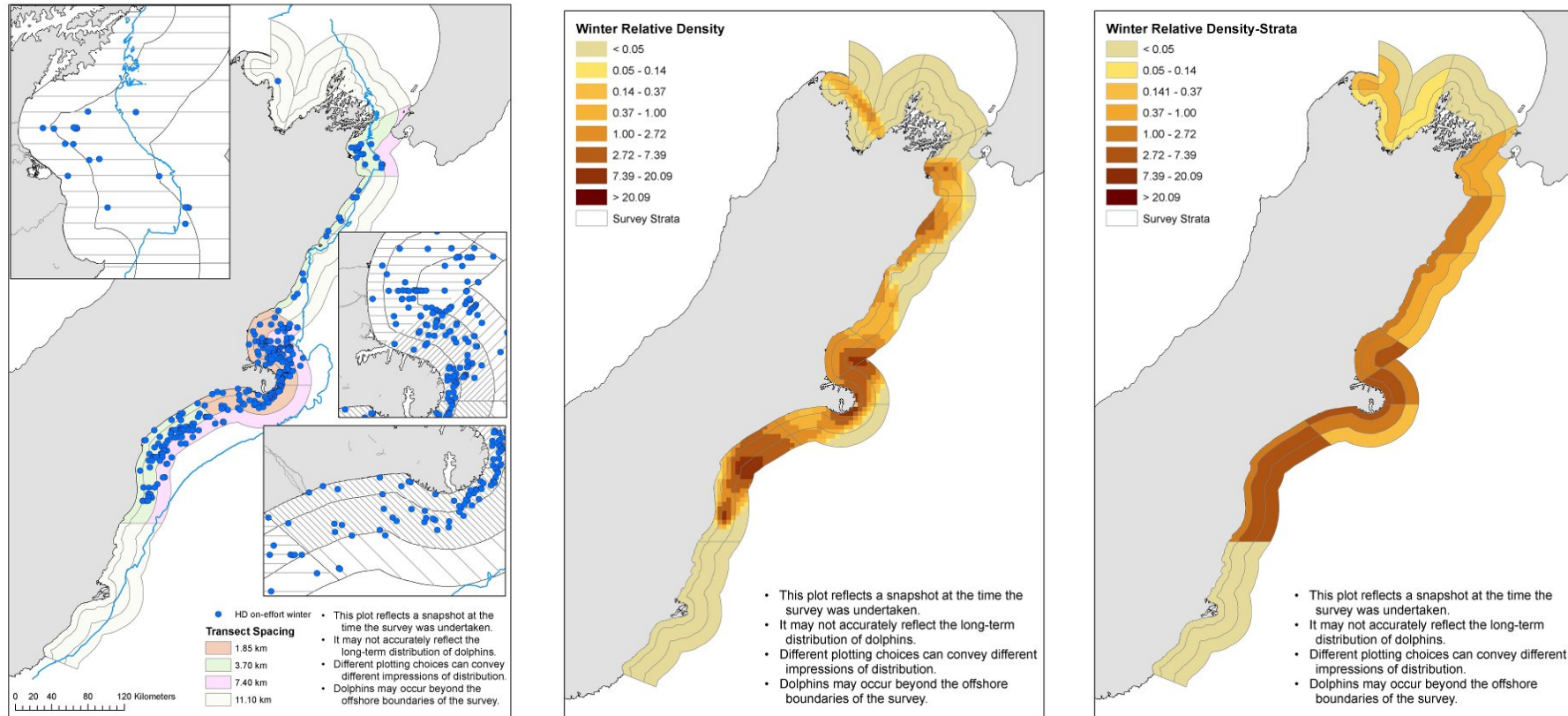


Figure 26a: Hecator's dolphin winter distribution assessed from aerial line-transect surveys. Panels represent patterns for an on-effort Hecator's dolphin sightings (left), the relative density of Hecator's dolphins within 5 km × 5 km grid cells generated from Density Surface Models with eight density categories (middle) and the relative density of Hecator's dolphins within survey strata generated from Density Surface Models (right). Relative densities greater than 1 indicate areas with density greater than the overall average density.

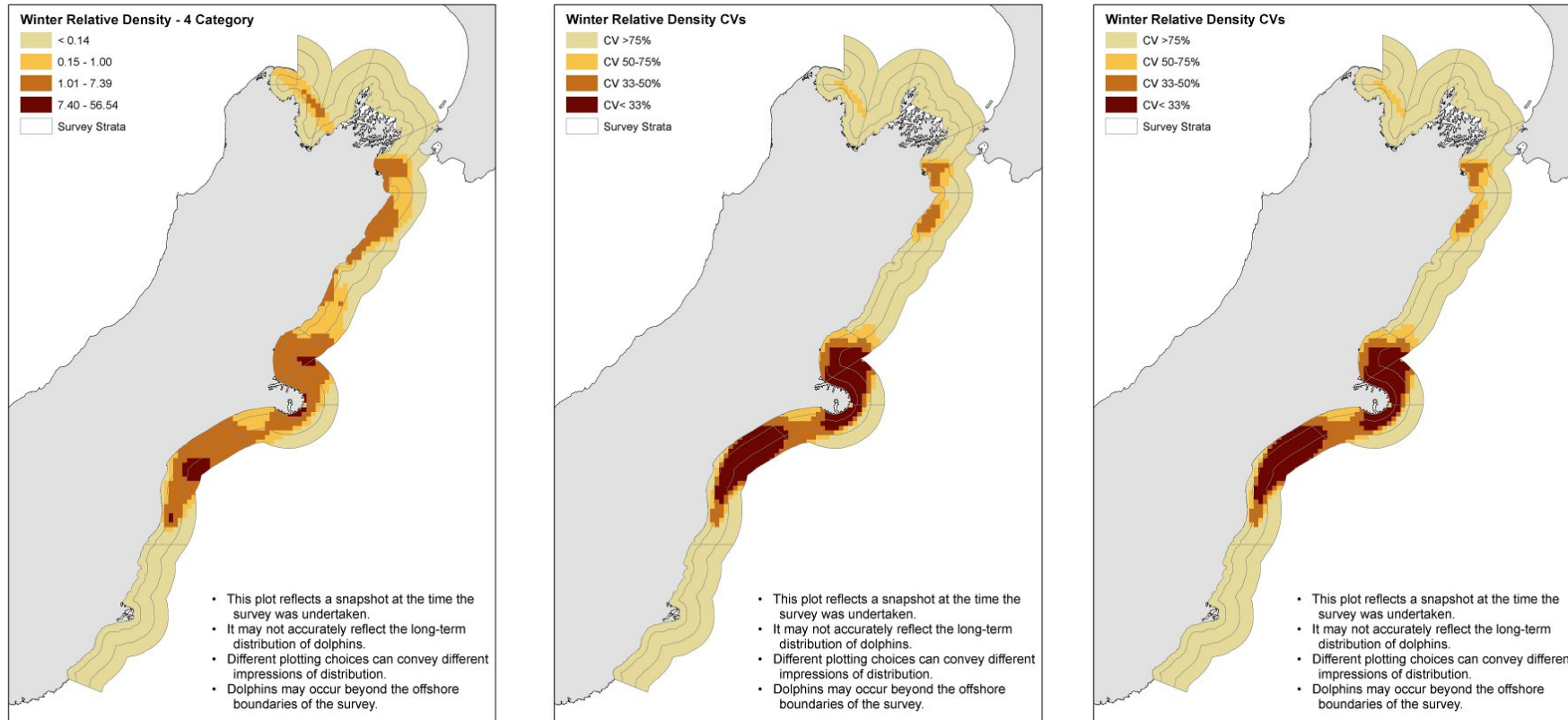


Figure 26b: Heceta's dolphin winter distribution assessed from aerial line-transect surveys. Panels represent the relative density of Heceta's dolphins within 5 km × 5 km grid cells generated from the Density Surface Model with four density categories (left), with density categories defined in terms of quartiles of estimated relative density values (middle), and precision of estimated relative density with darker colours indicating greater precision; i.e. smaller CVs (right). Relative densities greater than 1 indicate areas with density greater than the overall average density.

Table 30: Estimated summer and winter dolphin density (Density; per 100 km²) for each strata from DSM analyses. Standard errors (SE) obtained from a parametric bootstrap approach with 510 bootstrapped data sets for summer SE and 507 for winter SE.

	Offshore (nmi)	Stratum	Summer		Winter	
			Density	SE	Density	SE
Coastal Section						
Golden Bay North	0-4		0	0	5	10
	4-12		0	0	7	5
Golden Bay A	0-4		0	25	1	2
	4-12		0	0	6	3
	12-20		0	0	0	0
Golden Bay B	0-4		0	1	1	7
	4-12		0	0	2	2
	12-20		0	0	1	1
Marlborough Sounds	0-4		2	3	0	0
	4-12		0	0	0	0
	12-20		0	0	0	0
Cloudy/Clifford Bay	0-4		70	21	17	7
	4-12		31	8	13	4
	12-20		4	2	4	3
Kaikoura	0-4		39	17	20	15
	4-12		3	1	8	6
	12-20		2	1	5	4
Clarence	0-4		32	16	43	22
	4-12		1	1	21	11
	12-20		0	1	4	5
Pegasus Bay	0-4		88	31	24	9
	4-12		63	16	40	11
	12-20		56	22	92	24
Banks Pen. North	0-4		284	58	93	23
	4-12		109	29	66	16
	12-20		34	17	44	12
Banks Pen. South	0-4		228	40	52	11
	4-12		48	10	20	5
	12-20		2	1	6	3
Timaru	0-4		65	20	27	7
	4-12		40	7	61	11
	12-20		2	3	64	16
Otago	0-4		0	0	0	0
	4-12		0	0	0	0
	12-20		0	0	0	0
Overall			22	3	18	3

Table 31: Group-size frequency table used to randomly generate group sizes in the parametric bootstrap procedure. Given is the number of observed groups of size s (n_s), the expected probability of detecting a group of size s within the covered area ($E(p_{\bullet}(s))$), and is the estimated frequency of group size s (\hat{f}_s). The estimated number of groups in the covered area (\hat{N}_{gc}) was 483.77 in summer and 480.82 in winter.

Size	Summer			Winter		
	n_s	$E(p_{\bullet}(s))$	\hat{f}_s	n_s	$E(p_{\bullet}(s))$	\hat{f}_s
1	125	0.71	0.36	188	0.65	0.60
2	145	0.76	0.39	109	0.73	0.31
3	40	0.80	0.11	21	0.80	0.06
4	29	0.84	0.07	7	0.86	0.02
5	9	0.87	0.02	4	0.91	0.01
6	10	0.89	0.02	3	0.95	0.01
7	3	0.92	0.01			
8	3	0.93	0.00	1	0.99	0.00
9	2	0.95	0.00			
10	3	0.96	0.01			

Standard errors were obtained using 510 bootstrap data sets. This is a sufficient number for approximating standard errors (Manly 1997). Three bootstrap data sets for the winter analysis produced estimates of total dolphin abundance that were greater than 20 000 dolphins, which was considered extreme; hence; these data sets were not used for determining standard errors.

Total abundance was estimated from the DSM as 9244 (SE = 1376) for the summer and 7550 (SE = 1284) during the winter. These values are in very good agreement with the non-DSM estimates of abundance using the top-ranked detection function model and the helicopter-based estimates of availability (summer: 9334, SE = 1316, Table SM.K.1; winter: 7627, SE = 902, Table SM.M.1).

The relative precision (i.e., the CV) of DSM-based stratum-specific estimates tended to be better than non-DSM estimates, particularly for those strata with non-negligible estimates, although not in all instances (Table 32). While the CVs presented in Table 32 are for density estimates, the same CVs would hold for stratum-specific abundance estimates. A direct comparison is slightly impeded by the estimates from the two different approaches being somewhat different for some strata, which is primarily a result of the smooth density surface created by the GAM.

Table 32: Comparison of DSM-based estimates of dolphin density (per 100 km²) each season with those obtained from the corresponding non-DSM analyses (top-ranked models in Table SM.J.1 and SML.1 appendices).

Coastal Section	Offshore Stratum (nmi)	Summer				Winter			
		non-DSM	CV	DSM	CV	non-DSM	CV	DSM	CV
Golden Bay North	0-4							5	195%
	4-12							7	74%
Golden Bay A	0-4							1	141%
	4-12					12	107%	6	58%
	12-20								
Golden Bay B	0-4							1	622%
	4-12							2	145%
	12-20							1	222%
Marlborough Sounds	0-4			2	132%				
	4-12								
	12-20								
Cloudy/Clifford Bay	0-4	64	38%	70	30%	13	58%	17	38%
	4-12	39	36%	31	26%	26	39%	13	34%
	12-20			4	44%	22	70%	4	74%
Kaikoura	0-4	40	53%	39	43%	24	49%	20	75%
	4-12			3	44%			8	76%
	12-20			2	85%			5	86%
Clarence	0-4	27	84%	32	49%	63	52%	43	50%
	4-12			1	69%			21	52%
	12-20							4	127%
Pegasus Bay	0-4	82	29%	88	35%	10	81%	24	38%
	4-12	35	58%	63	25%	60	49%	40	27%
	12-20	48	94%	56	39%	64	40%	92	27%
Banks Pen. North	0-4	270	22%	284	20%	84	30%	93	24%
	4-12	129	37%	109	26%	64	23%	66	24%
	12-20	61	71%	34	52%	55	46%	44	27%
Banks Pen. South	0-4	225	19%	228	18%	60	28%	52	21%
	4-12	63	44%	48	22%	16	27%	20	23%
	12-20			2	69%	5	76%	6	42%
Timaru	0-4	52	36%	65	31%	18	34%	27	27%
	4-12	41	45%	40	18%	77	21%	61	18%
	12-20			2	130%	50	28%	64	25%
Otago	0-4								
	4-12								
	12-20								
Total		21	14%	22	15%	17	12%	18	17%

4 DISCUSSION

4.1 Abundance estimates

There is general agreement between our seasonal abundance estimates, confirming that the current population of Hector's dolphin along the ECSI is larger than expected from previous estimates. From Tables 25 and 27, it is clear that almost half of the population in summer and three-quarters of the winter population are occurring in strata beyond 4 nmi. Other recent aerial survey studies off Banks Peninsula (Rayment et al. 2010a), Clifford/Cloudy Bays (DuFresne & Mattlin 2009) and Pegasus Bay (DuFresne et al. 2010) have indicated that a larger than previously expected proportion of Hector's dolphins were regularly occupying these more offshore waters. Additional evidence of offshore occurrences of dolphins have been recorded by boat-based fisheries observers around Timaru and Banks Peninsula (Figure 27; Slooten 2013). Hence, a portion of the discrepancy between our study and previous results are likely to be due to the more extensive offshore coverage.

Summer abundance estimates are approximately four to five times greater than what have previously been suggested for Hector's dolphin abundance along ECSI (Dawson & Slooten, 1988; Dawson et al. 2004). All previous ECSI abundance estimates have been from boat-based summer surveys (Figure 27; Dawson & Slooten, 1988; Dawson et al. 2004), and while different methods were employed, both studies concluded an ECSI population size of about 1600–1900 individuals, firstly in 1984–1985, then again in 1997–2000. We have estimated that approximately 4500 dolphins are within 4 nmi of the ECSI over summer; about 2–2.5 times greater than the two previous boat-estimates. The difference in the current abundance estimate cannot be directly attributed to any one management regulation established before or since the previous abundance surveys.

Instead, discrepancies between estimates are more likely to be due to a combination of more optimistic population growth in recent years due to marine protected areas (Gormley et al. 2012) and differences in sampling intensity and methods (including methods to correct for responsive movement, availability and perception bias). The new methods that have been developed to estimate the detection functions are unlikely to be a source of over-estimation as they have been verified by simulation (SM §B) and provide similar estimates to those from a DISTANCE-style analysis on the reduced data (SM §O). The simulation results did suggest the potential for the constant dependence and limiting independence models to provide overestimates of abundance, but such results tended to occur when the correlation between the intercept terms of the detection and dependence functions were less than -0.9. Any detection function model that provided potentially unreliable results were excluded from the final inferences. It should also be remembered that each set of estimates has an associated level of uncertainty so it is conceivable that the actual abundances at different points in time may be more similar than the estimates would suggest.

This is the first time the entire region of the ECSI has been surveyed using aerial survey methods. However, the fact that the estimated abundance from an aerial survey is much greater than a boat-based estimate is not without precedent. Hector's dolphin abundance along the West Coast of the South Island (WCSI; Farwell Spit - Milford Sound) was estimated to be approximately 1300 individuals from a boat-based survey (Dawson & Slooten 1988). Slooten et al. (2004), using aerial surveys with similar line-transect methods to those used here, reported abundance estimates of about 5400 along the WCSI or over four times greater than the previous boat-based estimates. Boat-based abundance within Cloudy and

Clifford Bay was estimated at 160 animals (Dawson et al. 2004), while DuFresne & Mattlin (2009) recently estimated summer abundance at almost six times that; 951 from a three-year aerial survey project.

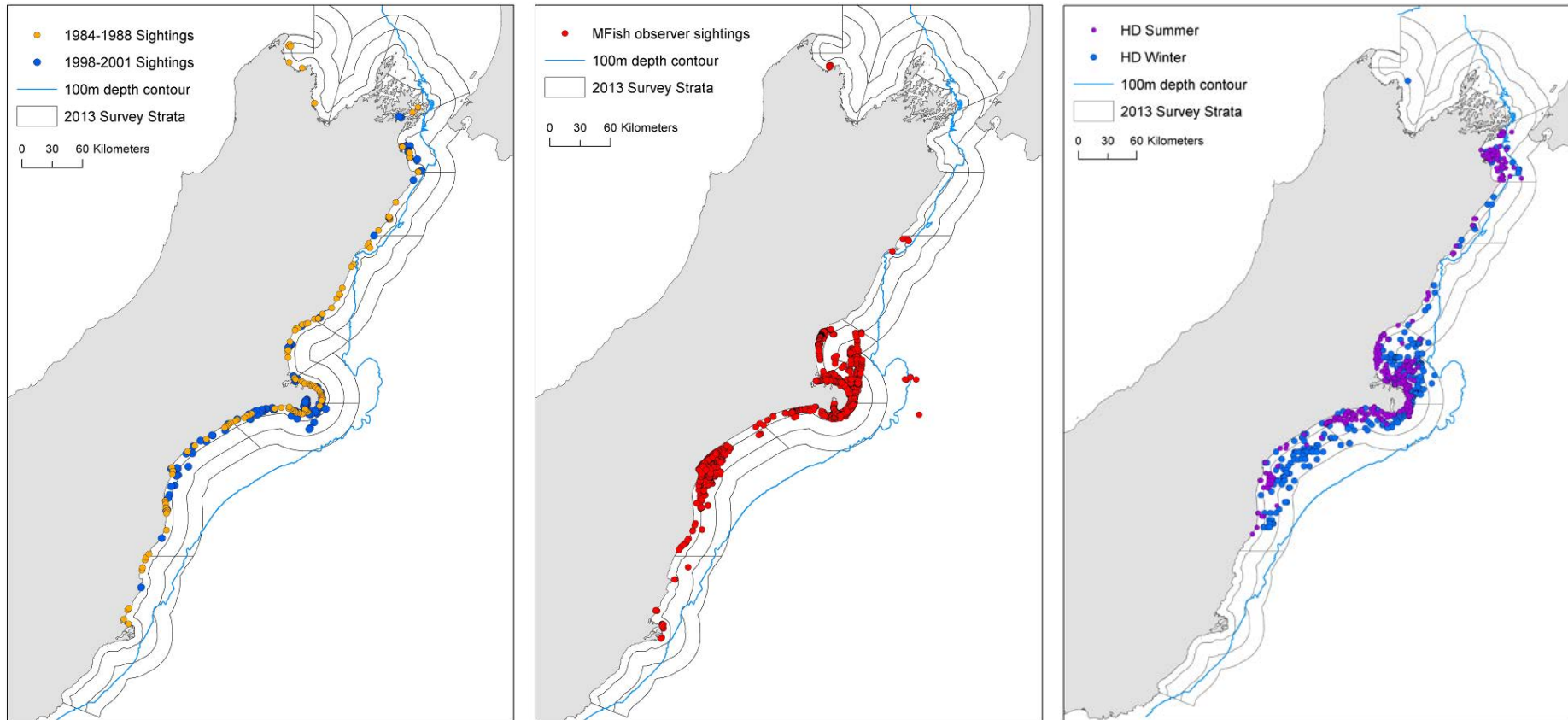


Figure 27: Locations of Hector's dolphin sightings along the ECSI from boat-based surveys (left), Ministry of Fisheries observers 2009-2010 (centre) and present survey (right).

Comparison of availability protocols

An advantage of the circle-back procedure is that it can be applied in areas that are beyond the range of single-engine helicopters and that the information on availability can be collected as the dolphin groups are detected rather than having to conduct an additional survey to first locate a group before collecting dive-cycle information. This has a real practical advantage given the differential costs between small fixed-wing aircraft and single-engine helicopters. The circle-back method also more closely resembles the sighting conditions from the real survey compared to the helicopter observation. A disadvantage is that a large number of circle-backs have to be performed to gain relatively precise estimates of availability (e.g. close to 100 circle-back passes would be desirable). Another disadvantage is the requirement of matching up groups from each pass to reliably record whether the same group was redetected or not. Misidentification of groups is likely to lead to some bias in the availability estimates, although sound protocols should minimise the potential for misidentification (detailed previously). Another potential source of concern could be the periodic sampling of a periodic process, which may introduce a bias if the process is consistently being observed at the same point in its cycle. However, given the degree of natural variation in the time taken to complete circle-backs (note that it was not a standard rate turn), and in Hector's dolphin dive cycles, the point in the dolphin's dive cycle at which the aircraft flies over the group could be considered random.

The potential for misidentification is much lessened with helicopter-based surveys of diving behaviour; however they do have their own shortcomings. One issue is the potential for censoring bias caused by longer dives; if a group performs a longer dive that exceeds the survey time limit or causes the observer to lose contact with the group that longer dive time will not be included in the dive data, resulting in a possible overestimate of availability. Another issue relates to the continuous nature of dolphins' dive cycle, which means that a group may become available/unavailable to the observers in the aircraft performing the line transect survey at any point while the area of ocean they inhabit is within the view of the observers. The time that a particular point in the ocean is visible to the observers in the aircraft, increases with distance from the aircraft. Ideally, any dive-cycle based availability estimate should take this aspect into account, although here only the average time objects are in view is used. Finally, the depth at which a dolphin becomes visible to airborne observers, and therefore available, will depend on viewing angle and most helicopter surveys are primarily conducted from a near-overhead position. Availability based on helicopter methods may therefore be an overestimate, particularly if dolphins spend a reasonable amount of time swimming just below the surface, relative to the actual survey conditions of a fixed wing aircraft flying along a transect where viewing angles will tend to be lower (i.e. further away).

It is our view that neither helicopter surveys nor circle-backs provide the ideal information about dolphin availability; both have some shortcomings and require some assumptions to be made in order to obtain useful estimates. We suggest that further work needs to be done on assessing field methods for reliably assessing availability of Hector's dolphins to aerial surveys. The methods used here are, however, two practical options that could be implemented within the budgetary constraints of the project and considered appropriate, as we are primarily interested in the level of consistency obtained in the abundance estimates while using each of the methods. Without knowledge of the truth, it is difficult to reliably conclude which approach might be more valid given that both require important caveats. The fact that both methods result in similar estimates of abundance provides some reassurance, especially in light of the fact that the dive-cycle-based estimates were in the same range as

those determined previously (Slooten et al. 2004, 2006; DuFresne & Mattlin 2009; Clement et al. 2011).

4.2 Distribution

There is a very strong indication of regional shifts in Hector's dolphin distribution between the summer and winter surveys, with fewer dolphins in the Cloudy/Clifford Bay, Pegasus Bay and around Banks Peninsula, and more dolphins offshore of Timaru and in the Clarence region over winter. However, the increase in winter abundance estimates within both Clarence and Timaru strata cannot fully account of winter declines in all other regions. There was also a general offshore shift in winter distribution, as has been noted by others previously (e.g. DuFresne & Mattlin 2009, Rayment et al. 2010). Several winter sightings of dolphin were observed on or near the 20 nmi boundary within both Pegasus Bay and Canterbury Bight suggesting that our survey limit may not fully encompass the offshore limits of this species. An unaccounted for offshore shift may help explain the large winter decline in both northern and southern Peninsula waters that are not fully accounted for in Timaru and Clarence waters.

It must be kept in mind, however, that a complete survey of most regions only took a few days to a little more than a week; hence it cannot be ascertained whether the observed shifts are of a relatively temporary nature that coincided with the surveys, or are truly representative of seasonal patterns. Verification beyond occurrence could only be achieved through additional surveys, although some of the observed shifts did match up with *a-priori* expectations from MacKenzie et al. (2012).

A DSM is a model-based method for assessing abundance and distribution based upon distance sampling methods. As with any model-based inference, the appropriateness of the conclusions depends upon the accuracy of the model at the scale of its application. While there are likely to be many factors that influence dolphin distribution that we have not considered, we have focused on coarse-scale factors given the intended usage of the DSM. The use of a bivariate spline term, involving the easting and northing coordinates of a transect segment where a dolphin sighting occurred, provides a flexible method for modelling spatial variation without attempting to identify the underlying factors that might be driving the spatial variation. As demonstrated with simulation by MacKenzie et al. (2012), using a bivariate spline term within a DSM produced useable results, even when the factors involved in the generating density survey were not included in the DSM. That is, the density estimation model did not include the same factors that were used in the density generation model. The DSM did not include a wider range of factors because the objective of the distribution modelling was to describe where the dolphins were, rather than to understand the underlying habitat preferences of Hector's dolphins (which would have required quite a different study).

As was expected, the relative precision of the stratum-level estimates of density obtained from the DSMs tended to be at least as good as what could be obtained from the stratum-specific abundance estimates using the non-DSM approach. This is because some information on spatial variation in density is shared across multiple strata through the GAM component of the DSM. In the non-DSM approach, while there is shared information in terms of a common detection function, a primary component of uncertainty occurs within the among-line variation in the estimated encounter rate that is estimated independently for each stratum.

The density estimates for each stratum tended to be different for the DSM and non-DSM approaches. Some of the discrepancy will be due to the resolution of the prediction grid (5 km × 5 km cells) with the whole cell being included in a stratum if its centroid was included. Discrepancies will also result as the DSM is producing a smooth surface; hence, in some cases the density could be pushed to another region as a result of the smoothing. This can result in non-zero density estimates for strata where no dolphins were sighted, which cannot occur in a non-DSM approach.

4.3 Spatial management areas

Banks Peninsula Marine Mammal Sanctuary (BPMMS)

The Banks Peninsula Marine Mammal Sanctuary (BPMMS) was created in 1988 to reduce the high level of Hector's dolphins being incidentally caught in both commercial and recreational gillnets (Dawson & Slooten 1993). The original BPMMS boundaries were established at a four nmi offshore limit and between the Rakaia River to the south and Sumner Head to the north, as the majority of animals were thought to occur within this area year-round (Figure 28; Dawson & Slooten 1993).

Despite year-round and seasonal fishery restrictions, the resident population continued to demonstrate low adult survival rates within the Sanctuary boundaries (Cameron et al. 1999, DuFresne 2005). Later boat and aerial survey work found that a reasonable number of dolphin sightings over summer occurred outside the BPMMS limits (e.g. about 19%; Rayment et al. 2010a) and that a substantial proportion of the total animals sighted within inshore waters over summer shifted outside the 4 nmi boundaries over winter (e.g. about 56% Rayment et al. 2010a, Clement 2005, DuFresne 2005). Several studies (e.g. Dawson & Slooten 2005, Slooten 2007, Davies et al. 2008) attribute the previous lack of recovery in survival rates to the continued bycatch of adult dolphin in fisheries occurring outside the boundaries of the BPMMS.

Extensions to the BPMMS in 2008 now exclude mining and seismic surveys offshore to 12 nmi and as far north as the Waipara River (see Figure 28; DOC 2008). However, the original four nmi boundaries still apply to commercial and recreational set-net fishing (with some harbour exceptions) and commercial trawl fishing is now prohibited within two nmi of the coast (DOC & MFish 2007). While current fisheries regulations now extend along most of the ECSI inshore regions, there are no current fishery restrictions beyond four nmi.

Figure 28 displays the location of current survey sightings in relation to the past and present boundaries of the BPMMS and current fisheries restriction zones (DOC & MFish 2007). Sixty-six percent of the estimated summer ECSI population is found around Banks Peninsula (combined Pegasus, Banks North and Banks South strata; Table 26). Apportioning the estimated abundance within each stratum based upon the number of dolphins seen inside/outside of the current boundaries of the Sanctuary from the full summer dataset; 45% of the local (i.e., Pegasus, Banks North and Banks South strata) summer population occurred within the 4 nmi fisheries restriction zone and 82% within 12nmi (Figure 28).

In winter, only 39% of the estimated winter ECSI population was observed in the general vicinity of the Peninsula (Table 28). Apportioning the stratum-specific abundance estimates based upon the number of dolphins seen inside/outside of the current boundaries of the

BPMMS from the full winter dataset; only 26% of the local winter population occurred within the 4 nmi fisheries restriction zone and 67% within 12 nmi (Figure 28).

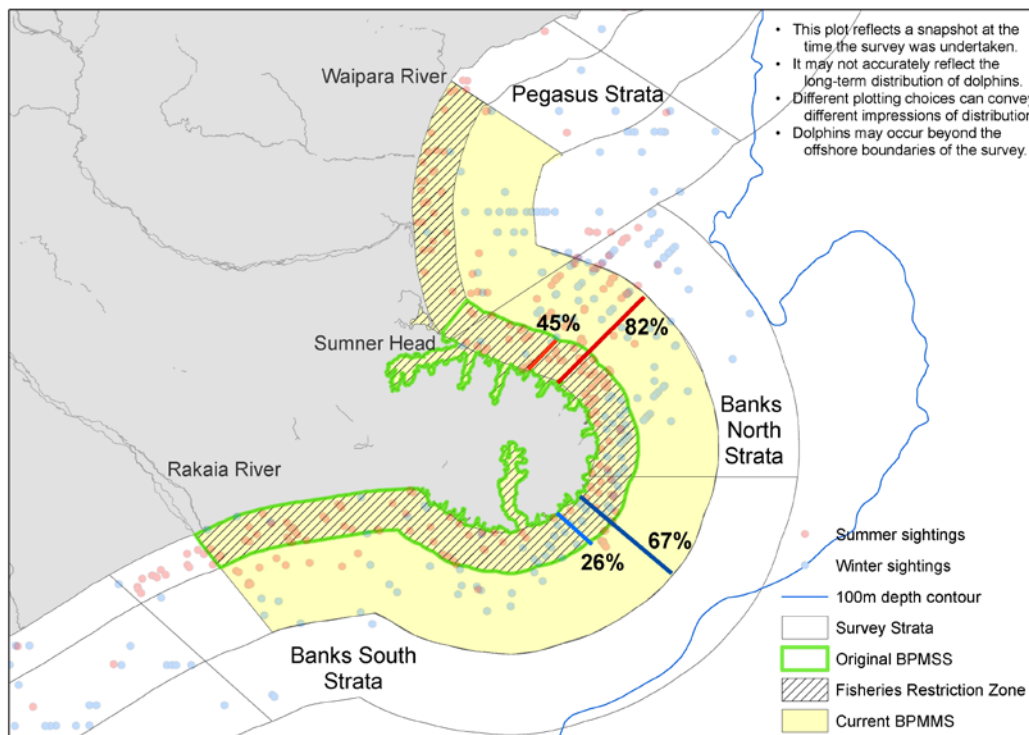


Figure 28: Survey sightings in relation to the BPMMS boundaries (previous and current). Red lines and associated percentages represent proportion of local summer population within 4 nmi and 12 nmi BPMMS, and blue lines and associated percentages denote winter.

Clifford and Cloudy Bay Marine Mammal Sanctuary (CCBMMS)

This region was not originally considered a high density area for Hector’s dolphins until more recent research found a sizable population present year-round (about 200–950 animals; DuFresne & Mattlin 2009). The Clifford and Cloudy Bay Marine Mammal Sanctuary (CCBMMS) was also created in 2008 as part of the new TMP regulations implemented to protect Hector’s dolphins by DOC and MFish in 2008 (Figure 29). The boundaries of this Sanctuary also extend out to 12 nmi offshore from Tory Channel to Cape Campbell. Similar commercial and recreational fishing regulations apply as to BPMMS with both commercial and recreational setnetting banned out to four nmi and commercial trawl fishing out to two nmi. A few exemptions have been made based on legal reviews of some closures, in particular the decision to allow both commercial and recreational fishing for butterfish using setnets within 200 m of the shore along the western edge of Cloudy Bay and Marlborough Sounds (from Rarangi to Cape Jackson; see Figure 29 for place locations).

During our summer, 10% of the ECSI population was within the Clifford and Cloudy Bay stratum (Table 26) and 9% in winter (Table 28). Apportioning the local estimated abundance based upon the number of individual dolphins sighted in the full data sets as above; 47% of

the local summer population appear to be within the 4 nmi fisheries restriction zone and 97% within the CCBMMS boundaries. In winter, 14% of the local population appear to be within the 4 nmi fisheries restriction zone and 74% within the CCBMMS boundaries (Figure 29).

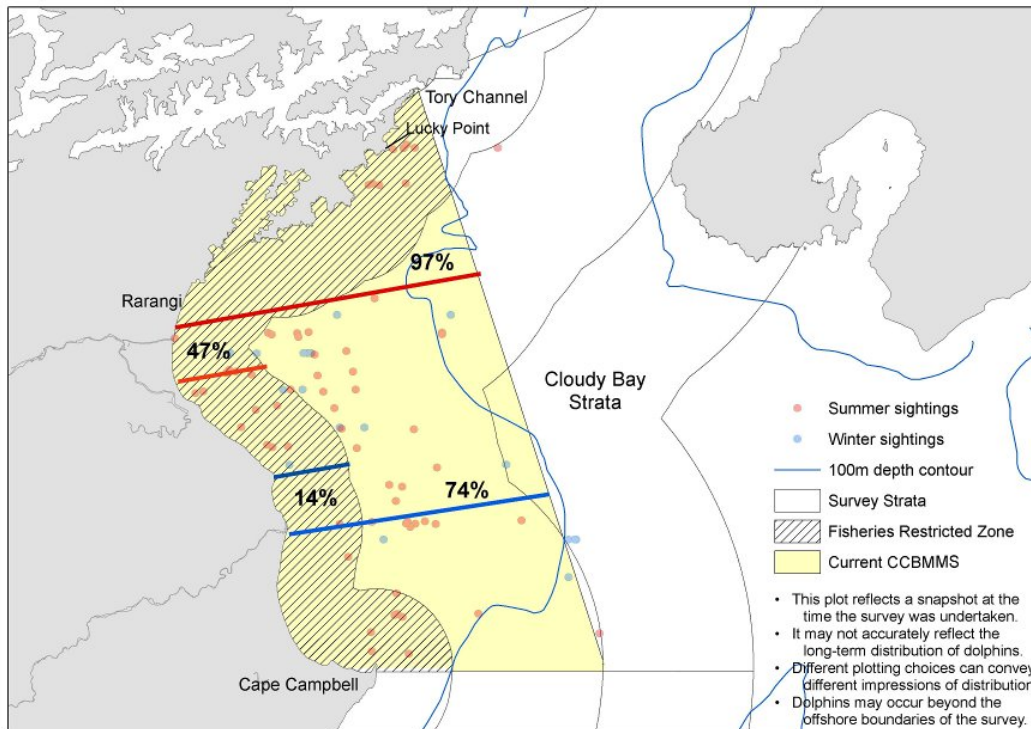


Figure 29: Survey sightings in relation to the CCBMMS boundaries. Red lines and associated percentages represent proportion of local summer population within 4 nmi and 12 nmi of CCBMMS, and blue lines and associated percentages denote winter.

In general, survey results suggest that, at least in summer, a large portion of the ECSI Hector's dolphin population occurs in waters around Banks Peninsula and within Clifford and Cloudy Bays. However, these results also suggest that reasonable numbers of dolphins can be found outside designated spatial management areas, in more offshore regions or along the Timaru and Kaikoura/Clarence coastline, during both summer and, in particular, winter.

5 ACKNOWLEDGMENTS

This work was completed for the Ministry for Primary Industries under project PRO2009-01C. It would never have been completed without the enduring patience and superb search image of the observer team that helped throughout various stages of the field work and data analysis. We would also like to thank all the supporting organisations and people that assisted in the field work portion of this project including: Flight Hauraki (Paul McSherry and William Hayman), the Omaka Aero club, Department of Conservation Golden Bay office, the Knightbridge Court Motel that became our home away from home, Blue Water Survival Training Specialists and the Helipro staff in both Christchurch and Wellington. Thanks also to Rachel Fewster and Rob Mattlin who have scrutinised various versions of this report.

6 REFERENCES

- Anderson, D.R. (2008) Model based inference in the life sciences. Springer. New York, USA.
- Baker, C.S.; Chilvers, B.L.; Constantine, R.; DuFresne, S.; Mattlin, R.H.; van Helden, A.; Hitchmough, R. (2010). Conservation status of New Zealand marine mammals (suborders Cetacea and Pinnipedia), 2009. *New Zealand Journal of Marine and Freshwater Research*, 44(2): 101 – 115.
- Borchers, D.L.; Laake, J.L.; Southwell, C.; and Paxton, C.G.M. (2006). Accommodating unmodeled heterogeneity in double-observer distance sampling surveys. *Biometrics* 62, 372–378.
- Buckland, S.T.; Anderson, D.R.; Burnham, K.P.; Laake, J.L.; Borchers, D.L.; Thomas, L.; (2001). Introduction to distance sampling: estimating abundance of biological populations. Oxford University Press, New York.
- Buckland, S.T.; Anderson, D.R.; Burnham, K.P.; Laake, J.L.; Borchers, D.L.; Thomas, L.; (2004). Advanced Distance Sampling: Estimating abundance of biological populations. Oxford University Press, New York.
- Buckland, S.T.; Laake, J.L.; Borchers, D.L. (2010). Double-observer line transect methods: levels of independence. *Biometrics* 66: 169–177.
- Burnham, K.P.; Anderson, D.R. (2002). Model selection and multimodel inference. 2nd Ed., Springer-Verlag, New York, USA.
- Cameron, C.; Barker, R.; Fletcher, D.; Slooten, E.; Dawson, S. (1999). Modelling survival of Hector's dolphins around Banks Peninsula, New Zealand. *Journal of Agricultural Biological and Environmental Statistics* 4 (2): 126–135.
- Clement, D.M. (2005). Distribution of Hector's dolphin (*Cephalorhynchus hectori*) in relation to oceanographic features. PhD Dissertation, University of Otago, Dunedin, New Zealand. 253 p.
- Clement, D.; Mattlin, R.; Torres, L. (2011). Abundance, distribution and productivity of Hector's (and Maui's) dolphins (Final Research Report, PRO2009-01A). Ministry of Fisheries. (Unpublished report held by Ministry for Primary Industries, Wellington.)
- Clement, D.; Slooten, E.; Dawson, S.; DuFresne, S. (2001). Line-transect survey of Hector's dolphin abundance between Farewell Spit and Motunau. DOC Science Internal Series 22. Department of Conservation, Wellington.
- Davies, N.M.; Bian, R.; Starr, P.; Lallemand, P.; Gilbert, D.; McKenzie, J. (2008). Risk analysis for Hector's dolphin and Maui's dolphin subpopulations to commercial set net fishing using a temporal-spatial age-structured model. Final Research Report for

- Ministry of Fisheries, project IPA 2006/05. [www.fish.govt.nz/NR/rdonlyres/B034115D-247A-42E5-B08F-F5D267046C59/0/Hector NIWA risk analysis.pdf](http://www.fish.govt.nz/NR/rdonlyres/B034115D-247A-42E5-B08F-F5D267046C59/0/Hector%20NIWA%20Ariskanalysis.pdf) (Unpublished report held by Ministry for Primary Industries, Wellington.)
- Dawson, S.; Slooten, E. (1988). Hector's Dolphin *Cephalorhynchus hectori*: Distribution and abundance. *Reports International Whaling Commission Special issue 9*: 315–324.
- Dawson, S.M.; Slooten, E. (1993). Conservation of Hector's dolphins: The case and process which led to establishment of the Banks Peninsula Marine Mammal Sanctuary. *Aquatic Conservation: Marine and Freshwater Ecosystems*:3: 207–221.
- Dawson, S.M.; Slooten, E. (2005). Management of gillnet bycatch of cetaceans in New Zealand. *Journal of Cetacean Research and Management* 7:59–64.
- Dawson, S.; Slooten, E.; DuFresne, S.; Wade, P.; Clement, D. (2004). Small-boat surveys for coastal dolphins: line-transect surveys for Hector's dolphin (*Cephalorhynchus hectori*). *Fishery Bulletin* 102(3): 441–451.
- Dawson, S.; Wade, P.; Slooten, E.; Barlow, J. (2008). Design and field methods for sighting surveys of cetaceans in coastal and riverine habitats. *Mammal Review* 38(1): 19–49.
- Department of Conservation, Ministry of Fisheries (2007). Hector's and Maui's dolphin threat management plan draft for public consultation. 5 March 2009. <http://www.fish.govt.nz/NR/rdonlyres/2088EFD2008C-E2207-4798-9315-C2000AF2002FC2006FFB2002/2000/DRAFTTMPFINAL.pdf>
- Department of Conservation (2008). Marine Mammals Protection (Banks Peninsula Sanctuary) Amendment Notice 2008. <http://www.doc.govt.nz/Documents/conservation/marine-and-coastal/marine-protected-areas/marine-mammals-protection-banks-amendment.pdf>
- DuFresne, S. (2005). Conservation biology of Hector's dolphin. PhD Dissertation University of Otago, Dunedin, New Zealand. 166 p.
- DuFresne, S.; Mattlin, R. (2009). Distribution and Abundance of Hector's Dolphin (*Cephalorhynchus hectori*) in Clifford and Cloudy Bays (Final report for NIWA project CBF07401). Marine Wildlife Research Ltd.
- DuFresne, S.; Mattlin, R.; Clement, D. (2010). Distribution and Abundance of Hector's Dolphin (*Cephalorhynchus hectori hectori*) and Observations of Other Cetaceans in Pegasus Bay. Final Report to the Marlborough Mussel Company, Baseline Monitoring for Environment Canterbury Consent CRC21013A.
- Gomez-Segura, A.; Hammond, P.S.; Canadas, A.; Raga, J.A. (2007). Comparing cetacean abundance estimates derived from spatial models and design-based line transect methods. *Marine Ecology Progress Series* 329: 289–299.
- Gormley, A.M.; Slooten, E.; Dawson, S.; Barker, R.J.; Rayment, W.; DuFresne, S.; Brager, S. (2012). First evidence that marine protected areas can work for marine mammals. *Journal of Applied Ecology* 49: 474–480.
- Hamner, R.M.; Oremus, M.; Stanley, M.; Brown, P.; Constantine, R.; Baker, C.S. (2012). Estimating the abundance and effective population size of Maui's dolphins using microsatellite genotypes in 2010–11, with retrospective matching to 2001–07. Department of Conservation, Auckland. 44 p.
- Hiby, L. (1999). The objective identification of duplicate sightings in aerial survey for porpoise, in *Marine Mammal Survey and Assessment Methods*, eds G.W. Garner, S.C. Amstrup, J.L. Laake, B.F.J. Manly, L.L. McDonald, and D.G. Robertson. Balkema, Rotterdam, pp. 179–189.
- Laake, J.L.; Borchers, D.L. (2004). Methods for incomplete detection at distance zero. Pp. 108–189 in *Advanced Distance Sampling*, eds S.T. Buckland, D.R. Anderson, K.P. Burnham, J.L. Laake, D.L. Borchers and L. Thomas. Oxford University Press, Oxford.

- MacKenzie, D.I.; Clement, D.; Mattlin, R. (2012). Abundance, distribution and productivity of Hector's (and Maui's) dolphins (Final Research Report, PRO2009-01B). (Unpublished report held by Ministry for Primary Industries, Wellington.)
- Manly, B.F.J. (1997). Randomization, bootstrap and Monte Carlo methods in biology. 2nd edition. Chapman and Hall, London, U.K.
- Manly, B.F.J.; McDonald, L.L.; Garner, G.W. (1996). Maximum likelihood estimation for the double-count method with independent observers. *Journal of Agricultural and Biological Statistics* 1: 170–189.
- Pichler, F.B.; Dawson, S.M.; Slooten, E.; Baker, C.S. (1998). Geographic isolation of Hector's dolphin populations described by mitochondrial DNA sequences. *Conservation Biology* 12:676–682
- Rayment, W.; Clement, D.; Dawson, S.; Slooten, E.; Secchi, E. (2010b). Distribution of Hector's dolphin (*Cephalorhynchus hectori*) off the west coast, South Island, New Zealand, with implications for the management of bycatch. *Marine Mammal Science* 27: 398–420.
- Rayment, W.; Dawson, S.; Slooten, E. (2010a). Seasonal changes in distribution of Hector's dolphin at Banks Peninsula, New Zealand: implications for protected area design. *Aquatic Conservation: Marine and Freshwater Ecosystems* 20: 106–116.
- Reeves, R.R.; Dawson, S.M.; Jefferson, T.A.; Karczmarski, L.; Laidre, K.; O'Corry-Crowe, G.; Rojas-Bracho, L.; Secchi, E.R.; Slooten, E.; Smith, B.D.; Wang, J.Y.; Zhou, K. (2008). *Cephalorhynchus hectori maui*. In: IUCN 2011. IUCN Red List of Threatened Species. Version 2011.1.<http://www.iucnredlist.org>
- Slooten, E.; Dawson, S.; Rayment, W. (2004). Aerial surveys for Hector's dolphins: abundance of Hector's dolphins off the South Island west coast, New Zealand. *Marine Mammal Science* 20: 477–490.
- Slooten, E.; Dawson, S.; Rayment, W.; Childerhouse, S. (2006). A new abundance estimate for Maui's dolphin: What does it mean for managing this critically endangered species? *Biological Conservation* 128: 576–581.
- Slooten, E. (2007). Conservation management in the face of uncertainty: effectiveness of four options for managing Hector's dolphin bycatch. *Endangered Species Research* 3:169–179.
- Slooten, E. (2013). Effectiveness of area-based management in reducing bycatch of the New Zealand dolphin. *Endangered Species Research* 20: 121–130.
- Thomas, L.; Buckland, S.T.; Rexstad, E.A.; Laake, J.L.; Strindberg, S.; Hedley, S.L.; Bishop, J.R.B.; Marques, T.A.; Burnham, K.P. (2010). Distance software: design and analysis of distance sampling surveys for estimating population size. *Journal of Applied Ecology* 47: 5–14.
- Turek, J.; Slooten, E.; Dawson, S.; Rayment, W.; Turek, D. (2013). Distribution and abundance of Hector's dolphins off Otago, New Zealand. *New Zealand Journal of Marine and Freshwater Research* 47: 181–191. DOI:10.1080/00288330.2013.771687